



SUDAN UNIVERSITY of SCIENCE and
TECHNOLOGY



COLLEGE of GRADUATE STUDIES and RESEARCH
STRUCTURES ENGINEERING

Numerical Investigation on Burial Corrugated Steel
Culverts Design

التحقق العددي لتصميم البرابح الفولاذية
الموجه المدفونة

By

MOSAB ABDELHALIM ABDELKARIM MAKKI

B.Sc. in Civil Engineering (Structures), 2010

A Thesis Submitted to Sudan University of Science and Technology
in Partial Fulfilment of the Requirements for the Degree of M.Sc. in
Structures Engineering

Supervised by

Dr. ABUSAMRA AWAD ATTAELMANAN

February 2015

Abstract

A full analysis and design theories have been reviewed conducted to determine response of a buried corrugated steel structural plate culvert for four exceptional shapes as; a round pipe, horizontal ellipse, arch and low profile arch. The select of culverts span, cover, and exceptional live load have been applied and all were have the same value. AASHTO LRFD Method has been used to measure the result of analysis and design by using manual and computer program techniques. Data collected by using computer controlled data acquisition system.

The ultimate design strength of these type of culverts determined by manual analysis and CANDE finite element program. CANDE used to determine numerical results of factored thrust force and displacement of the shell at many point during the loading sequence.

The CANDE numerical results compared with the manual analysis and design. Where the magnitude did not agree well between the manual results and the numerical simulations. The round pipe was the best choice from the other forms of the culvert shapes, due to it showed results in this study.

مستخلص

في هذا البحث تمت مراجعة وإجراء نظريات التحليل والتصميم لتحديد الاستجابة لبرابح من ألواح الفولاذ المموج المدفون لأربعة أشكال تم اختيارها؛ أنبوب مستدير، والبيضاوي الأفقي، والقوس، والقوس المنخفض. وكان اختيار طول بحر القنوات، وغطاء الردم، والحمل الحي الاستثنائي المطبق بأن يكون لهم نفس القيمة. وقد تم استخدام طريقة الـ AASHTO LRFD لقياس نتائج التحليل والتصميم باستخدام الحسابات اليدوية وتقنية البرامج. حيث تم جمع البيانات باستخدام نظام الحصول على البيانات بالكمبيوتر.

فإن مقاومة التصميم الحدية لهذه الأنواع من البرابح يحددها التحليل اليدوي أو برنامج العناصر المحدودة CANDE. فهذا البرنامج استخدم لتحديد النتائج العددية لقوة الضغط المحورية الناتجة على سمك الجدار وإزاحة الجدار في العديد من النقاط أثناء تسلسل التحميل.

وقد تم مقارنة النتائج العددية لبرنامج CANDE مع نتائج التحليل والتصميم اليدوي. حيث وجد ان مقدار التطابق بين النتائج اليدوية والمحاكاة العددية للبرنامج لم تتوافق جيداً، ووجد أيضاً أن الأنبوب المستدير أفضل خيار إذا تم مقارنته مع أشكال البرابح الأخرى وذلك نتيجة لما تم الوصول إليه في هذه الدراسة.

Table of Contents

Abstract.....	ii
مستخلص	iii
Table of Contents.....	iv
List of Tables	vi
List of Figures.....	vii
Acknowledgements.....	x
Dedication.....	xi

Chapter 1 Introduction

1.1. General Statement	1
1.2. Research Problem.....	2
1.3. Objectives.....	4
1.4. Hypothesis	4
1.5. Methodology	4
1.3. Outline of Thesis	5

Chapter 2 Literature Review

2.1. Introduction	6
2.2. Corrugated Sheets	9
2.3. Corrugated Steel Culvert.....	14
2.4. Salient Researches of Corrugated Metal Culverts	28
2.5. Corrugated Metal Culverts by Finite Element Method.....	33

Chapter 3 Case Study

3.1. Introduction	42
3.2. Structural Analysis and Design by Load and Resistance Factor Design.....	44
3.3. CANDE Input Flow	52
3.4. CANDE Solution Methods and Formulations	54
3.5. Hydraulics of Culverts	70

Chapter 4 Analysis of Results and Discussion

4.1. Manual Analysis and Design Calculations	72
4.2. CANDE Results	75
4.3. End Area Value	88

Chapter 5 Conclusions and Recommendations

5.1. Summary	90
5.2. Conclusions	90
5.3. Recommendations	92

References	93
-------------------------	----

Appendixes	95
-------------------------	----

List of Tables

Table 2.1. Shapes and uses of corrugated conduits	15
Table 3.1. Sectional properties for corrugated 152 x 51 mm	43
Table 3.2. Ultimate longitudinal seam strength for 152 x 51 mm.....	43
Table 3.3. Soil types by UCS classification	43
Table 3.4. Live Loads for H20 highway loadings	48
Table 3.5. Resistance Factors for LRFD Design	50
Table 3.6. Corrugated Metal Design Criteria	57
Table 3.7. Load factors for corrugated metal pipe or arch	70

List of Figures

Figure 2.1. Structural plate pipe for an irrigation ditch crossing	8
Figure 2.2. Section of arc-and tangent-type corrugated sheets	9
Figure 2.3. Radius-to-depth ratio versus pitch-to-depth ratio at various web angles	12
Figure 2.4. Factor C_5 versus pitch-to-depth ratio at various web angles.....	12
Figure 2.5. Factor C_6 versus pitch-to-depth ratio at various web angles.....	13
Figure 2.6. Factor λ versus pitch-to-depth ratio at various web angles.....	13
Figure 2.7. Tangent-to-depth ratio versus pitch-to-depth ratio at various web angles	14
Figure 2.8. Commonly used corrugations	19
Figure 2.9. Configuration of structural plate sheets	20
Figure 2.10. Alternate structural plate configuration	21
Figure 2.11. Dimensions of bolts and nuts for structural plate	22
Figure 2.12. Hook bolts and nuts for embedment in headwalls	23
Figure 2.13. Hook bolt and base channel	23
Figure 2.14. General dimensions of unbalanced channels for structural plate arches	23
Figure 2.15. Deep Corrugated Structural Plate Type I plate configuration	25
Figure 2.16. Additional details for deep corrugated structural plate Type I	26
Figure 2.17. Deep Corrugated Structural Plate Type II plate configuration	27
Figure 2.18. Sketch of applying load with hydraulic jacks	30
Figure 2.19. Results of Utah loading tests on corrugated steel pipe	31
Figure 2.20. Diagram showing how load partly carried by a soil arch over the pipe	31
Figure 2.21. Options to define input data for CANDE	34

Figure 2.22. Hot-dipped galvanized steel structural plates stocked at the warehouse	39
Figure 2.23. Steel structural plate pipe is bolted by modular plates	40
Figure 2.24. Corrugated steel pipe culverts	40
Figure 2.25. Steel structural plate Arch culvert.....	41
Figure 3.1. Four shapes of corrugated culverts structure	42
Figure 3.2. Minimum covers orientation.....	45
Figure 3.3. Minimum permissible spacing for multiple installations	46
Figure 3.4. CANDE level 2 input flowchart.....	53
Figure 3.5. Nodal strip load and surface-pressure strip load.....	59
Figure 3.6. Converting pressure strip to equivalent nodal forces.....	60
Figure 3.7. Single wheel load distribution along axis of culvert.....	60
Figure 3.8. Two-wheel load distribution along axis of culvert	62
Figure 3.9. Squeeze-layer method for compaction loads on culvert	66
Figure 4.1. AASHTO Design Truck (H-20).....	75
Figure 4.2. Loads steps for Round Pipe and Horizontal Ellipse shapes.....	79
Figure 4.3. View for Round Pipe and Horizontal Ellipse shapes	79
Figure 4.4. Loads steps for Arch and Low Profile Arch shapes	80
Figure 4.5. View for Arch and Low Profile Arch shapes.....	81
Figure 4.6. The comparison of thrust force between manual and CANDE analysis	82
Figure 4.7. The comparison of Percentage thrust force between manual and CANDE program.....	83
Figure 4.8. The comparison of displacements in x-direction of four types of culverts by CANDE program	84

Figure 4.9. The comparison of displacements in y-direction of four types of culverts by CANDE program.....	85
Figure 4.10. The comparison of percentage displacements in x-direction using CANDE program.....	86
Figure 4.11. The comparison of percentage displacements in y-direction using CANDE program.....	87
Figure 4.12. Results of End area value of four culvert shapes using CANDE program.....	88
Figure 4.13. The comparison of percentage of end area value.....	89

Acknowledgements

I thank almighty God for giving me the courage and the determination, as well as guidance in conducting this research study, despite all difficulties.

I would like to express my gratitude to my advisor **Dr. Abusamra Awad Attaelmanan** for giving me the opportunity to obtain my Master of Science at Sudan University of Science and Technology in structural Engineering. He made me believe that I had so much strength and courage to persevere even when I felt lost. I also extend my heartfelt gratitude to **Eng. Emil Yousif Salama** for his helpful suggestions and comments throughout the course of this thesis. Sincere thanks goes to **Prof. Dr. Isam Mohammed Abdel-Magid** and his family for the endless help and kindness they provided.

Finally, I thank all those who assisted, encouraged and supported me during this research, be assured that the Lord will bless you all for the contributions you made.

Dedication

To my parents, thanks you for your unconditional support with my studies. I am honoured to have you as my parents. Thank you for giving me a chance to prove and improve myself through all my occupations. I love you. I would like to thank you for your endless love and support you have given me throughout my years at Sudan University of Science and Technology.

To my family, thank you for believing in me; for allowing me to further my studies. You showed me light in a tunnel where everything was dark. You were very tolerant and determined to see me through. Please do not ever doubt my dedication and love for you.

To my brothers and sisters, hoping that with this research I have proven to you that there is no mountain higher as long as God is on our side. You were such wonderful motivators even when the coping seemed tough for me.

CHAPTER 1

Introduction

1.1. General Statement

Underground conduits have served to improve people's standard of living since the dawn of civilization. Remnants of such structures from ancient civilizations have been found in Europe, Asia, and even the western hemisphere, where some of the ancient inhabitants of South and Central America had water and sewer systems.

These early engineering structures are often referred to as examples of the art of engineering. Nevertheless, whether art or science, engineers and scientists still stand amazed at these early water and sewer projects. They seem to bridge the gap between ancient and modern engineering practice. The gap referred to here is that period known as the "dark ages" in which little or no subsurface construction was practiced a time when most of the ancient "art" was lost.^[1]

Therefore, engineers and planners realize that the subsurface infrastructure is an absolute necessity to the modern community. It is true that "build down" must be before "build up". The underground water systems serve as arteries to the cities and the sewer systems serve as veins to carry off the waste. The water system is the lifeblood of the city, providing culinary, irrigation, and fire protection needs. The most peoples on the street takes these systems for granted, being somewhat unaware of their existence unless they fail.^[1]

Years of dependable service and a multitude of wide ranging installations have led the corrugated steel industry to play a major role in modern engineering technology for drainage systems. Today, Flexible steel underground conduits serve in diverse applications such as culverts,

storm sewers, sub drains, spillways, underpasses, conveyor conduits, service tunnels, detention chambers and recharge systems; for highways, railways, airports, municipalities, recreation areas, industrial parks, flood and conservation projects, water pollution abatement. In addition, many other programs such as gas lines, telephone and electrical conduits, oil lines, coal slurry lines, and heat distribution lines. It is now possible to use engineering science to design these underground conduits with a degree of precision comparable with that obtained in design buildings and bridges.

Corrugated metal buried conduits have been used as drainage structures for many years in the world so structural plate corrugated metal culverts have been used in engineering with the first application in 1931. Since that time, the popularity of these structures has increased dramatically. The reasons for this development are lightweight, lower material cost, relatively easy handling and installation procedures. These structures other than the very smallest culverts constructed by bolting together curved and corrugated metal plates. The most popular type of corrugated metal culverts has been the corrugated steel pipes and arches culvert. The pipe culverts do not require concrete footings and are advantageous over some other corrugated metal culverts where headroom is hydraulic capacity is demand.

1.2. Research Problem

In the last years in Sudan, there have been many investigations dealing with analysis and design of culverts. Most of these reported studies are relating to the concrete culverts under various backfill and normal live-load conditions. However, no investigations have been focus on the corrugated metal maximum load carrying capacity and the failure mechanism of these soil-structure systems. This is because the low

knowledge on the strength of a culvert depends on properties of backfill material, plate and soil structure interaction and there is no manufacture for this type of product in Sudan.

Four shapes of corrugated structural plate culvert structure were analysed and designed as a Round Pipe, Horizontal Ellipse, Arch and Low Profile Arch, had a nominal spans or diameters of 4 m. The embankment fill reached a height of approximately 0.6 m over the crown of the culvers. Numerical investigation of the culvers was accounting for by measuring the pressure distribution around the culvers as well as the displacements of the culvers during Soil compaction and construction increments.

Digital computers, combined with finite element techniques and sophisticated soil models, have given the engineering profession design tools, which have produced, and will undoubtedly continue to produce, even more precise designs. The study of the culvers also included comparing manual analysis and design with numerical predictions given by a finite element computer program. One of the most popular programs for culverts analysis is CANDE-2013, which stands for **C**ulvert **A**nalysis and **D**Esign. CANDE, based on the finite element method, is a powerful tool for the analysis and design of culverts. It is important to check the finite element predictions against manual analysis and design. If CANDE proves effective, it can used to design future large span or diameter corrugated metal culverts in Sudan.

1.3. Objectives

The objectives of this study are summarized as follows:

- To compare pressure distribution around different shapes of buried corrugated steel culverts.
- To compare the obtained ultimate thrust force using AASHTO analysis and design guidelines and CANDE Finite Element Method predictions.
- To evaluate displacements of the culverts under dead and live loads.
- To identify more effective geometrical shape of the culverts due to structural design.
- To perform the finite element analysis of the corrugated steel plate culverts by using CANDE.
- To understanding, corrugated steel culverts design.

1.4. Hypothesis

- Manual and CANDE computer program analysis and design results should be the same for the four shapes studied.
- The four shapes studied are assumed to have the same displacements.

1.5. Methodology

Methodology of research work undertaken focused on the following vital research methods and areas:

- Data of the research for the four culvert shapes are assumed, and the methods of analysis and design for the structures were selected for comparison purposes.

- Results of force and displacements from AASHTO-LRFD of manual analysis and design to be compared with corresponding values from a model built with a finite element-based on computer program CANDE.
- Design of different shapes and compare the obtained results with the finite element model.

1.6. Outline of Thesis

Chapter 1 is the introduction chapter for the thesis and it were illustrated the research problem, objectives, hypothesis, methodology and outline of Thesis. **Chapter 2** provides a review of relevant literature on the Corrugated Sheets of corrugated steel culverts and Corrugated Steel Culvert product details and shapes. Literature review consists of previous researches and using the finite element program CANDE to simulate, analysis and design of corrugated metal culverts. **Chapter 3** is a project methodology overview describing the specifications of the culverts used in this study, soil types and soil properties at the study of the steel-soil structure system. The discussion of the culverts specifications includes size, shape, and corrugation as well as wall properties. In addition, describes the method used to analyse and design the culverts with the manual analysis and design and finite element computer program CANDE. In this chapter, CANDE discussed in detail, including a solution method and formulation, design criteria, and modelling techniques of the live load and construction increments model used. **Chapter 4** provides the results of the manual analysis and design in comparison with the numerical data from CANDE results. **Chapter 5** presents the summary and conclusions of this thesis. Conclusions of the performance of the culverts, based on manual analysis and design and the performance of CANDE discussed.

CHAPTER 2

Literature Review

2.1. Introduction

A corrugated metal culvert is often considered a flexible pipe standing by itself is often so flexible that in order to maintain its cross-sectional shape, it has to brace by ties and struts. The pipe derives its soil-load carrying capacity from its flexibility. The pipe on its own is unable to sustain much loading, but when combined with radial support from good quality backfill the load bearing capacity of the pipe and backfill, working together as a system, increased substantially. The gravity load of soil placed on a pipe causes the metallic shell to deform laterally and press against the backfill, thereby generating lateral pressures. The backfill soil around the pipe performs two roles in this situation. In one role, it is responsible for the load that the shell of the pipe called upon to sustain; in the other, it provides the necessary support to the shell to enable it to sustain its own weight.^[1, 2]

The failure of a corrugated metal pipe is often due to one of the following three factors separately or combined; yielding of the wall, buckling of the wall, or failure of the seams. Local yielding may develop in the conduit wall because of the initially unsupported condition of the pipe and the no uniform loading imposed by the placement of the backfill soil layers during construction. Leonards and Juang stated that such local yielding is not necessarily detrimental, if the pipe shape is not too asymmetrical and the soil backfill has good support characteristics. They also stated that in the absence of buckling, yielding in the pipe walls could result in a favourable redistribution of soil pressures, thereby permitting the pipe to support the overburden loads more efficiently.

Thus, buckling of buried metal pipes has been shown to be an important failure mode. Elastic buckling is an unlikely mode of failure if the backfill is well compacted. It has shown by Duncan, with good backfill, the buckling load was greater than the seam strength, even for flexible pipes. Thus for structures backfilled with quality soil it appears to be sufficient to design against seam compression and wall crushing without separate consideration of buckling.^[3] The longitudinal seams, unlike the circumferential seams, of corrugated metal pipes have to transmit mainly thrusts from one plate segment to another. The compressive strength of the metal and the bolted seams must be sufficient to withstand the axial forces in the structure to keep it from having seam failure. If the structure can carry the imposed ring compression forces without seam compression failure, wall compression failure, or buckling, the structure will not collapse.

Soil arching is a factor in the pressure distribution on pipes. The soil pressure around the pipe influenced by the vertical settlement ratio between the pipe and the adjacent soil column. When a rigid pipe installed, the soil columns adjacent to the pipe are more compressive; therefore, they settle more than the soil column located directly above the pipe. Thus, a downward shear force develops on the sides of the soil column directly above the pipe. Therefore, the load on the pipe increased, becoming greater than the weight of the soil column above the pipe. This called negative soil arching. Positive soil arching occurs in the opposite manner. When a flexible pipe installed, the soil column above the pipe is more compressive. The shear force reversed and the load on the pipe is now less than the weight of the soil column above the pipe.^[2]

Corrugated steel pipe is available with a wide variety of protective coatings that have proven to meet the requirements of demanding environments. No matter the location or application, corrugated steel pipe

has a coating to meet the needs of the situation. This provides the engineer or contractor an end result of optimum service life for the structure at the lowest cost. Service life exceeding 100 years can be obtained using the proper coating, specific to location and application.

Steel contains the highest percentage of recycled material among products used for drainage structures. The recycled content of corrugated steel pipe, up to 96%, is rated as significant. Accordingly, specifying CSP can greatly assist in earning Leadership in Energy and Environmental Design (LEED®). Additionally, steel is certified to meet specifications even with recycled material. While other drainage products may claim to be eco-friendly, care should be taken to ensure that these products conform to the AASHTO drainage pipe design and product specifications. Corrugated steel pipe, while having a high recycled content, conforms to and is routinely certified for compliance to AASHTO specifications.^[4]



Figure 2.1. Structural plate pipe for an irrigation ditch crossing.^[4]

2.2. Corrugated Sheets

Corrugated sheets been used in a wide range of construction since about 1784 as shown in **Figure 2.2**. This is one of the oldest types of cold-formed steel products. At present, many manufacturers are producing numerous types of corrugated sheets with different coatings. Several standard corrugated steel sheets are generally available for building construction and other usage.

In general, certain simplified formulas for computing the sectional properties of standard corrugated steel sheets can used in design. The Institute issued following an investigation conducted by the American Iron and Steel Institute (AISI) during 1955-1957, a publication entitled “Sectional Properties of Corrugated Steel Sheets” in 1964 to provide the necessary design information for corrugated sheets.

Corrugated steel sheets frequently used for roofing and siding in buildings because the sheets are strong, lightweight, and easy to erect. In many cases, they used as shear diaphragms to replace conventional bracing and to stabilize entire structures or individual members such as columns, beams and exterior curtain wall panels. The application of unusually large corrugated sections in frameless stressed skin construction. In addition, corrugated steel pipe of galvanized sheets long been used in drainage structures. Other corrugated steel products been used for retaining walls, guardrails, aerial conduits, and other purposes.^[5]

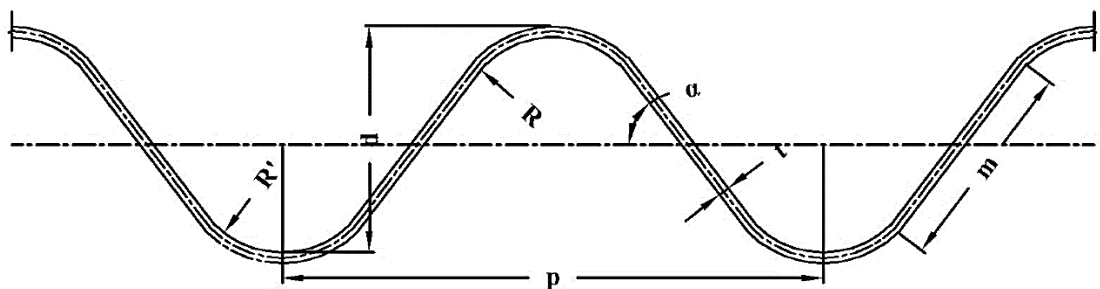


Figure 2.2. Section of arc-and tangent-type corrugated sheets.^[5]

During recent years, corrugated sheets been used in flooring systems for buildings and bridge construction. These products also been used as web elements for built-up girders in order to increase web stiffness instead of using a relatively thicker plate or a thin web with stiffeners.

In 1934, Blodgett developed a method to compute the sectional properties of arc-and tangent-type corrugated sheets. Wolford has simplified the computation of the moment of inertia and the section modulus for standard corrugated sheets. In the computation, design curves and tables can be used to determine factors C_5 and C_6 in Equations 2.1 and 2.2:

$$I = C_5bt^3 + C_6bd^2t \quad 2.1$$

$$S = \frac{2I}{d+t} \quad 2.2$$

Where I = moment of inertia, in.⁴

S = section modulus, in.³

b = width of sheet, in.

d = depth of corrugation, in.

t = thickness of sheet, in.

C_5, C_6 = factors depending on shape of arc-and-tangent-type corrugation.

Using Wolford's charts, as shown in **Figure 2.3 – 2.7**, the values of the moment of inertia, section modulus, area, radius of gyration, and length of tangent can computed by the following procedure:

1. Compute the mid thickness radius R' .

$$R' = R + \frac{1}{2}t \quad 2.3$$

2. Compute values of q and K ,

$$q = \frac{R'}{d} \quad 2.4$$

$$K = \frac{p}{d} \quad \mathbf{2.5}$$

Where p is the pitch.

3. From **Figure 2.3**, determine the angle α for the computed values of q and K.
4. From **Figure 2.4** and **2.5**, determine C_5 and C_6 by using K and angle α .
5. From **Figure 2.6** and **2.7**, determine λ and the m/d ratio.
6. Compute S and I by using **2.1** and **2.2**.
7. Compute

$$A = \lambda bt \quad \mathbf{2.6}$$

8. The radius of gyration is

$$r = \sqrt{\frac{I}{A}} \quad \mathbf{2.7}$$

9. The length of the tangent is $d \times m/d$.

Based on the method outlined above, the sectional properties of several types of corrugated sheets have developed. The accuracy of Equations **2.1** and **2.2** has verified by beam tests conducted under the sponsorship of the AISI.

The inelastic flexural stability of corrugations studied by Cary. In determining the load-carrying capacity of corrugated sheets, the nominal flexural strength can computed in a conventional manner as follows:

$$M_n = SF_y \quad \mathbf{2.8}$$

Where S = section modulus.

F_y = yield stress of steel.

The available flexural strength can be computed by using $\Omega_b = 1.67$ for ASD and $\phi_b = 0.95$ for LRFD. ^[5]

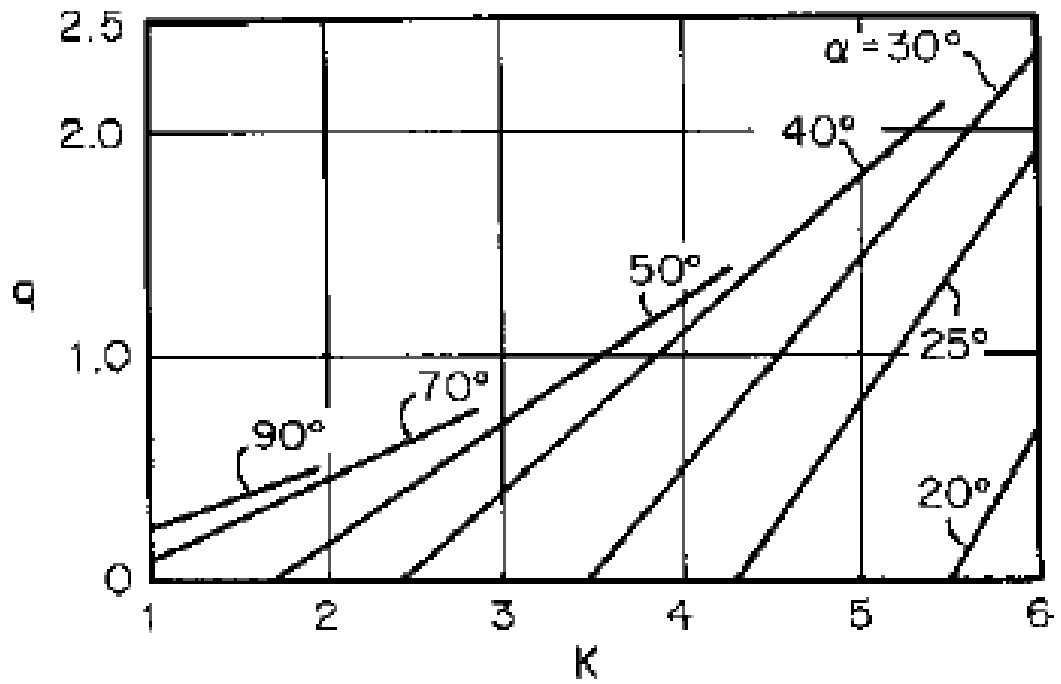


Figure 2.3. Radius-to-depth ratio versus pitch-to-depth ratio at various web angles.^[5]

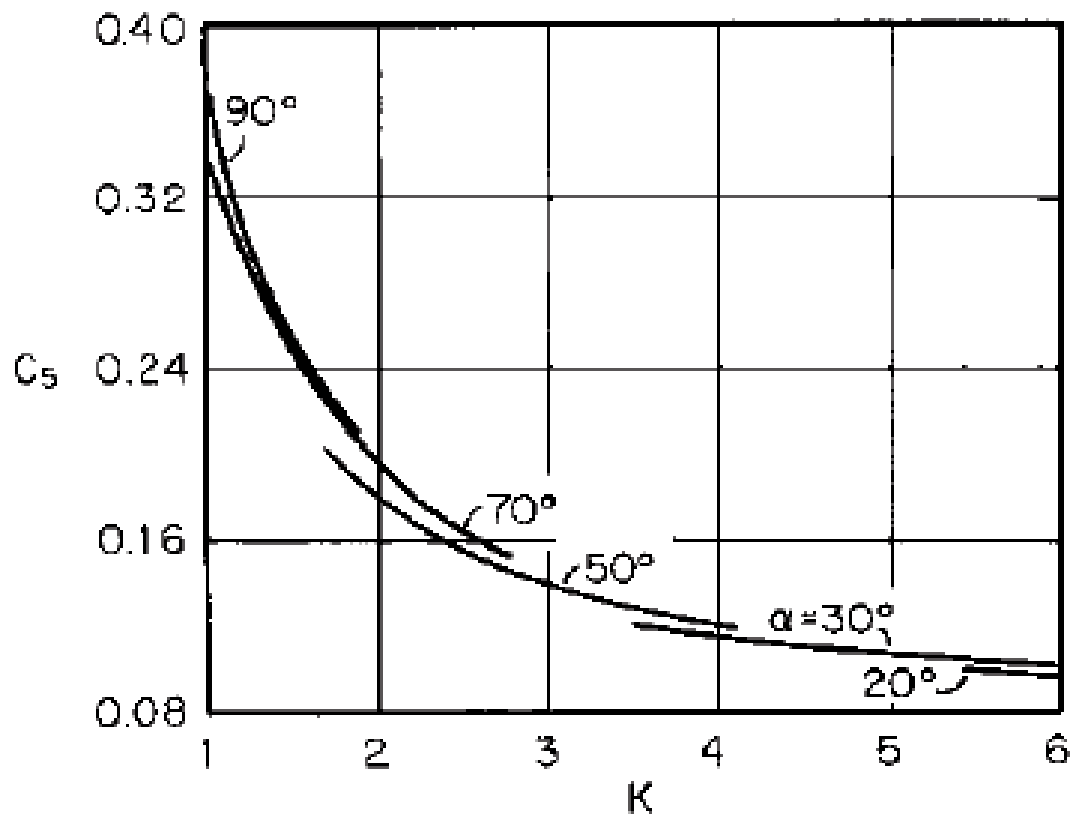


Figure 2.4. Factor C_5 versus pitch-to-depth ratio at various web angles.^[5]

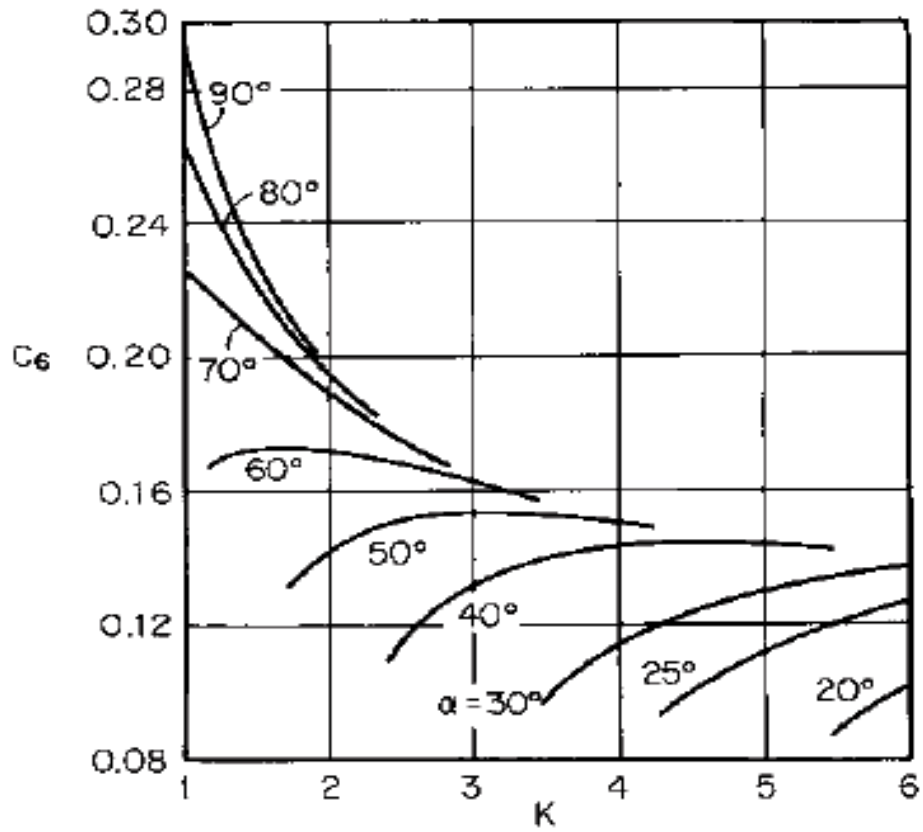


Figure 2.5. Factor C_6 versus pitch-to-depth ratio at various web angles.^[5]

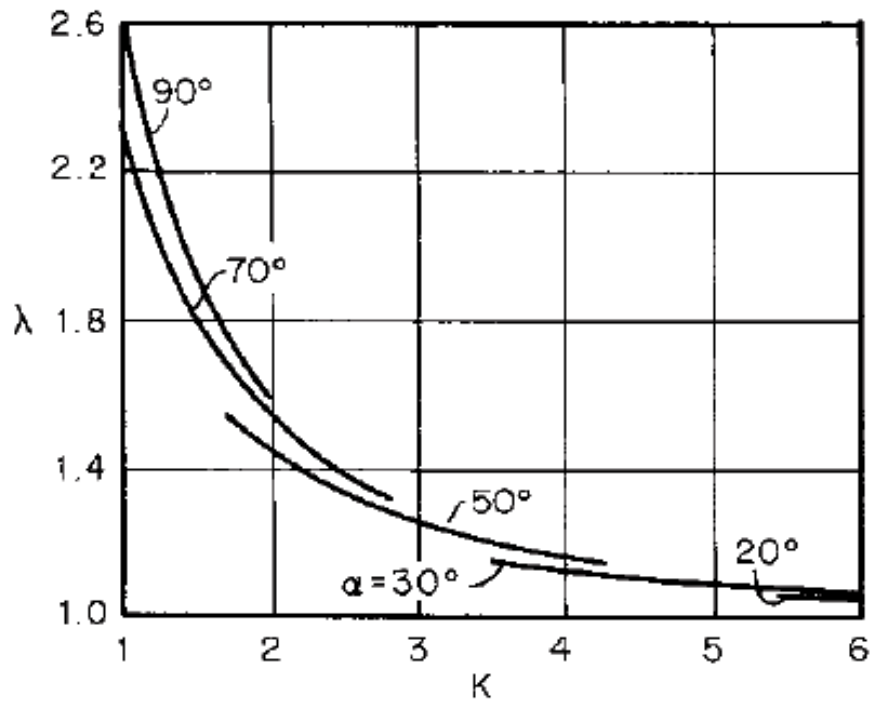


Figure 2.6. Factor λ versus pitch-to-depth ratio at various web angles.^[5]

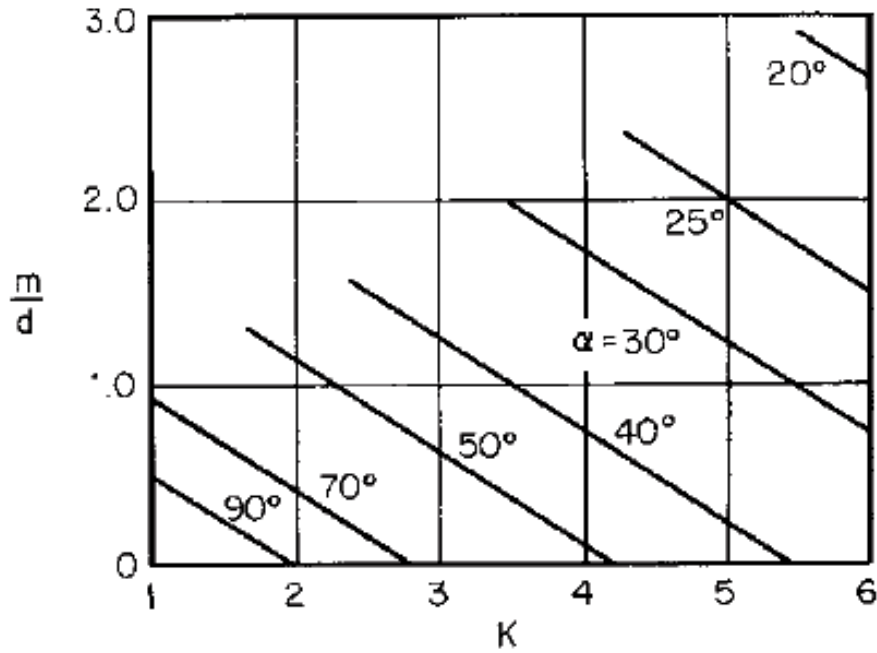


Figure 2.7. Tangent-to-depth ratio versus pitch-to-depth ratio at various web angles.^[5]

2.3. Corrugated Steel Culvert

Corrugated steel pipe was first developed and used for culverts in 1896. As experience gained in the use of this thin-wall, lightweight, shop-fabricated pipe, and the diameters gradually increased to 2400 mm and larger. Fill heights became greater, even exceeding 30 m. Diameters up to 8 m and arch spans up to 18 m have being install successfully.

Various design challenges and the application of corrugated steel pipe and other products to the solution of those challenges, have been describe above are not all-inclusive or complete solutions. They are intended only to show the adaptability and wide acceptance of one material - steel - for aiding in the solution of some of the problems facing the design engineer.


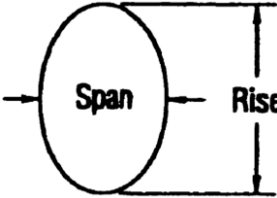
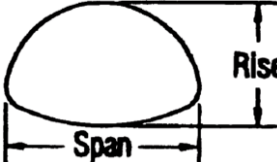
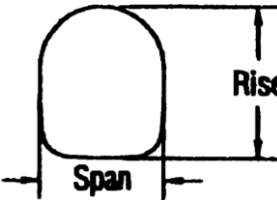
So vast are the annual expenditures for construction that the skills of resourceful qualified engineers are required to analyse, select, design and apply the available materials and products that most economically

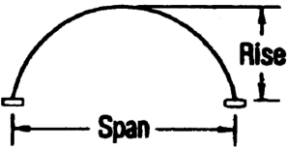
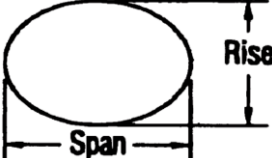
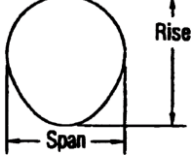
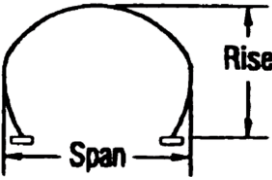
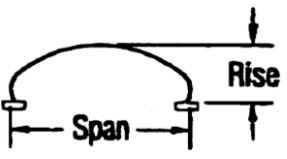
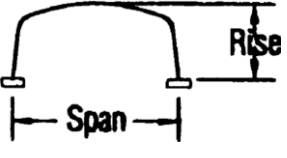
serve their purpose. The need for carefully considering the economics of providing and maintaining these facilities is obvious.^[6]

2.3.1. Shapes

The designer has a wide choice of standard cross-sectional shapes of corrugated steel and structural plate conduits as shown in **Table 2.1**. Size and service use may control the shape selected, with strength and economy as additional factors.^[6]

Table 2.1. Shapes and uses of corrugated conduits.^[6]

Shape	Range of Sizes	Common Uses
Round 	150 mm to 15.8 m	Culverts, sub drains, sewers, service tunnels, etc. For medium and high fills.
Vertical ellipse 5% nominal 	2440 mm to 6400 mm nominal; before elongation	Culverts, sewers, service tunnels, recovery tunnels. For appearance and where backfill compaction is only moderate.
Pipe-arch 	Span × Rise 450 × 340 mm to 7620 × 4240 mm	Where headroom is limited. Has hydraulic advantages at low flows.
Underpass 	Span × Rise 1755 × 2005 mm to 1805 × 2490 mm	For pedestrians, livestock or vehicles.

Arch		Span × Rise 1520 × 810 mm to 20 × 10 m	For low clearance large waterway openings and aesthetics.
Horizontal Ellipse		Span 1.6 m to 11.8 m	Culverts, grade separations, storm sewers, tunnels.
Pear		Span 7.2 m to 8.6 m	Grade separations, culverts, storm sewers, tunnels.
High Profile Arch		Span 6.3 m to 23.0 m	Culverts, grade separations, storm sewers and tunnels. Ammunition magazines, earth covered storage.
Low Profile Arch		Span 6.1 m to 15.0 m	Low, wide waterway enclosures, culverts, storm sewers.
Box Culverts		Span 3.2 m to 12.3 m	Low, wide waterway enclosures, culverts, storm sewers.
Specials		Various	Special fabrication for lining old structures or other special purposes.

i. Corrugated Steel Pipes

The principal profiles for corrugated steel pipe shown in **Figure 2.8**. Corrugations commonly used for pipes are described by pitch, depth and inside forming radius. Pitch is measuring at right angles to the corrugations from crest to crest. A corrugation is name as “pitch by depth”.

For riveted pipe with circumferential seams, the corrugations are 68 by 13 mm. For lock seam pipe, the seams and corrugations run spirally around the pipe. For small diameters of sub drainage pipe the corrugation is nominally 38 x 6.5 mm. Larger sizes use 68 x 13 mm, 76 x 25 mm and 125 x 25 mm corrugations.

Another corrugation used for lock seam pipe is the rib profile. The pipe wall is spirally formed. This unique profile configuration was developed for providing flow characteristics equal to those piping systems normally considered smooth wall. One profile configuration is available, with nominal dimensions 19 x 19 x 190 mm (rib pitch x rib depth x rib spacing), covering diameters from 450 through 2700 mm.^[6]

ii. Structural Plate and Deep Corrugated Structural Plate Products

1. Structural Plate

Structural plate pipes are structures where corrugated steel sections are bolted together to form the shape of the structure. The sections commonly refer to as plates. The 152 x 51 mm corrugation is the standard in the structural plate industry. The corrugation as shown in **Figure 2.8**.

The corrugations are at right angles to the length of the plate. The length of a plate is measured in a direction parallel to the length of the structure. The width of a plate is therefore measured in a direction perpendicular to the length of the structure, around the periphery of the structure.

Standard plates are fabricated in three lengths and several widths, as shown in **Figures 2.9** and **2.10**. The plate width designation, N, is used to describe the various plate widths available. N is the distance between two circumferential bolt holes, or one circumferential bolt hole space (circumferential refers to the direction around the periphery of the structure, at right angles to the length of the structure). The bolt hole space, N, is 243.84 mm (244 mm nominal).^[6]

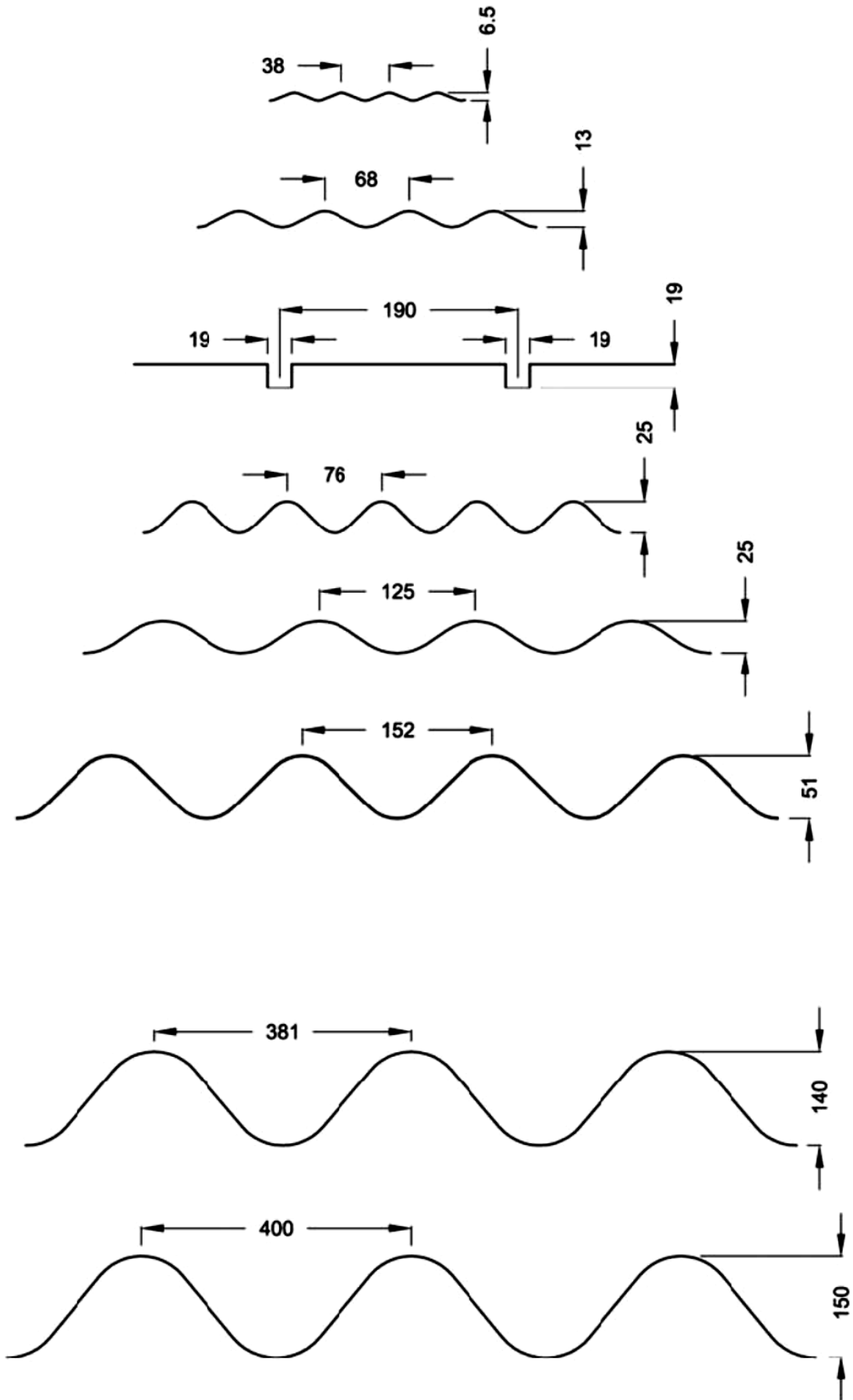


Figure 2.8. Commonly used corrugations.^[6]

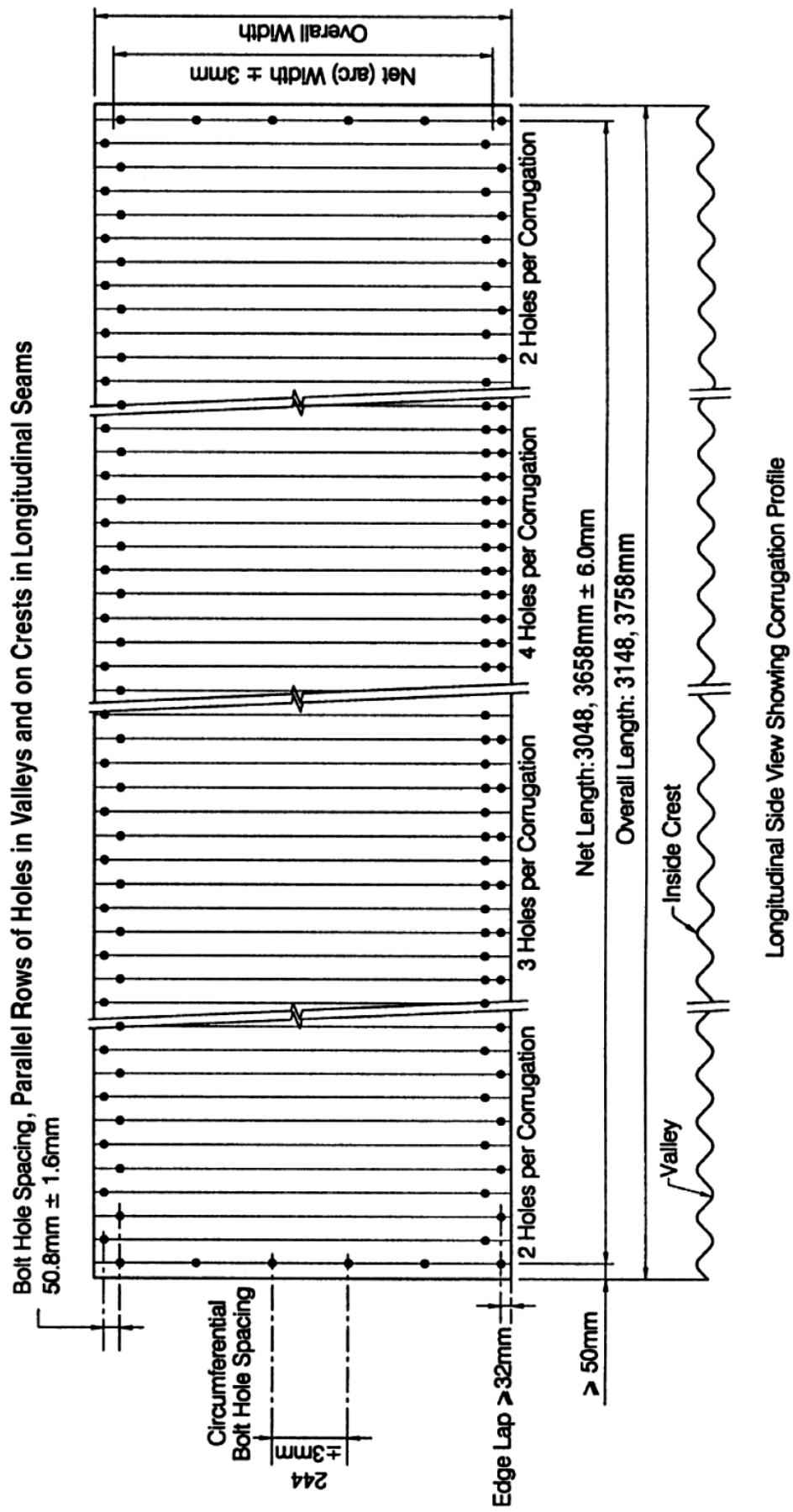


Figure 2.9. Configuration of structural plate sheets.^[6]

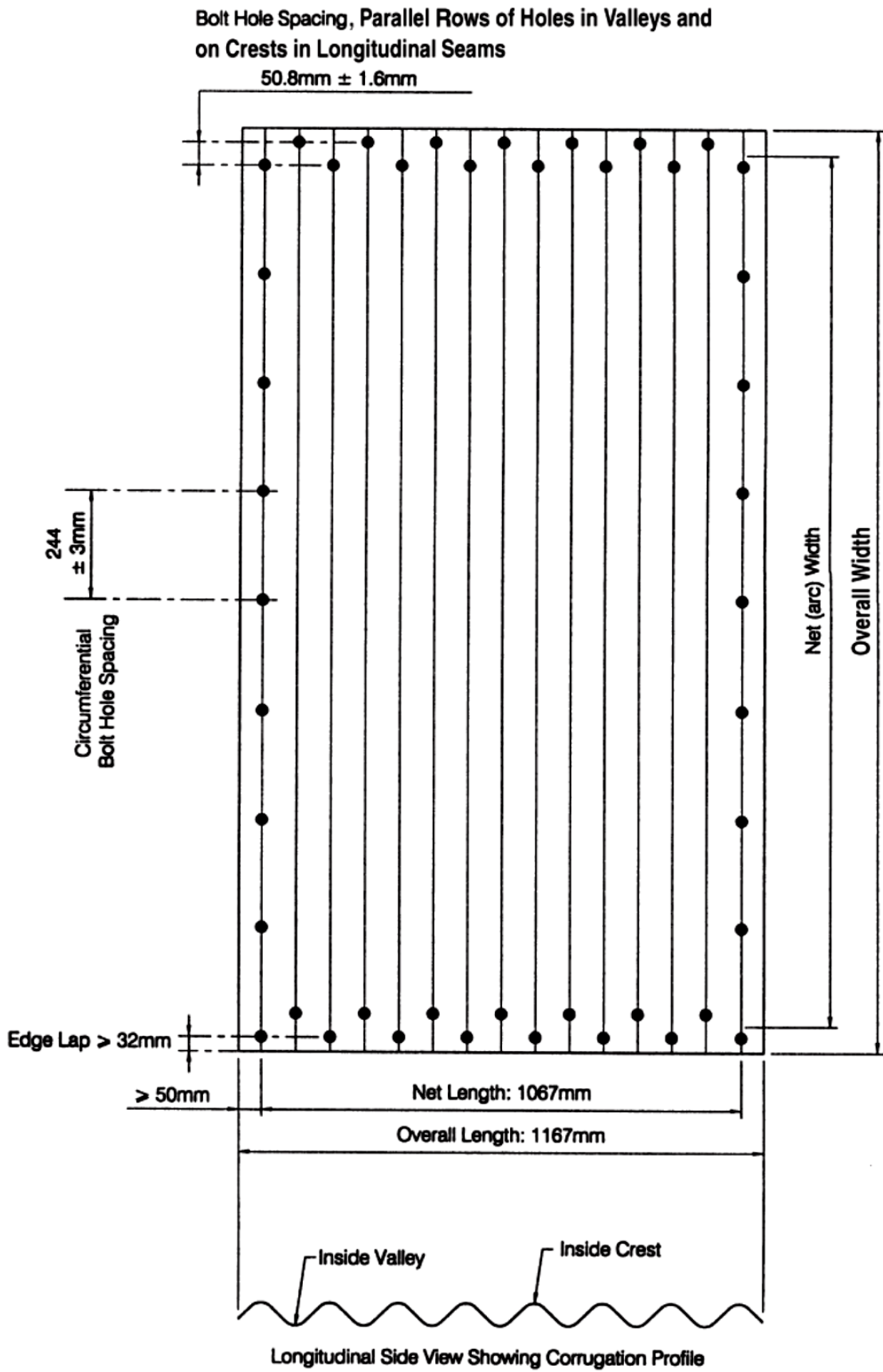


Figure 2.10. Alternate structural plate configuration.^[6]

Galvanized 19 mm diameter bolts of special heat-treated steel meeting ASTM Specification A 449 or ASTM Specification F568 Class 8.8, are used to assemble structural plate sections. Galvanized nuts meet the requirements of ASTM A 563 Grade 12. The galvanizing on bolts and nuts must meet ASTM Specification A 153, CSA-G164 Class 5 or ASTM B 695 Class 50 Type II. See **Figure 2.11** for dimensions of bolts and nuts. Lengths include 32, 38, 44, 51 and 76 mm. The containers and bolts are colour coded for ease in identification. These are designed for fitting either the crest or valley of the corrugations, and to give maximum bearing area and tight seams without the use of washers. Power wrenches are generally used for bolt tightening, but simple hand wrenches are satisfactory for small structures.

Anchor bolts are available for anchoring the sides of structural plate arches into footings, and the ends of structural plate conduits into concrete end treatments as shown in **Figures 2.12** and **2.13**. Material for these special 19 mm bolts must conform to ASTM Specification A 307, and nuts to ASTM A 563 Grade C. Galvanizing of anchor bolts and nuts must conform to ASTM A 153.^[6]

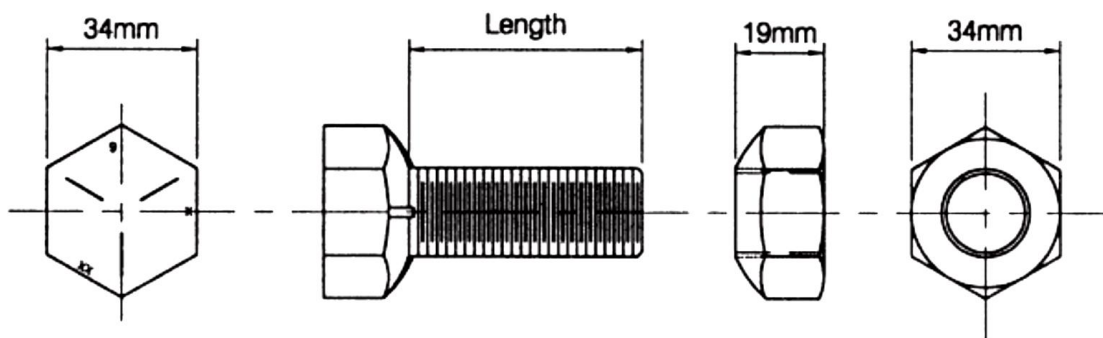


Figure 2.11. Dimensions of bolts and nuts for structural plate.^[6]

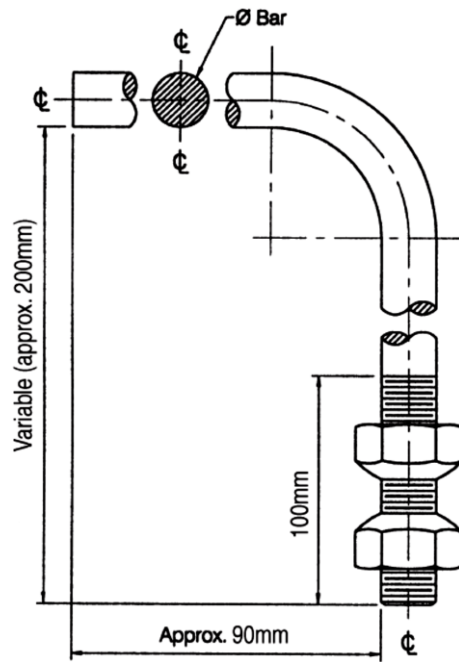


Figure 2.12. Hook bolts and nuts for embedment in headwalls.^[6]

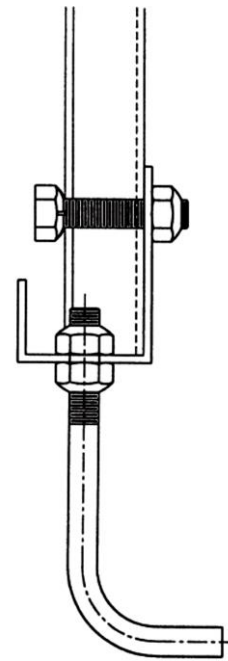


Figure 2.13. Hook bolt and base channel.^[6]

For arch seats, galvanized unbalanced channels are available for anchoring the arch to concrete footings. The unbalanced channel is anchored to the footing either by anchor bolts or by integral lugs that are bent and twisted as shown in **Figure 2.14.^[6]**

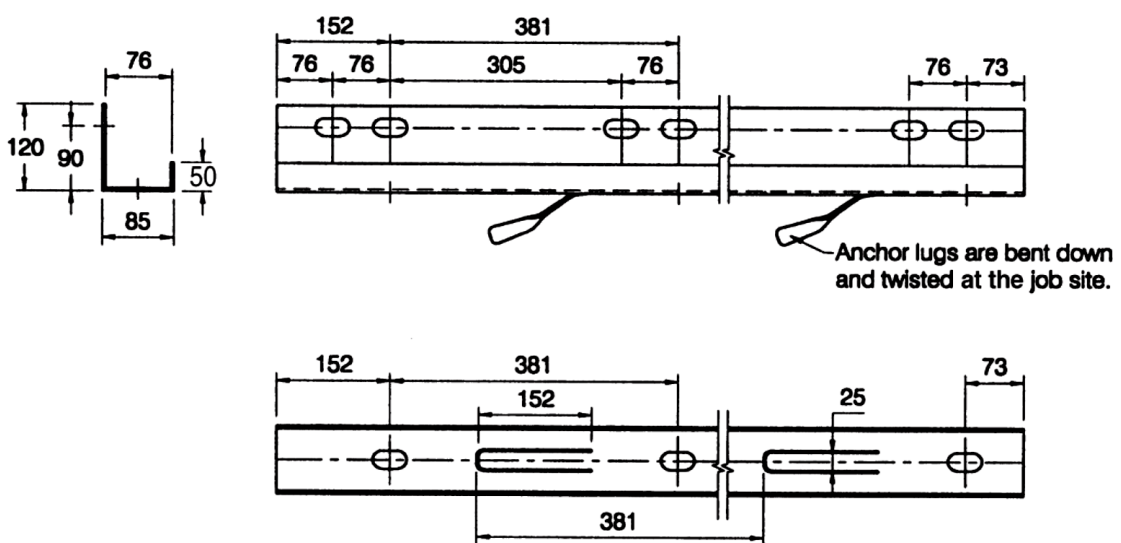


Figure 2.14. General dimensions of unbalanced channels for structural plate arches.^[6]

2. Deep Corrugated Structural Plate (DCSP)

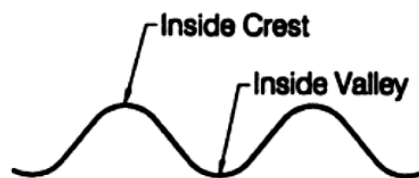
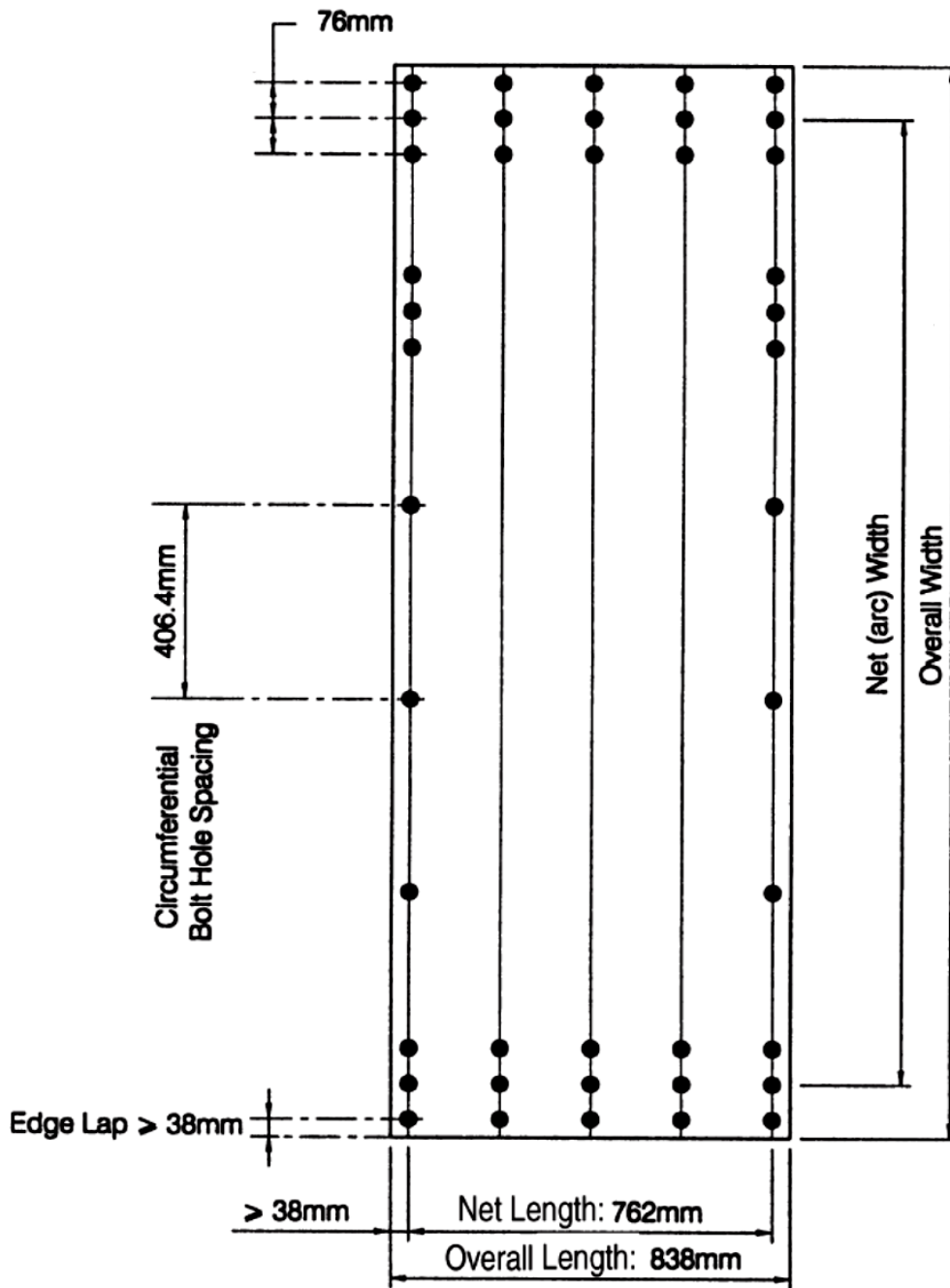
Deep corrugated structural plate is also a bolted structure. It has either a 381 x 140 mm corrugation (DCSP Type I) or a 400 x 150 mm corrugation (DCSP Type II), which are shown in **Figure 2.8**.

Type I plates are fabricated in one length and several widths, as shown in **Figures 2.15** and **2.16**. The coverage length is 762 mm. The plate width designation, S, is used to describe the various plate widths available. S is the distance between circumferential bolt holes, or one circumferential bolt hole space (circumferential refers to the direction around the periphery of the structure, at right angles to the length of the structure). For instance, a 5 S plate has a net width of 5 circumferential bolt hole spaces as **Figure 2.15**. The bolt hole space, S, is 406.4 mm (406 mm nominal).

Type II plates are fabricated in one length and several widths, as shown in **Figure 2.17**. The coverage length (excluding the side lips) is 1200 mm. The plate width designation, H, is used to describe the various plate widths available. H is the distance between circumferential bolt holes, or one circumferential bolt hole space (circumferential refers to the direction around the periphery of the structure, at right angles to the length of the structure). For instance, a 9 H plate has a net width of 9 circumferential bolt hole spaces as in **Figure 2.17**. The bolt hole space, H, is 425 mm.

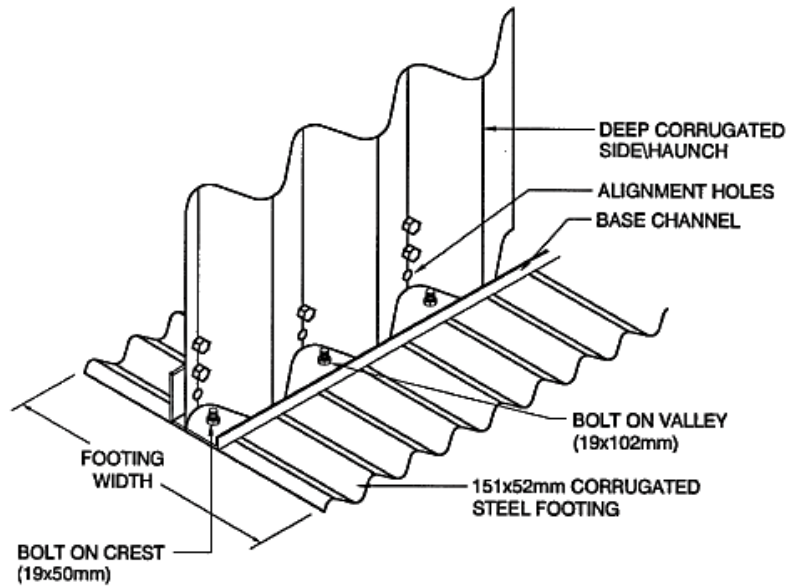
Plates are furnished curved to various radii and are identified with a permanent mark which shows information such as the plate geometry. This marking is provided to simplify field erection and to make identification of the structure details, in the future, as easy as possible.^[6]

Bolt Hole Spacing, Parallel Rows of Holes in Valleys and on Crests in Longitudinal Seams

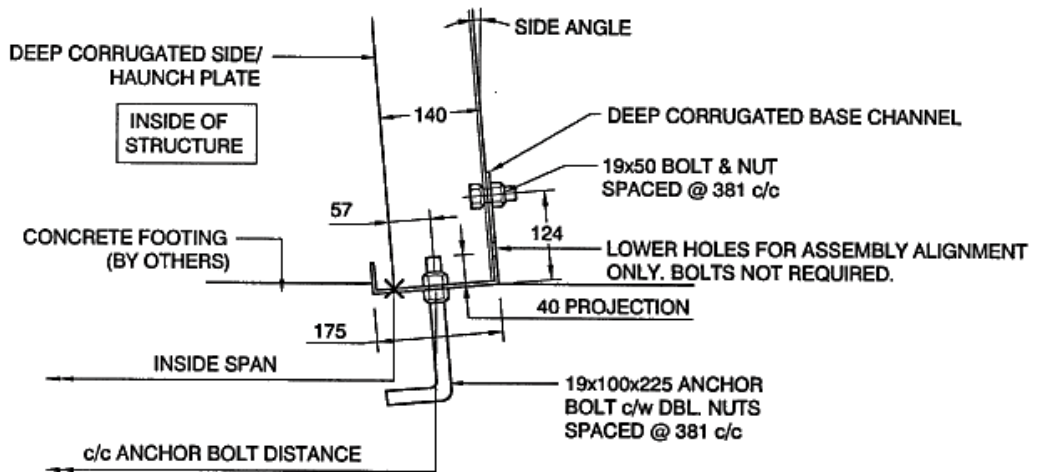


Longitudinal Side View Showing Corrugation Profile

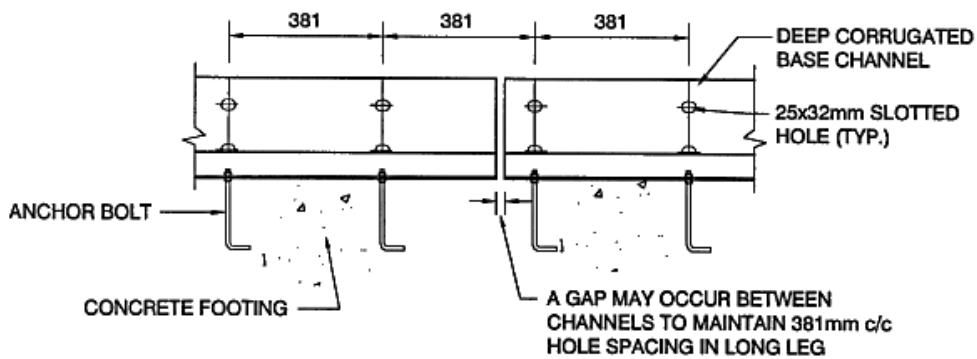
Figure 2.15. Deep Corrugated Structural Plate Type I plate configuration.^[6]



Detail - Typical Steel Footer



X WORK POINT IS TAKEN AT THE BASE OF STEEL ON THE INSIDE CREST



Details - Base Channel

Figure 2.16. Additional details for deep corrugated structural plate Type I.^[6]

Bolt Hole Spacing, Parallel Rows of Holes in Valleys and on Crests in Longitudinal Seams

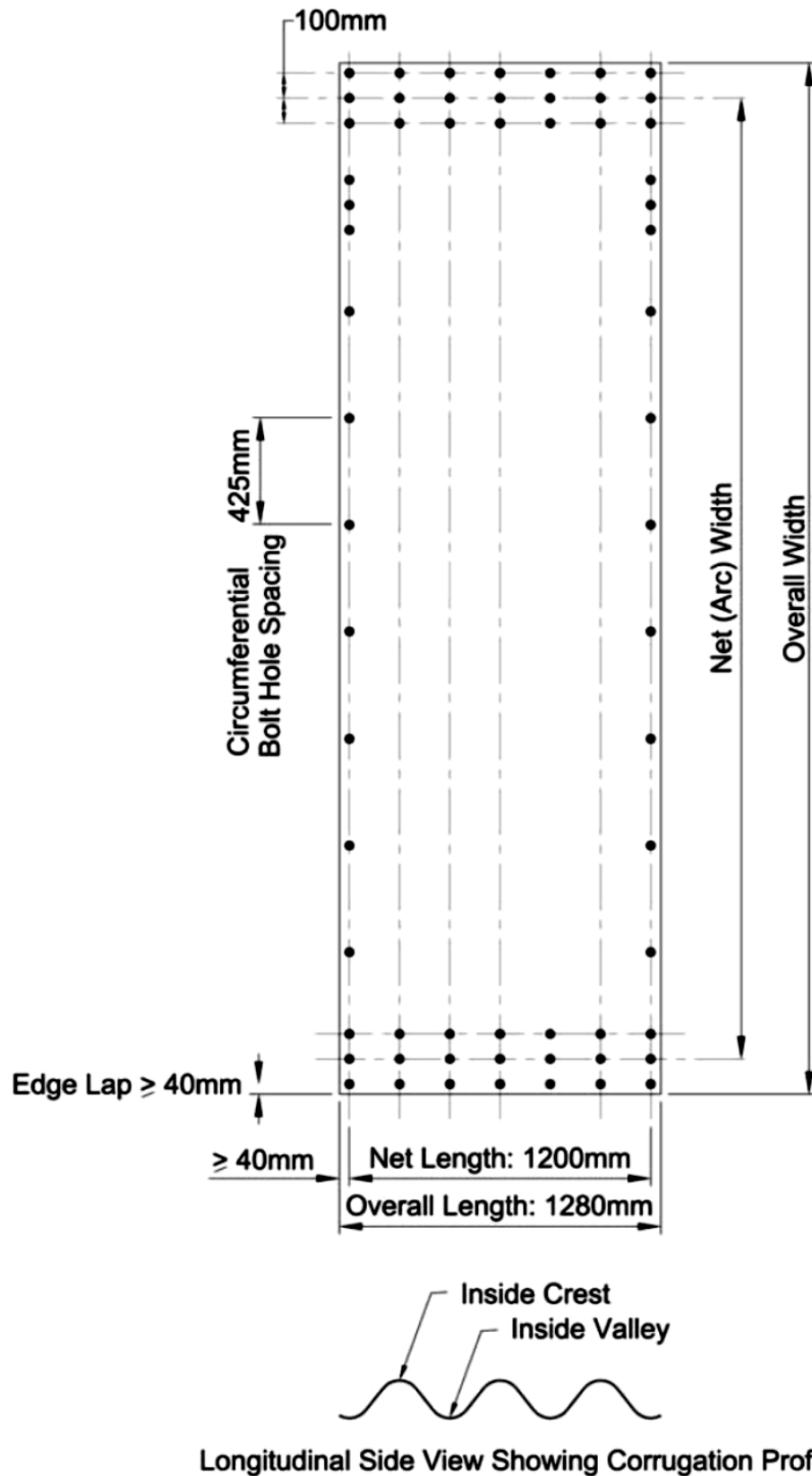


Figure 2.17. Deep Corrugated Structural Plate Type II plate configuration.^[6]

2.4. Salient Researches of Corrugated Metal Culverts

Engineers and contractors are an imaginative lot, seeking improved ways of designing and building their projects. Steel manufacturers and fabricators have cooperated, through their research and manufacturing staffs, to provide engineers and contractors with better materials, products and installation methods.

Manufacturers' sales staffs and associations are made up largely of experienced professional engineers, knowledgeable in the construction industries problems, who constitute a prime information source on applications, specifications and installation of their products.

Mechanical properties of steel are controlled in the mill, and the finished product is fabricated to exacting specifications. The strength and integrity of soil/steel structures is extremely predictable as the result of current research in laboratory and field installations.^[4]

2.4.1. Utah Test Program

Dr. R. K. Watkins and associates conducted extensive research at Utah State University during 1967 - 1970 under the sponsorship of the American Iron and Steel Institute. This was the first time that numerous full-size CSP installed in a backfill were loaded to their ultimate performance limit in a field laboratory. Approximately 130 pipes, 20 ft. long, in sizes from 24 in. to 60 in. diameter were loaded to their performance limit in low-grade soil backfills compacted from 70% to 99% standard AASHTO density. Riveted, spot welded and helical pipe fabrications were included in both 2-2/3x1/2 in. and 3x 1 in. corrugations. Confined compression tests made on six different soils to correlate results to commonly used backfill materials.

The pipes installed and loaded in 24 feet long, 15 feet wide and 18 feet high test cell constructed of 5/8 inch steel plate of elliptic cross-section as shown in **Figure 2.18**. Steel trusses pinned to the top of the cell walls supported hydraulic cylinders, which applied a uniform pressure up to 20,000 psf. on the upper surface of the soil. The backfill material was a silty sand installed in lifts and compacted with manually operated mechanical compactors. Compactive effort and moisture contents varied to obtain densities from 70% to 99% standard AASHTO.

After backfill, steel plates placed on top of the soil to improve the bearing of the hydraulic rams. Load applied in planned increments with the following readings taken: loading force, soil pressure on the pipe, vertical pipe displacements, and ring profile. Testing terminated when the hydraulic ram pressure could no longer increased. It is significant that, in this condition, the pipe could continue to deform in the test cell. Soil arching made the structure stable under applied loads much higher than those recorded in the test did.

Results of the test plotted for five degrees of standard AASHTO density for the backfill shown in **Figure 2.19**. Assuming the load applied by the hydraulic rams equals the pressure acting on the pipe, the ultimate steel stresses plotted on a buckling chart. It is immediately apparent that most of the steel stresses calculated by this criterion are fictitious because they greatly exceed the yield point. This explained by **Figure 2.20**, which illustrates how the applied load actually carried in part by the soil arch formed in the compacted backfill as load applied thereto and pipe and soil strains occur. Because the stresses on the ordinate in **Figure 2.19** calculated from the total load, with no reduction taken for the load carried by the soil in arching action, they designated as apparent stresses.

A prime objective of the Utah program was to establish a practical correlation between backfill density and pipe behaviour. The Utah

program provided, for the first time, ultimate performance data on full-scale soil-steel installations, utilizing a low-grade backfill soil and normal field methods and equipment. The Utah research confirmed what has observed in field installations for decades. The quality and density of backfill required to permit the pipe to carry high stress levels, to or near the yield point, is of ordinary magnitude comparable to current common practices for most highway embankments. The test results in **Figure 2.19** plotted on an outdated buckling stress graph where dashed lines show buckling curves that correlated to an unrealistically high level of soil compaction. The wide disparity between the $K = 0.44$ curve for 85% compaction and the actual performance results at 85% is readily apparent.

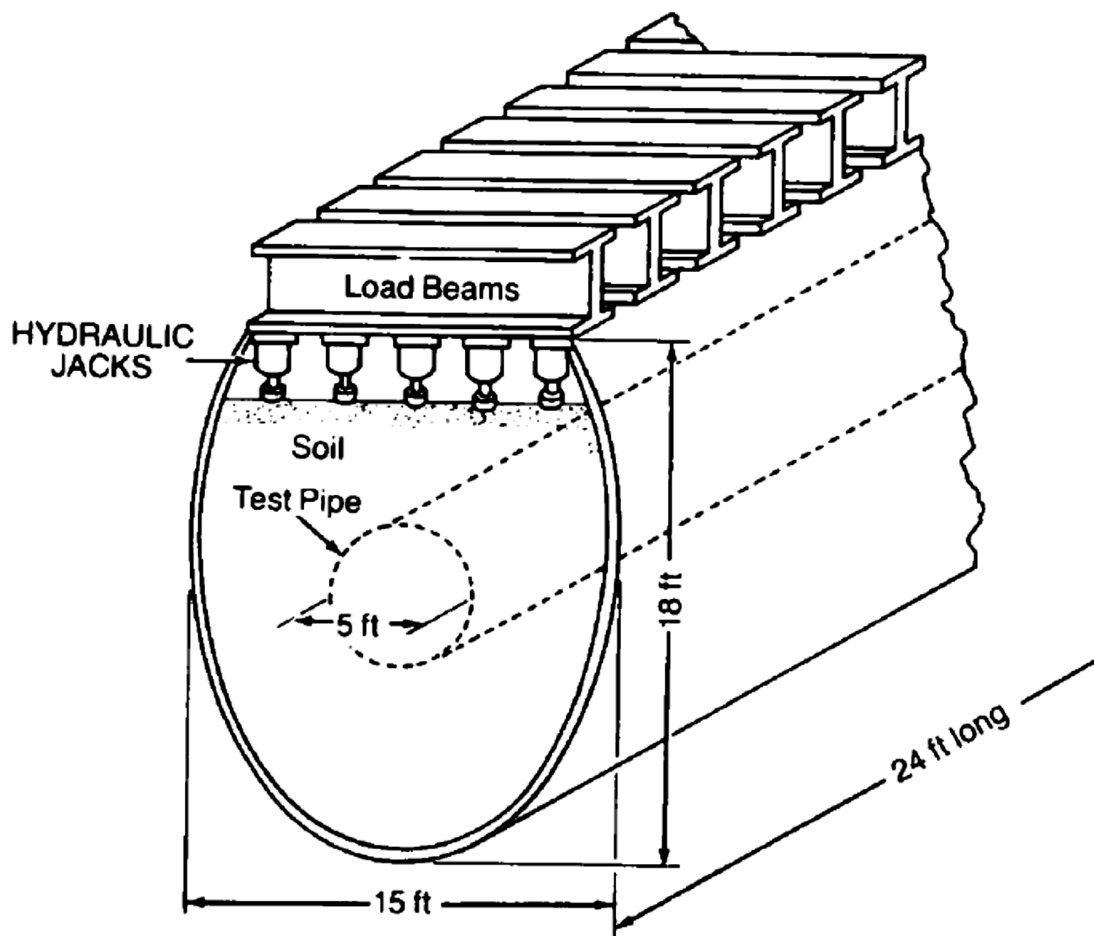


Figure 2.18. Sketch of applying load with hydraulic jacks.^[4]

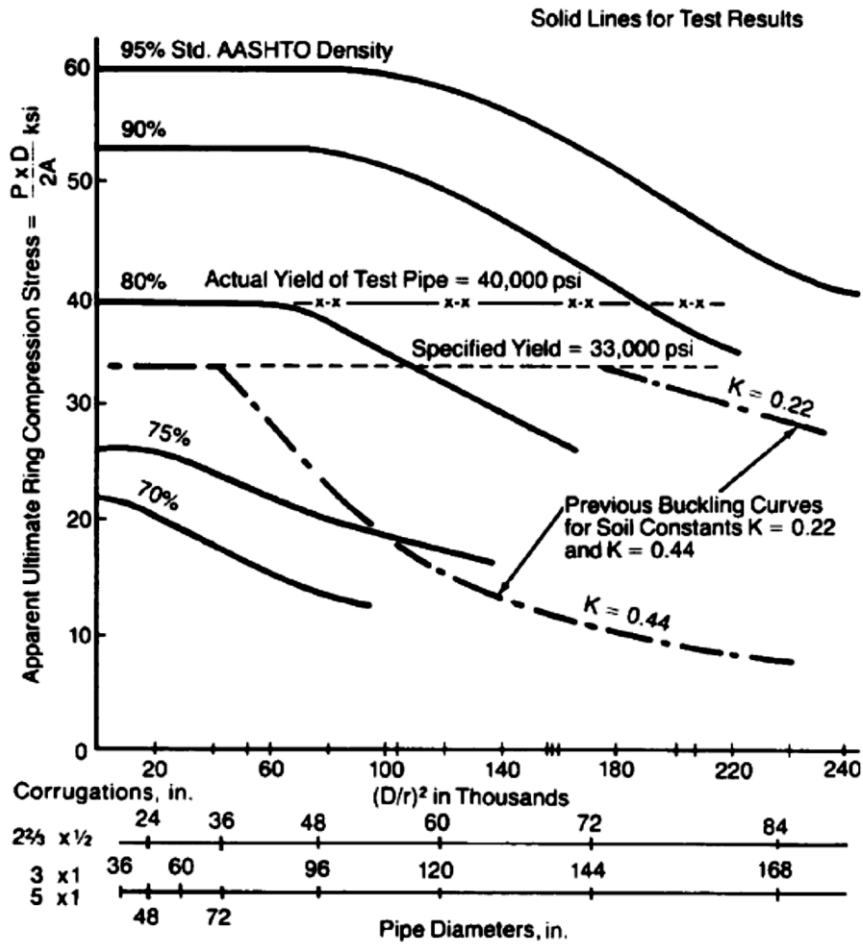


Figure 2.19. Results of Utah loading tests on corrugated steel pipe.^[4]

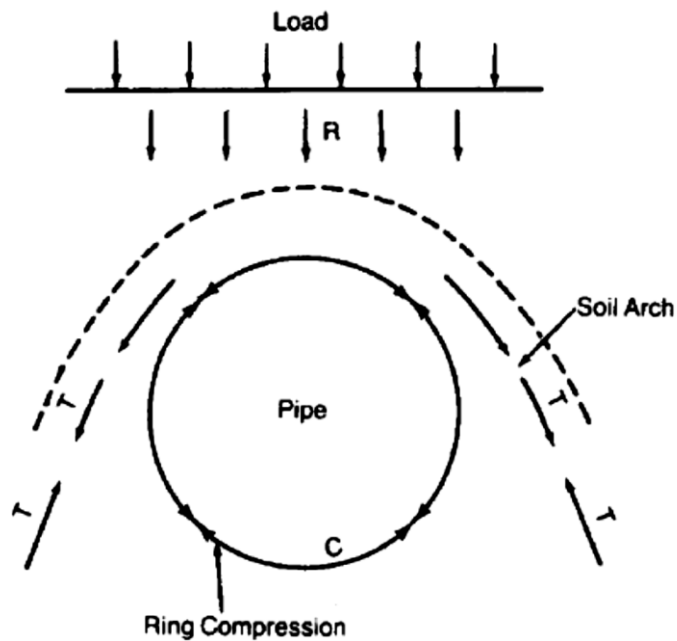


Figure 2.20. Diagram showing how load partly carried by a soil arch over the pipe.^[4]

This research established a zone of “critical density” between 70% and 80% standard AASHTO density. The critical density represents a level of backfill compaction that will allow the pipe to carry ring compression stress at or near the yield point. At a conservative value of 80% standard AASHTO density, there is enough soil support to preclude deflection collapse and the pipe carries stress near the yield point.

The test soil used in the Utah research considered a low-grade material for pipe backfill. Specifically, it a silty sand that bulked very easily and could be placed to a wide range of standard densities, something very necessary to a good test program. The tests confirmed that pipe backfill could designed, specified, and evaluated based on percent standard AASHTO density, regardless of soil type. The only exceptions are unstable soils, such as those which turn plastic with moisture, even though they have been well compacted to 85% or more standard AASHTO and confined in the fill. Such soils would of course, not be suitable for a high embankment base, much less for pipe backfill.

[4]

2.4.2. Caltrans Tests

A significant research study led by A. E. Bacher of Caltrans in 1975 provided important data on a full-scale installation under high fills. This project involved a 10 feet diameter structural plate pipe with a 0.109-inch wall, drastically under-designed to magnify the response and expected to fail. It was loaded with a fill of almost 200 feet, likely the record for this type of test. In addition to demonstrating the remarkable strength of the pipe, measurements of wall stresses and soil pressures contributed to the body of knowledge and gave confidence to design methods used by specifying agencies. [4]

2.5. Corrugated Metal Culverts by Finite Element Method

The finite element method (FEM), sometimes referred to as finite element analysis (FEA), is a computational technique used to obtain approximate solutions of boundary value problems in engineering. Simply stated, a boundary value problem is a mathematical problem in which one or more dependent variables must satisfy a differential equation everywhere within a known domain of independent variables and satisfy specific conditions on the boundary of the domain. Boundary value problems are also sometimes called field problems. The field is the domain of interest and most often represents a physical structure. The field variables are the dependent variables of interest governed by the differential equation. The boundary conditions are the specified values of the field variables (or related variables such as derivatives) on the boundaries of the field.^[8]

With the development of the finite element method, finite element analysis of engineering problems has become very prevalent. The finite element method has been used frequently to provide a representation of the complex soil-structure interaction surrounding corrugated metal culverts. This section represents a review of past studies involving finite element analyses on corrugated metal structures. The review includes studies validating the finite element predictions with actual field measurements.

In addition to the development of analysis and design method noted previously, there have been many additional studies made on the performance of corrugated steel pipe.

2.5.1. Finite Element Computer Program (CANDE)

CANDE is a finite element computer program developed by Michael Katona in 1976. CANDE was developed specifically for the structural analysis, design and evaluation of buried culverts and other soil-structure systems. There are three solution levels available in CANDE, which corresponds to successive increases in analytical power and modelling detail. Level 1 is based on a closed form, plain strain elastic solution for a circular conduit in an elastic half space. Level 2 and level 3 are based on the finite element method in a two dimensional setting. Level 2 uses a mesh generated automatically to cover most culvert installations. Level 3 allows the user to generate his/her own mesh, making it a powerful tool when uncommon installations are being modelled.^[9]

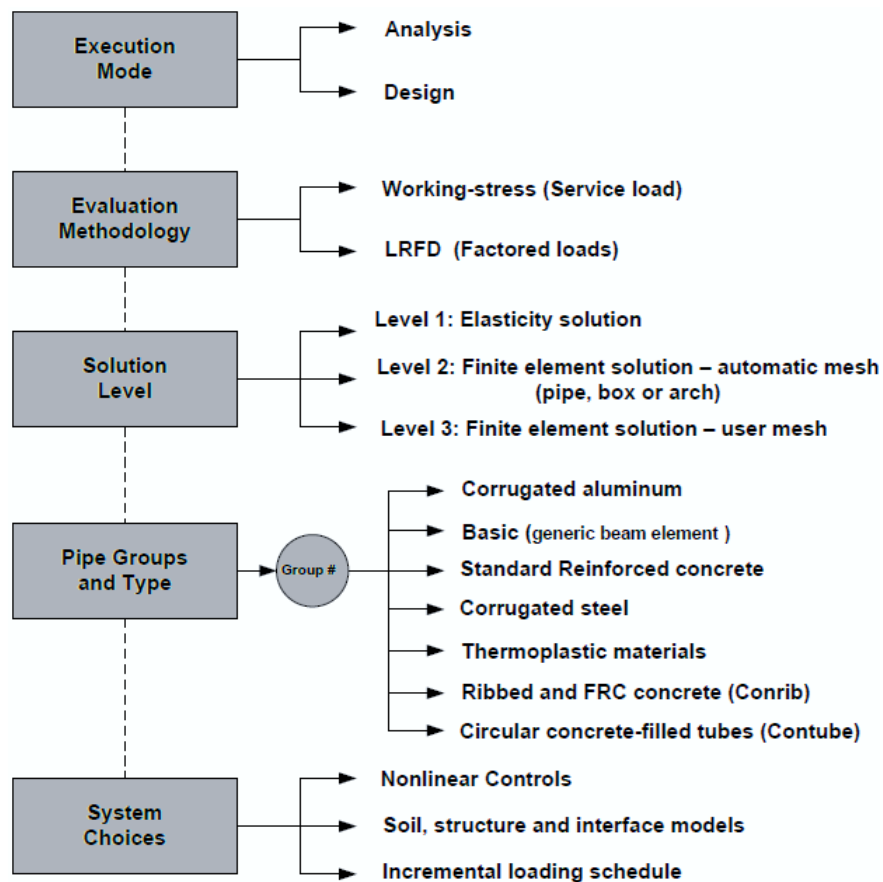


Figure 2.21. Options to define input data for CANDE.^[9]

2.5.2. Katona - Analyses of Culverts by The Finite Element Method

The intent was to provide a study of the analyses of long span culverts by the finite element method that would be a foundation for future studies. Two finite element programs were used; ADINA and CANDE. The two programs were used to examine large deformation theory versus small deformation theory. ADINA uses large deformation theory while CANDE uses small deformation theory. Katona noted from his findings that the large deformation solution is not significantly different from the small deformation solution; the differences at most were 8% at the crown. Katona stated small deformation theory and infinitesimal stress-strain laws may be used for analysing long span systems if the percentage of crown deflection remains within practical limits.

Katona also investigated the effects of modelling the structure monolithically versus an incremented structure sequence. The monolithic system was not incapable of tracking the history of deformations such as maximum peaking, nor was it able to consider compaction loads. The incremental solution showed peaking behaviour similar to what is seen in the field. Katona concluded incremented construction techniques should be used over the monolithic technique.

In addition, the sensitivity of the following parameters was determined: compaction loads and soil stiffness. It was noted that as compaction pressure increases, maximum peaking increases substantially. Compaction pressure placed on each soil layer increment produced peaking several times greater than the gravity weight of the soil, correlating with field observations. Therefore, Katona stated compaction loads should be included in long span analyses. It was found that maximum peaking and maximum flattening occur almost in inverse

proportion to soil stiffness. Katona noted that deflection is directly controlled by soil stiffness, whereas thrust was not appreciably changed.^[16]

2.5.3. Chang, Espinoza, and Selig - Computer Analysis of A Corrugated Steel Culvert

Chang, Espinoza and Selig compared finite element predictions from CANDE to the field measurements of a buried corrugated steel arch. The steel arch had a 26 foot span, 15 foot rise and 23 feet of soil cover. During construction, measurements were made for bending and thrust stresses in steel, deflections of the culvert, backfill stresses, and backfill strains. Three soil models, linear elastic, overburden dependent, and the extended Hardin's model, were used in the finite element analyses.

Field data showed a substantial amount of circumferential shortening during the placement of the backfill, especially when the height of the backfill was below the crown of the culvert. Circumferential shortening may have occurred due to slippage in bolted seams because the holes punched in the corrugated steel plates are larger in diameter by 1/8 inch.

The predicted thrust stresses, displacements, and vertical soil stresses at the crown were found to be satisfactory. Vertical and horizontal soil stress at the spring-line showed considerable discrepancy with the field measurements. Major discrepancies were found between the measured and predicted behaviour in the earlier stages of construction before the backfill was above the crown. This may have been caused by incorrect modelling by neglecting the effect of compaction during backfilling and slip occurring at the bolted seams that permits a circumferential shortening of the structure shell. It may also have been caused by the limitations of the stress-strain model assumed for the soil

according to Chang, Espinoza and Selig. The behaviour calculated by the finite element method was found to agree very well with measured changes after the backfill was above the crown. However, they stated that the proper values for the soil moduli must be used and the bolted seam compressibility must be represented.^[16]

2.5.4. Sharma and Hardcastle - Evaluation of Culvert Deformations Using the Finite Element Method

Sharma and Hardcastle performed a finite element analysis using CANDE on a rib reinforced, low profile and long span steel arch culvert. The culvert is 3.42 m high with a span of 10.52 m. The culvert suffered from unexpected deformations (sag) during the first few months after installation. A major emphasis was placed upon modelling the construction sequence during the analysis phase in order to obtain a realistic assessment of deformations and stress. The non-linear soil model was chosen over the constant elastic moduli on the basis that it would provide a better simulation of the anticipated behaviour of the culvert and supporting soils. The sub-soil profile was developed from data collected from soil borings at the site. For this study, the analysis considered three sets of model parameters corresponding to good, average, and poor soil conditions. The non-linear analysis with poor soil condition parameters generated the lowest factor of safety. The deformations computed by CANDE were smaller than the maximum observed values. CANDE was unable to predict deformations that closely agreed with observations, yet the relative deformations with respect to the footing elevation were predicted within reasonable accuracy.^[16]

2.5.5. Andrew Moreland - Experimental and Numerical Investigation of A Deeply Buried Corrugated Steel Multi Plate Pipe

This study evaluated the structural performance of a corrugated steel plate pipe installed under deep cover during and after construction was completed. The pipe installed at this project was 252 inches in diameter. The overall centerline length of the structure was 439 feet exclusive of the bevelled ends or 477 feet in length at the invert. The embankment fill reached to a height of approximately 75 feet over the crown of the pipe, at its highest point. The thickness of each steel plate was 0.375 inches. The corrugation profile was 6 x 2 inches.

Field performance of the pipe was monitored by measuring the pressure distribution around the pipe as well as the deflection of the pipe during and after construction. The study of the pipe also included comparing measured field performance with numerical predictions given by a finite element computer program CANDE-89.

The pipe's behaviour stabilized from the end of construction to the end of the field monitoring according to the relatively unchanging pressure distribution around the pipe.

The CANDE finite element computer program was not able to predict accurately the field performance of the corrugated steel plate pipe. CANDE had a tendency to under predict the pipe deflections and to over predict the soil pressure acting against the pipe.

When interface elements were used to model the boundary between the soil and pipe, the program would not converge. This problem has been reported in previous studies. A model that includes interface elements would probably yield improved CANDE predictions of the culvert behaviour, due to the interface slippage expected during the

construction phase due to movement of the pipe due to circumferential shortening.

CANDE was unable to predict the peaking behaviour experienced by the culvert during initial backfilling up to the crown. This problem has also been reported in previous studies of CANDE. Simulated compaction effects had very little effect in helping to predict the peaking behaviour.^[16]



Figure 2.22. Hot-dipped galvanized steel structural plates stocked at the warehouse.^[7]



Figure 2.23. Steel structural plate pipe is bolted by modular plates.^[7]



Figure 2.24. Corrugated steel pipe culverts.^[10]



Figure 2.25. Steel structural plate Arch culvert.^[11]

CHAPTER 3

Case Study

3.1. Introduction

In this study, four shapes of corrugated structural plate culvert structure were analysed and designed by load and resistance factor design (LRFD) method using manual and CANDE-2013. Those shapes listed as a Round Pipe, Horizontal Ellipse, Arch and Low Profile Arch, with spans of 4 m and cover height 0.6 m as show in **Figure 3.1**. The mechanical properties are Minimum Yield Point 225 MPa, Minimum Tensile Strength 310 MPa, Min Elongation is 50 mm and Modulus of Elasticity 200×10^3 MPa. The sectional properties are provide in **Table 3.1**. Ultimate longitudinal seam strengths are list in **Table 3.2** for bolted structural plate. Recommended limit of Flexibility Factor FF, for structural plate is 0.114 mm/N for ordinary round and the maximum limit of FF, for arch shape is increased as $FF \leq 1.5 \times FF$ shown for round pipe. In selecting soils for backfill, the grouping of soils according to the ASTM United Classification System (UCS), **Table 3.3** provides soil descriptions and a comparison of this system. After completion of the LRFD analysis and design method by manual and CANDE level 2, data collected and recorded.

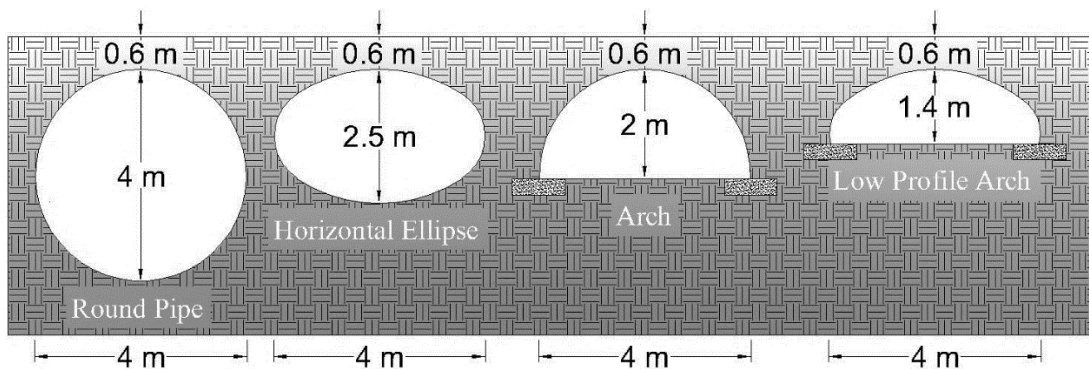


Figure 3.1. Four shapes of corrugated culverts structure.

Table 3.1. Sectional properties for corrugated 152 x 51 mm.

Specified Thickness, mm								
2.82	3.56	4.32	4.79	5.54	6.32	7.11	8.08	9.65
Moment of Inertia, mm ⁴ /mm								
990.1	1280	1576	1770	2080	2395	2717.5	3113.5	3802
Area of Wall Cross Section, A, mm ² /mm								
3.294	4.24	5.184	5.79	6.77	7.74	8.72	9.89	11.89
Radius of Gyration, r, mm								
17.3	17.4	17.4	17.5	17.5	17.6	17.7	17.7	17.9

Table 3.2. Ultimate longitudinal seam strength for 152 x 51 mm.

Structural Plate Thickness, mm	Bolt Diameter, mm	Bolts per Corrugation	Seam Strength, kN/m
2.82	M20	2	613
3.56	M20	2	905
4.32	M20	2	1182
4.79	M20	2	1357
5.54	M20	2	1634
6.32	M20	2	1926
7.11	M20	2	2101
7.11	M20	3	2626
7.11	M20	4	2830
8.08	M22	4	3430
9.65	M22	4	4159

Table 3.3. Soil types by UCS classification.

UCS Soil Classification	Soil Description
GM SM SP SM	Gravelly sand
GM SM ML SP GP SC GC GM SC GC SC GC	Sand and gravel with low plasticity silt Sand and gravels with elastic silt Sands with clay fines Sands with highly plastic clay fines
SW SP SM	Fine sands, such as beach sand
ML CL OL	Low compressibility silts

3.2. Structural Analysis and Design by Load and Resistance Factor Design

This section presents procedures for the design of corrugated culvert structures.

Load and Resistance Factor Design (LRFD) is a method of proportioning structural elements (the pipe) by applying factors to both load factors and the nominal strength levels (resistance factors). The specified factors based on the mathematical theory of reliability and a statistical knowledge of load and material characteristics. The load factors are multipliers (typically greater than 1.0) that take account of the variability of different types of loads, such as earth loads and live loads. Thus, the pipe must design to resist a combination of factored earth loads and factored live loads plus impact.

Resistance factors are typically 1.0 or lower. They account for the possible reduction in the strength of the structural materials involved. While LRFD designs do not openly display the degree of safety (the factor of safety) as such, it is essentially the ratio of the factored load divided by the factored resistance.

LRFD methods may found in both the AASHTO *LRFD Bridge Design Specifications* and in ASTM Standard Practice A796/A796M. AASHTO has set a goal to use the LRFD method for all new construction. ASTM A976/A796M includes both Allowable Stress Design (ASD) and LRFD as alternative procedures. ASTM LRFD is a simplified version of AASHTO LRFD, which involves additional factors and alternative live loads. The referenced documents should referred to for complete details.^[4]

The structural design process consists of the following steps:

1. Check minimum allowable cover.
2. Check minimum spacing.
3. Select the backfill and other soil densities required or expected.
4. Calculate the design pressure.
5. Compute the Factored Thrust.
6. Compute the Wall Resistance.
7. Check Buckling Stress.
8. Check minimum handling stiffness.
9. For bolted or riveted pipe only, check seam strength.
10. Arch only: check rise to span ratio (≥ 0.3) and calculate footing reactions.
11. Check deflection.

3.2.1. Minimum Covers

Minimum covers for H20 and H25 highway loads taken as the greater of span/8 or 300 mm for all corrugated steel pipe. The minimum cover measured from the top (inside rise) of the pipe to the bottom of the asphalt pavement course and to the top of rigid pavements.^[4]

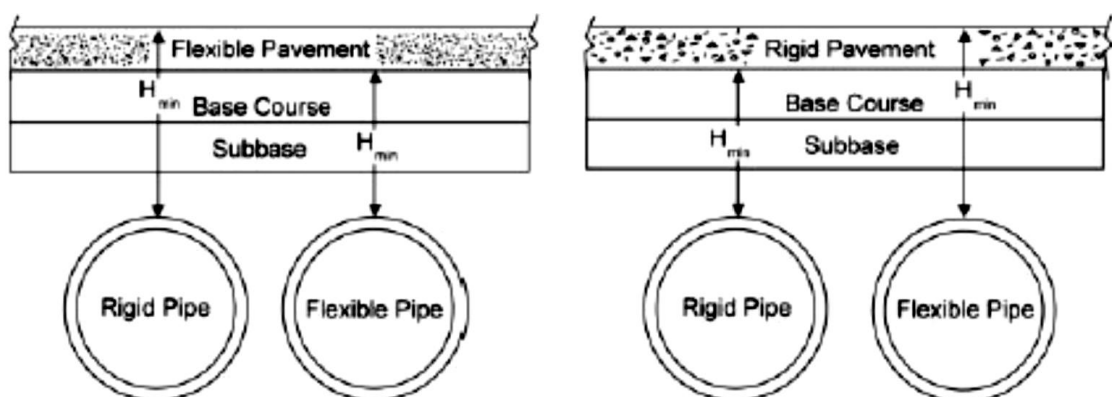


Figure 3.2. Minimum covers orientation.^[15]

3.2.2. Minimum Spacing

When two or more steel drainage structures installed in parallel lines, the space between them must be adequate to allow proper backfill placement, hunching and compaction. The minimum spacing requirement depends upon the shape and size of the structure as well as the type of backfill material. **Figure 3.3** provides the recommended minimum spacing for pipe, pipe arch and arches when standard backfill materials are used. The minimum spacing provides adequate room to fill under the haunches and to compact the backfill.^[4]

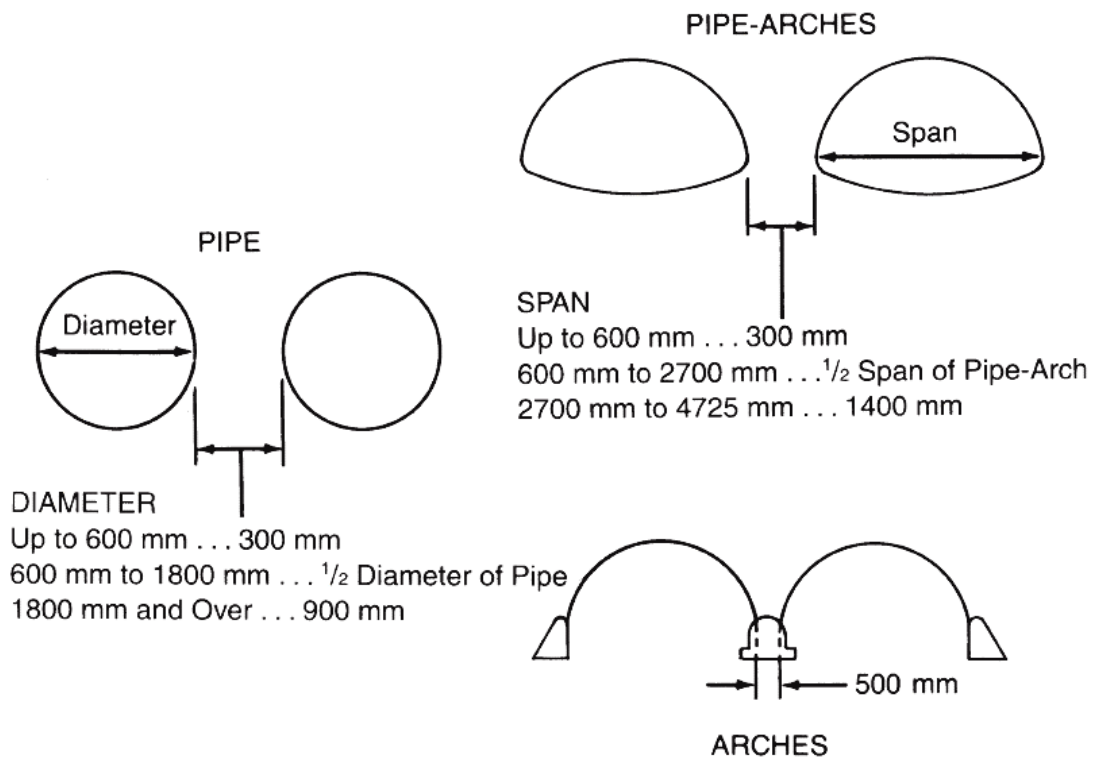


Figure 3.3. Minimum permissible spacing for multiple installations.^[6]

3.2.3. Backfill Design

Requirements for selecting and placing backfill material around and near a pipe are similar to those for selecting a roadway embankment fill. The main differences in requirements are because the pipe generates more lateral pressure than the earth within the embankment would if no

structure existed. In addition, the backfill material must be placed and compacted around the pipe without distorting its shape. However, in the end, the quality of the backfill may be dictated by the need to support the pavement over the conduit.

The quality of the backfill is characterized by the soil stiffness, a property that results from the nature of the soil and the level of compaction. The best backfill materials are non-plastic sands and gravel (GW, GP, GM, and SW). Compaction to a minimum density of 90 percent of standard Proctor is generally sufficient.

Often, the backfill for corrugated culvert structures may be selected from the materials available at the job site. Although highly plastic or organic soils are unsuitable, materials with some degree of plasticity, (SM, GM, etc.) can be used in most instances. The stiffness of corrugated steel pipe allows these materials to be placed and compacted to the density necessary to support the pipe. AASHTO requires that backfill materials meet AASHTO M145 requirements compacted to 90 percent of standard Proctor density.^[4]

3.2.4. Design Pressure^[12]

When the height of cover is equal to or greater than the minimum cover of the structure, and then determine the factored design pressure, P_f , acting on the steel.

The design load or pressure on a pipe is comprised of earth load (EL), live load (LL), and impact load (IL). These loads are applied as a fluid pressure acting on the pipe periphery.

For steel pipe buried in a trench or in an embankment on a yielding foundation, loads are defined as follows:

- i. The earth load (EL) is the weight of the soil column directly above the pipe:

$$(EL) = Hw \quad \text{ASTM clause 6.2.1}$$

Where,

(EL) = earth load, kPa

H = depth of fill above top of pipe, m

w = unit force from 1 m³ of fill material above the pipe, kN/m³.

- ii. The live load (LL) is that portion of the weight of vehicle, train, or aircraft moving over the pipe that distributed through the soil to the pipe. Live Loads for H20 highway loadings, including impact effects, shown in **Table 3.4**.

Table 3.4. Live Loads for H20 highway loadings.^[12]

Height of Cover, m	Live Load, kPa
0.30	86.2
0.61	38.3
0.91	28.7
1.22	19.2
1.52	12.0
1.83	9.6
2.13	8.4
2.44	4.8
over 2.44	Neglect

The pipe shall be designed to resist the following combination of factored earth load (EL) and live load plus impact (LL + IL):

$$P_f = 1.95 (EL) + 1.75 (LL + IL) \quad \text{ASTM clause 9.1}$$

Where,

(IL) = pressure from impact load, kPa

(LL) = pressure from live load, kPa

P_f = factored crown pressure, kPa

3.2.5. Factored Thrust^[12]

The factored thrust, T_f , per unit length of wall shall be determined from the factored crown pressure P_f as follows:

$$T_f = P_f S/2 \quad \text{ASTM clause 9.2}$$

Where,

S = pipe diameter or span, m

T_f = factored thrust in pipe wall, kN/m

3.2.6. Factored Resistance^[12]

The factored resistance (R_f) shall equal or exceed the factored thrust. R_f shall be calculated for the limit states of wall resistance, resistance to buckling, and seam resistance (where applicable) as follows:

$$R_f = \phi R_n \quad \text{ASTM clause 9.3}$$

Where,

R_f = factored resistance for each limit state, kN/m

R_n = nominal resistance for each limit state, kN/m

ϕ = resistance factor

The resistance factor (ϕ) shall be as specified in **Table 3.5**. The axial nominal resistance (R_n) per unit length of wall without consideration of buckling shall take as:

$$R_n = f_y A \quad \text{ASTM clause 9.4}$$

Where,

A = required wall area, mm²/mm

f_y = specified minimum yield strength, MPa

Table 3.5. Resistance Factors for LRFD Design.^[12]

Type of Pipe	Limit State	Resistance Factor, ϕ
Helical pipe with lock seam or fully welded seam	Minimum wall area and buckling	1.00
Annular pipe with spot-welded, riveted, or bolted seam	Minimum wall area and buckling	1.00
	Minimum seam strength	0.67
Structural plate pipe	Minimum wall area and buckling	1.00
	Minimum seam strength	0.67

3.2.7. Critical Buckling Stress^[12]

Check section profile with the required wall area for possible wall buckling. If the critical buckling stress f_c is less than the minimum yield stress f_y , recalculate the required wall area using f_c instead of f_y .

$$\text{If } s < \frac{r}{k} \sqrt{\frac{24E}{f_u}} \text{ then } f_c = f_u - \frac{f_u^2}{48E} \left(\frac{ks}{r}\right)^2 \quad \text{ASTM clause}$$

8.1.2

$$\text{If } s > \frac{r}{k} \sqrt{\frac{24E}{f_u}} \text{ then } f_c = \frac{12E}{\left(\frac{ks}{r}\right)^2} \quad \text{ASTM clause 8.1.2}$$

Where,

E = modulus of elasticity = 200×10^3 MPa

f_c = critical buckling stress, MPa

f_u = specified minimum tensile strength, MPa

k = soil stiffness factor = 0.22 for good side-fill material compacted to 90% of standard density

r = radius of gyration of corrugation, mm

s = pipe diameter or span, mm

3.2.8. Handling and Installation^[12]

The pipe shall have enough rigidity to withstand the forces that are normally apply during shipment, handling, and installation. Both shop- and field-assembled pipe shall have strength adequate to withstand compaction of the side fill without interior bracing to maintain pipe shape. Handling and installation rigidity is measure by the following flexibility requirement.

$$(FF) = s^2 / EI \quad \text{ASTM clause 10.1}$$

Where,

(FF) = flexibility factor, mm/N

I = moment of inertia of corrugated shape, mm⁴/mm

3.2.9. Required Seam Strength^[12]

Since helical lock seam and welded-seam pipe have no longitudinal seams, this criterion is not valid for these types of pipe.

For pipe fabricated with longitudinal seams (riveted, spot-welded, or bolted) the seam strength shall be sufficient to develop the thrust in the pipe wall. The safety factor on seam strength (SS) is 3.

$$(SS) = T_f (SF) \quad \text{ASTM clause 9.6}$$

Where,

(SF) = safety factor

(SS) = required seam strength, kN/m

3.2.10. Foundation Design

The supporting soil beneath pipe is generally refer to as the pipe foundation. The foundation under the pipe is not of great concern in most cases. However, standard designs assume the foundation carries the full

soil column above the pipe without appreciable settlement. If differential settlement between the pipe and the adjacent backfill does occur, it is desirable for the pipe to settle more than the backfill. This helps to defray any drag down loads that otherwise could occur. The bearing strength of the foundation should equal or exceed wH .^[4]

3.2.11. Deflection Limits

The application of deflection design criteria is optional. Long-term field experience and test results have demonstrated that corrugated steel pipe, properly installed using suitable fill material will experience no significant deflection. Some designers, however, continue to apply a deflection limit.

Generally, deflections of 5% of the rise are not considered excessive, provided the shape change has stopped, the shape is suitable for the intended function and the backfill has become suitably consolidated.^[4]

3.3. CANDE Input Flow

As illustrated in the following charts, the input data is structure into the five parts (A, B, C, D and E) as listed below:

- Part A – Master control selections.
- Part B – Pipe type material properties and options.
- Part C – Solution Level 2 input.
- Part D – Soil model material properties.
- Part E – Load factors for LRFD analysis/design.

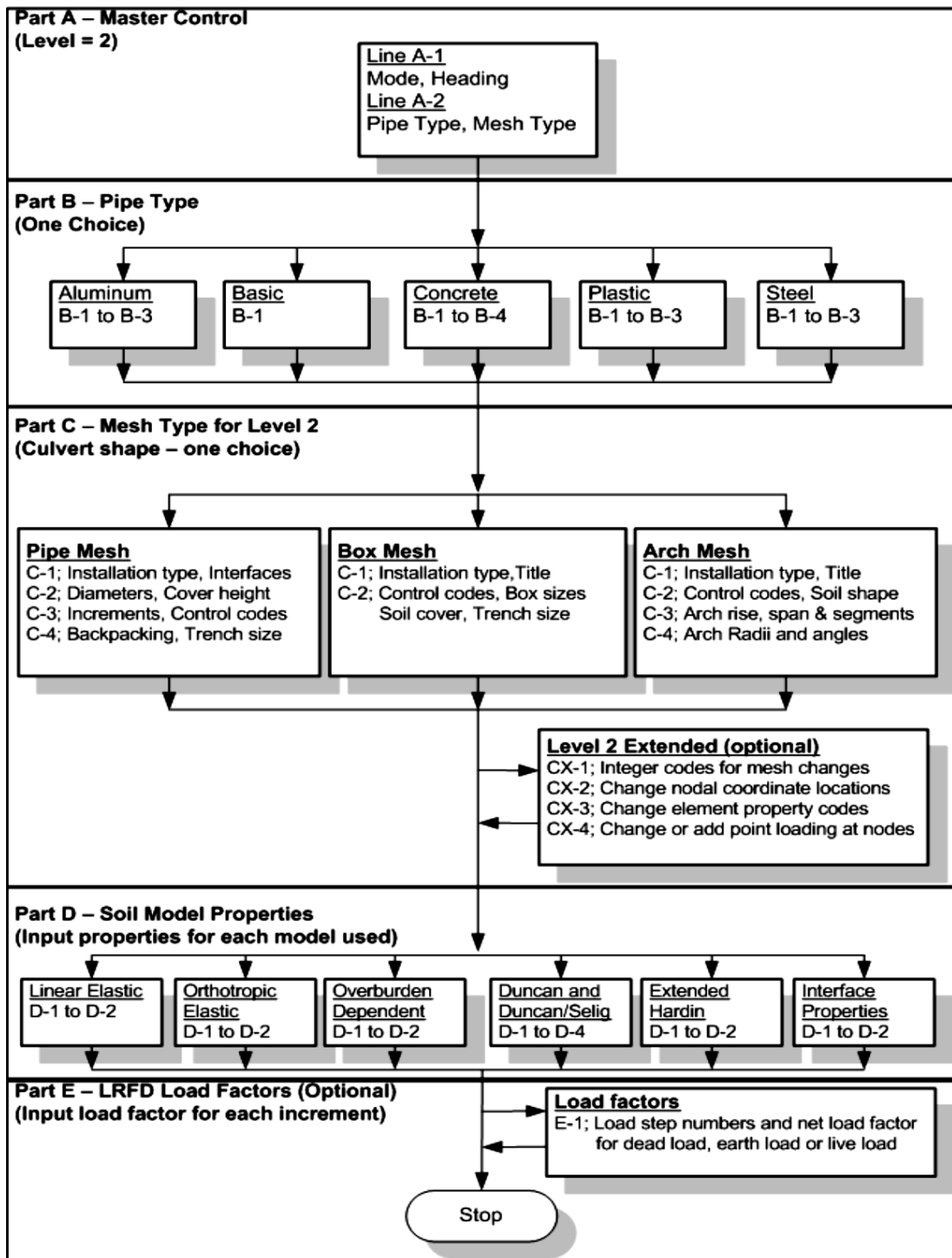


Figure 3.4. CANDE level 2 input flowchart.^[9]

3.4. CANDE Solution Methods and Formulations

Two distinct solution methods are contained in CANDE. The first is call Level 1 and is an extension of a closed-form elasticity solution by Burns and Richard. The second is a finite element methodology modified and extended from Herrmann. Input for the finite element method has two input options called Level 2 and Level 3. Level 2 offers a completely automated mesh generation scheme but it is restricted to basic culvert shapes and symmetric installations, whereas Level 3 is virtually unrestricted in modelling capability, but requires the user to define the mesh topology.^[13]

3.4.1. Beam-Column Elements – Pipe Type Models^[13]

Presented in this section a complete development of the beam-column elements used for modelling corrugated metal, reinforced concrete and thermoplastic pipe materials (or any two-dimensional structure). The initial development focused on the general finite-element formulation that is applicable to all pipe-type material models. Subsequent developments describe specific stress-strain models that distinguish one pipe-type material from another.

i. General Form

The major assumptions and limitations used for the beam-column element listed below:

1. Two-dimensional framework in a plane strain formulation.
2. Bernoulli-Euler beam kinematics without shear deformation.
3. Small deformation theory.
4. Material nonlinearity is a function of normal stress-strain and their history.
5. Incremental virtual work formulation with incremental stress-strain relationships.

ii. Design criteria for corrugated metal

Design criteria for corrugated metal includes strength limits for thrust stress against material yielding in hoop compression, global buckling and seam strength rupture. Although not yet required by AASHTO, another meaningful strength criterion is a limit on the amount of plastic penetration through the cross section. For deep corrugations with corrugation heights ≥ 5.0 inches, the combined thrust-moment criterion is more stringent than the separate requirements of the thrust stress and plastic penetration criteria. Finally, a performance limit on the allowable deflection completes the set of design criteria. The design criteria summarized in **Table 3.6**.

The above design criteria are equally applicable to working stress or LRFD design methodologies. For the working stress approach, the demand and the capacity quantities are un-factored, and the design evaluation given by safety factors defined as capacity divided by demand. Typically, safety factors about 2.0 are desirable for strength-related criteria. For the LRFD approach, the demand and the capacity quantities factored, and the design evaluation given by ratios of demand-to-capacity. Demand-to-capacity ratios less than or equal to 1.0 are acceptably safe. Further discussion on the design criteria provided below:

1. Thrust-stress demand determined by finding the element with the largest thrust force, N_{\max} , and dividing by the cross-sectional area. The corresponding yield-strength capacity is typically 33,000 psi for steel and 24,000 psi for aluminium.
2. For the buckling-strength capacity, CANDE offers the user three choices; (1) an approximate and generally conservative estimate based on the simplified AASHTO LRFD equations 12.7.2.4-1-2, (2) another approximate AASHTO LRFD equation 12.8.9.6-1 intended for deep corrugations, and (3) a much more accurate

solution based on CANDE's large deformation formulation with linearized buckling prediction.

3. If longitudinal bolted seams are present in the corrugated metal culvert, the seam-strength capacity is typically less than the material yield strength. In the absence of experimental test data, seam-strength capacity often specified as 67% of material yield-strength capacity.
4. On the demand side, the percentage of the cross-section that strained into the plastic range from thrust and bending calculated directly from the nonlinear corrugated metal model. The limit of plastic penetration is 100% of the cross section, meaning cross section is incapable of carrying any additional load. Note that some amount of plastic yielding expected to occur in the outer fibres of most well designed corrugated metal culverts under service loading. The plastic penetration design criterion is a precaution against full 100% yielding of the entire cross section, not against moderate outer fibre yielding.
5. This relatively new AASHTO criterion intended for deep corrugations whose corrugation height is greater or equal to 5.0 inches. For LRFD evaluation, the ratio defining the combined moment-thrust criterion implies that numerators include load factors and the denominators include resistance factors, whereas for working stress evaluation they do not.
6. Computed deflection is the relative vertical movement between the top and bottom of the culvert structure, and the percent deflection is relative the vertical distance. The service load limit for allowable deflection generally taken as 5% for all corrugated metal structures.

Table 3.6. Corrugated Metal Design Criteria.^[13]

Design Criterion (Strength limits)	Demand	Capacity
(1) Thrust stress	$\sigma_{\max} = N_{\max} / A$	$F_y =$ yield strength
(2) Global Buckling	$\sigma_{\max} = N_{\max} / A$	$F_b =$ buckling capacity: *AASHTO Eq. 12.7.2.4-1, or *AASHTO Eq. 12.8.9.6-1, or
(3) Seam strength	$\sigma_{\max} = N_{\max} / A$	$f =$ seam strength
(4) Plastic Penetration *(%)	pp = percent of cross-section plastically deformed.	failure = 100%
(5) Combined Moment-Thrust Criterion (ratio). (For deep corrugations only)	<i>Ratio</i> $= \left \frac{M_{\max}}{M_z} \right + \left(\frac{N_{\max}}{A f_y} \right)^2$	Ratio Limit = 1.00
(Performance Limits) (at Service Load)	Demand	Capacity
(6) Allowable deflection *(%)	$\Delta_{\max} =$ computed deflection%	Allowable = 5% of the rise

N_{\max} = max thrust force, M_{\max} = max moment, A = area, M_z = plastic moment

3.4.2. Modelling Techniques^[13]

When applying CANDE to analyse or design any culvert installation (or more generally any soil structure interaction problem), modelling questions always arise. Some common questions are; what extent of the insitu soil should be included in the finite element mesh, what soil models should be used for insitu and backfill soil, should interface elements be included between structure and soil, how many construction increments should be used, and is large deformation theory

required. There is no clear-cut answer to these and similar modelling questions because each problem is unique and modelling assumptions that are appropriate for one case may not be appropriate for another.

The best advice is to try as many modelling approaches as can be practically undertaken for a particular problem. Sometimes it will be found that the differences in solutions from alternative modelling assumptions are inconsequential. At other times, a particular modelling assumption may substantially alter the structural behaviour, affecting the safety of the design. In all cases, however, useful information is obtained that guides our insight into soil-structure interaction and permits a more intelligent assessment of the problem.

i. Live Loads

External loads (as opposed to element body weight loads) defined by boundary-condition input data described in CANDE's user instructions. All external loads applied at nodes as force components in the global x and y directions per unit length in the z direction. Alternatively, if desired, the force components can be defined in rotated x - y coordinates defined by the user.

Figure 3.5 illustrates F_x and F_y force components acting along a particular node strip along the z -direction. Also shown in the figure is a uniform surface-pressure strip load with a uniform pressure P_0 .

Pressure strip loadings are converted to equivalent nodal strip loads by distributing the pressure load acting on each element to the neighbouring nodes and summing the results to determine the equivalent force strips, F_x and F_y . **Figure 3.6** and the accompanying table shows an example of converting a pressure-strip load to nodal-strip loads in the negative y -direction.

The live-load modelling problem summarized as follows. If the actual patch pressure (say 80 psi representing an HS-20 truck tire) is used in a CANDE model or any two-dimensional model, will be over predicted the loads on the culvert.

The AASHTO LRFD load spreading method is a simple concept that assumes the pressure patch load spreads uniformly with soil depth in the overall shape of a truncated pyramid. The top plane of the truncated pyramid has the patch pressure and area, $L \times W$. The base-plane at any depth H assumed to expand in the x - y plane and the y - z plane at a constant angle. The total force on any base-plane area remains constant so that the uniform pressure decreases in proportion the increase in base-plane area.

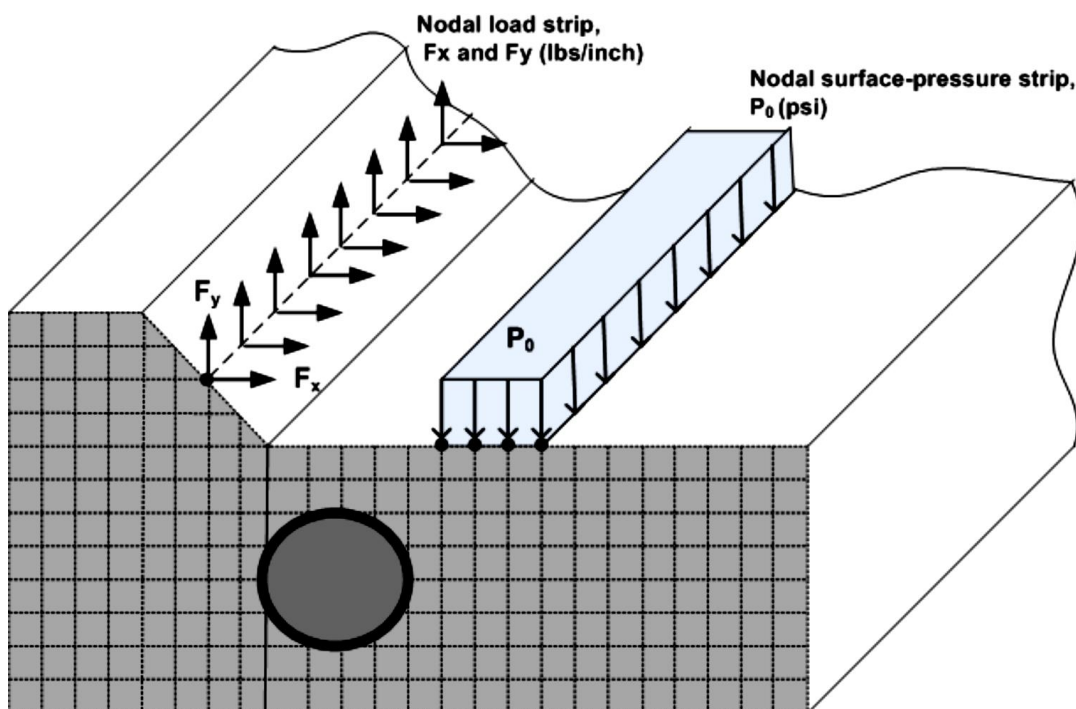


Figure 3.5. Nodal strip load and surface-pressure strip load.^[13]

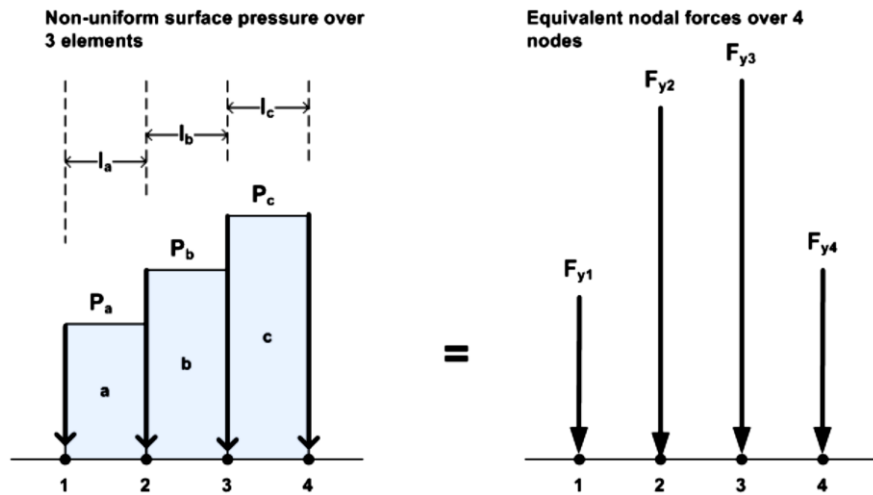


Figure 3.6. Converting pressure strip to equivalent nodal forces.^[13]

Single wheel correction. In order to adapt the AASHTO method to correct the strip pressure problem, it will be recognized that only the y-z plane needs to be corrected because the pressure distribution in the x-y plane accurately determined by the plane-strain solution. The AASHTO approximation for load spreading in the y-z plane, which is along the length of the culvert shows in **Figure 3.7**.

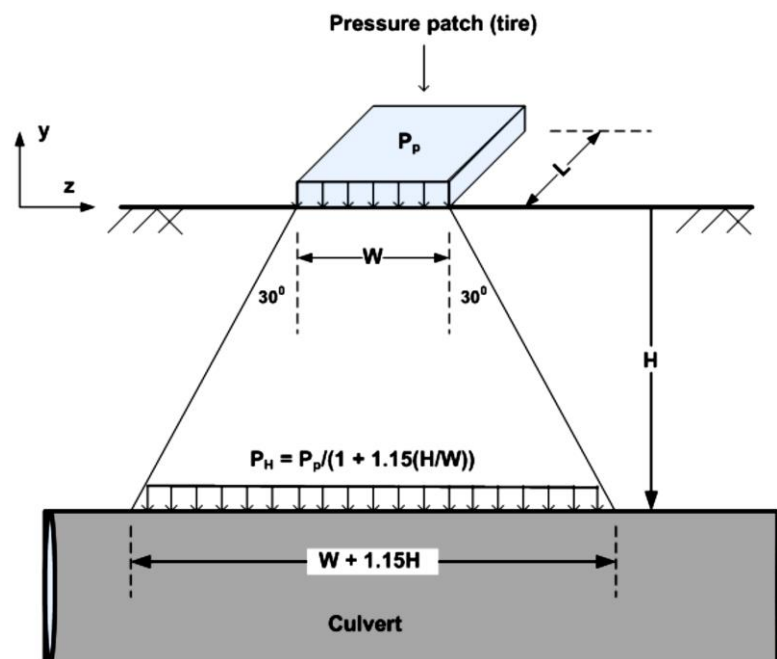


Figure 3.7. Single wheel load distribution along axis of culvert.^[13]

As illustrated in **Figure 3.7**, the base-line pressure along the length of the culvert given by,

$$P_H = P_P \frac{1}{\left(1+1.15\frac{H}{W}\right)} \quad \mathbf{3.1}$$

Where,

P_H = reduced pressure, kPa

P_P = surface pressure, kPa

H = depth to culvert crown, m

W = width of pressure patch along axis of culvert, m

Since the CANDE pressure strip does not account for the pressure reduction along the culvert axis, it follows that reduction factor is given as,

$$r = \frac{P_H}{P_P} = \frac{1}{\left(1+1.15\frac{H}{W}\right)} \quad \mathbf{3.2}$$

Again, the “r” ratio is the reduction factor applied to P_p to get the corrected strip pressure P_s for CANDE analysis.

Two wheel correction. One useful feature of the AASHTO approach is that the interaction of two tires separated by a distance, S , can be accommodated by a simple extension of the one-wheel method. Typically, the spacing distance S represents the truck axle length separating two tires.

The two-wheel approach should be used whenever the culvert cover depth is deeper than the so-called wheel interaction depth given by

$$H_{int} = \frac{S-W}{2 \tan(30^\circ)} = \frac{S-W}{1.15} \quad \mathbf{3.3}$$

Where,

H_{int} = wheel interaction depth, m

S = spacing between wheels, centre to centre, m

W = patch or tire width in y-z plane, m

When the culvert buried deeper than H_{int} , the portion of the culvert between the wheels begins to experience soil pressure from both wheels. When pressure overlap begins to occur, the AASHTO load spreading method assumes the pressure remains uniform over the entire interaction zone. The total force from the two tires equilibrates the force from the pressure distribution along the culvert. The above concepts are summarized and illustrated in **Figure 3.8**.

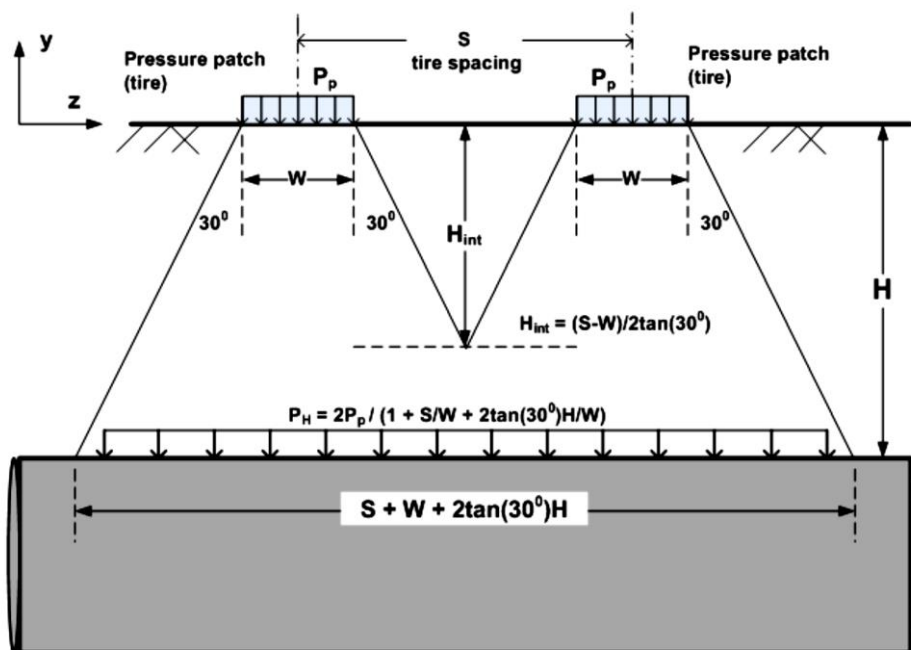


Figure 3.8. Two-wheel load distribution along axis of culvert.^[13]

As illustrated in **Figure 3.8**, the uniform pressure along the length of the culvert given by,

$$P_H = 2P_P \frac{1}{\left(1 + \frac{S}{W} + 1.15 \frac{H}{W}\right)} \quad 3.4$$

Where,

P_H = reduced pressure, kPa

P_P = surface pressure of tire 1 and tire 2, kPa

H = depth to culvert, providing $H > H_{int}$, m

Following the same argument as presented for the single wheel correction, the two-wheel reduction factor is determined as,

$$r = \frac{P_H}{P_P} = \frac{2}{\left(1 + \frac{S}{W} + 1.15 \frac{H}{W}\right)} \quad 3.5$$

As before, r is the reduction factor to compute strip pressure, $P_s = rP_p$ for CANDE analysis.

ii. Construction Increments

Incremental construction is the physical process of placing and compacting soil layers, one lift at a time, below, alongside and above the culvert as the installation is constructed. Analytically this achieved by adding incremental solutions from successive finite element configurations, where each new configuration contains additional soil elements (and/or structural elements) that mimics the real-world build-up of the soil-structure system, one load step at a time.

The terms “load step” and “construction increment” closely related terms and often used interchangeably; however, they have slightly different meanings. Load step is an all-encompassing term referring to any incremental solution, which may or may not include a construction increment. For example, a load step may only include boundary-condition loads without additional elements added to the system. A construction increment is a special kind of load step wherein additional elements added to the global stiffness matrix usually representing an additional layer of soil. The body weight of added elements form the load increment associated with the load step along with any boundary loads such as soil compaction pressures, discussed subsequently.

The last technique to be describe is the modelling of soil compaction using the so-called squeeze layer method first. The purpose of soil compaction is to densify soil after it laid down in loose layers and

then compacted to achieve a specified density usually stated in terms of AASHTO T-99 relative density.

Compaction equipment ranging from hand-held compactors to large-tracked bulldozers used to compress each soil layer by creating a temporary vertical pressure to compact the soil. As the soil is compressed vertically (squeezed), it tends to expand laterally due to the Poisson effect, which creates horizontal pressure on the sides of the culvert. These lateral pressures cause inward movement of the culvert sides and peaking at the culvert crown, that is, a reverse deformation pattern from that caused by overburden loading. Large culverts such as long-span corrugated metal structures often experience as much as 2% crown peaking because of compacting soil layers between the footing and the crown.

Compaction loads are beneficial not only in compacting the soil to achieve the desired soil stiffness properties but also in introducing reverse deformations and bending moments into the culvert, which provides the culvert with additional capacity to resist the opposite bending deformations that subsequently come from soil placed on top of the culvert.

The squeeze layer technique is a simple modelling concept that simulates the effect of soil compaction and is applicable to both linear and nonlinear soil models. The concept will be illustrated in **Figure 3.9** and discussed below:

1. To start, a uniform compaction pressure representing the compaction equipment, typically on the order 5-psi pressure, placed on the surface of the in-situ soil at the level of the footing.

2. Next, the 2nd construction increment (first layer of backfill soil with body weight) added to the system along with another uniform compaction pressure applied to its top surface. At the same time,

however, the first compaction pressure removed by applying an equal but opposite compaction pressure to the bottom surface. These two opposing pressures squeeze the soil layer and increase the lateral pressure on the arch via the Poisson effect.

3. The intermediate construction increments 3rd, 4th and 5th are treated exactly like the 2nd construction increment so that each layer is squeezed, increasing lateral pressure on the arch and inducing more peaking. Note that after the 5th load increment (or more generally, the increment before the crown-level increment) all the temporary compaction pressures have been removed except the compaction pressure on the surface of 5th construction increment.

4. The squeeze layer process is terminated with the 6th construction increment (i.e., crown-level increment). As the 6th construction increment is added to the system with its stiffness and body weight, the last remaining compaction pressure from the 5th construction is removed.

5. All the remaining construction increments, representing soil layers above the crown, added in the normal manner with body weight but without any compaction pressures.

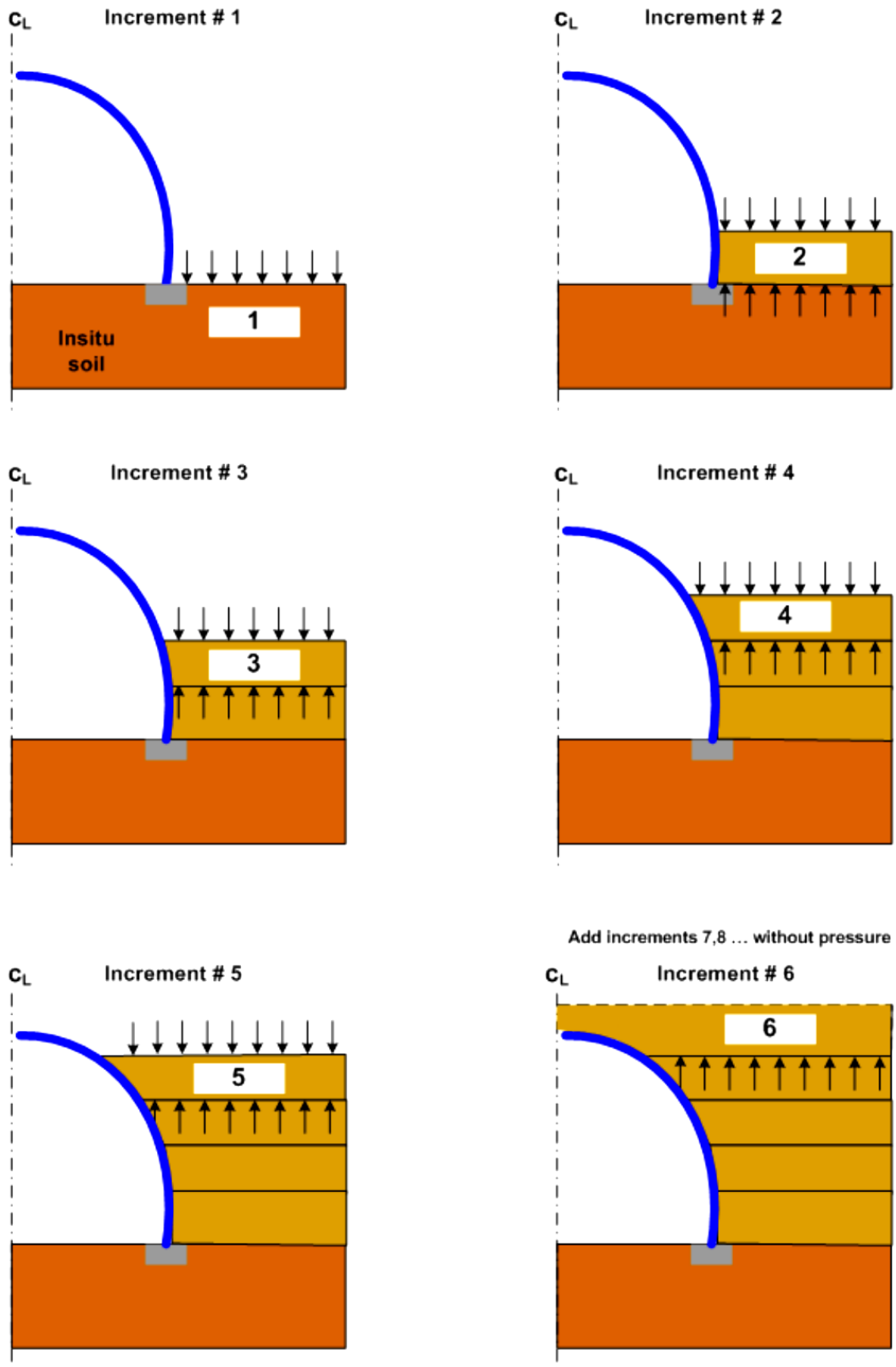


Figure 3.9. Squeeze-layer method for compaction loads on culvert.^[13]

3.4.3. Design Criteria^[13]

The probabilistic-based design philosophy known as load and resistance factor design (LRFD) has adopted into the AASHTO LRFD Bridge Design Specifications wherein the specifications for buried structures are primarily contained in Section 12. One of the tasks in the NCHRP CANDE Upgrade project was to incorporate LRFD methodology for all culvert materials into CANDE in addition to the traditional working stress design (WSD) methodology.

The WSD approach uses service loads and un-factored capacities to compute safety factors defined as capacity divided by service-load demand. The LRFD approach uses factored loads and factored capacities to compute ratios of factored demand divided by factored capacity for strength related design criteria, and service-load demand divided by performance limits for service related design criteria.

LRFD methodology for buried structures includes both service limit states and strength limit states. One consequence of the two limit states when using a comprehensive solution method is that two separate solutions may need to be obtained, one with service loading and one with factored loading. The definitions of service loading and factored loading provided in the following discussion along with tables summarizing the specified load factors. To augment this discussion, guidance provided on applying these factored loads in the context of a comprehensive finite element solution methodology.

i. Service Loads

A common example of a design criterion that is associated with service loading is the allowable deflection of flexible culverts. In the case of rigid culverts, a common example is the allowable concrete crack width. Later, the exact form of these and other design criteria will

discussed and quantified. For present purposes, it is only necessary to understand that a solution at the service load level is required in order to evaluate the service design criteria. For a culvert system to successfully pass the service load design criteria, the predicted response such as the percent deflection must be less than or equal to the allowable limit.

The service load level is the actual design load experienced by the culvert system as if one were performing a working stress analysis. Service loads include the following conditions:

1. Dead load of structure.
2. Earth load on the soil.
3. Live load pressure on the structure transmitted through soil.
4. Live load multiplier due to vehicle impact.
5. Live load multiplier due to multiple lane presence.
6. Other design load considerations such as hydrostatic or thermal loading.

In terms of finite element modelling, the structure dead load (body weight of the culvert) typically applied in the first load step after consideration of in situ soils, followed by a sequence of load steps composed of soil element layers, which placed around and above the culvert up to the design cover height. Each soil layer is loaded with its own body weight according to the soil density associated with the region. Live loads typically applied in the last load step(s) on the soil surface as a pressure boundary condition, representing the tire footprint pressures from the design-truck. AASHTO specifications also require that service-load tire pressures increased by multipliers to account for dynamic impact and the effects of multiple lane presence, which prescribed as follows:

- Impact multiplier = $1 + 0.33(1.0 - H/8.0) \geq 1.0$.
- Multiple-lane-presence multiplier = 1.2.

The multiple lane presence factor is 1.2 for a single loaded lane and considers that a single truck has a high likelihood of overloaded. While LRFD allows reduced values of the multiple presence factor when more than one lane is loaded, calculations for culverts under live load show that the single loaded lane condition virtually always controls the design.

As a side comment, it is noted that the prescription of the basic live load tire pressure presents a special problem for two-dimensional, plane strain finite element programs because the tire foot print area extends to infinity in the out-of-plane direction, thereby overestimating the actual loading on the culvert as compared to the actual footprint width of finite dimensions.

ii. LRFD Loads for Strength-limit States

For strength limit states such as the yield strength, ultimate strain, or global buckling capacity of the soil-structure system, the LRFD methodology assigns net multiplying factors to the service loads. The resulting structural responses, which are at higher levels of stress than the service load responses, called the factored demands. Concurrently, resistance factors, whose values are typically 1.0 or less, multiplied by the strength values and the resulting products called factored capacities. The test of a successful culvert design using the LRFD methodology is that the factored capacities are greater or equal to the corresponding factored demands for all the strength-state design criteria. In a simplistic sense, the ratio of the effective load factor to the resistance factor is comparable to the safety factor concept used in working stress design methodology. However, it generally accepted that LRFD methodology offers a more logical design assessment than WSD methodology.

Load Factors Currently specified in AASHTO LRFD specifications as shown in **Table 3.7**. A general observation that should fit well with

reader's intuition is that γ_{\max} increases in value from the dead load case to the earth load case to the live load case.

Table 3.7. Load factors for corrugated metal pipe or arch.

Dead Load Culvert (DC)		Earth fill Loading (EB)		Live Load (LL)
γ_{\max}	γ_{\min}	γ_{\max}	γ_{\min}	γ_{\max}
1.25	0.9	1.95	0.9	1.75

Where,

γ_{\max} = maximum load factor dependent on load case and culvert type.

γ_{\min} = minimum load factor dependent on load case and culvert type.

3.5. Hydraulics of Culverts

Engineer's interpretation of field data and hydrology is often influenced by personal judgement, based on experience in a given locality.

However, hydrology and hydraulic research are closing the gap to move the art of designing a culvert closer to becoming a science.

Up to this point, the design procedure has consisted of collecting field data, compiling facts about the roadway and making a reasonable estimate of flood discharge. The next step is to design an economical corrugated steel structure to handle the flow (including debris) with minimum damage to the slope or culvert barrel. Treatment of the inlet and outlet ends of the structure must also be considered.

An ASCE Task Force on Hydraulics of Culverts offers the following recommendations for "Attributes of a Good Highway Culvert":

1. The culvert, appurtenant entrance and outlet structures should properly take care of water, bed-load, and floating debris at all stages of flow.

2. It should cause no unnecessary or excessive property damage.
3. Normally, it should provide for transportation of material without detrimental change in flow pattern above and below the structure.
4. It should be design so that future channel and highway improvement can be made without too much loss or difficulty.
5. It should be design to function properly after fill has caused settlement.
6. It should not cause objectionable stagnant pools in which mosquitoes may breed.
7. It should be designed to accommodate increased runoff occasioned by anticipated land development.
8. It should be economical to build, hydraulically adequate to handle design discharge, structurally durable and easy to maintain.
9. It should be design to avoid excessive ponding at the entrance which may cause property damage, accumulation of drift, culvert clogging, saturation of fills, or detrimental upstream deposits of debris.
10. Entrance structures should be design to screen out material which will not pass through the culvert, reduce entrance losses to a minimum, make use of the velocity of approach in so far as practicable, and by use of transitions and increased slopes, as necessary, facilitate channel flow entering the culvert.
11. The design of the culvert outlet should be effective in re-establishing tolerable non-erosive channel flow within the right-of-way or within a reasonably short distance below the culvert.
12. The outlet should be design to resist undermining and washout.
13. Energy dissipaters, if used, should be simple, easy to build, economical and reasonably self-cleaning during periods of easy flow.^[4]

CHAPTER 4

Analysis of Results and Discussion

In this chapter, the manual analysis and design of the four shapes of culverts by AASHTO LRDFD method compared with the finite element results from CANDE-2013 programme were done. The approach used to simulate the analysis and design of the culverts presented in detail in **Chapter 3**.

4.1. Manual Analysis and Design Calculations

In this section, manual analysis and design of different culverts shapes using load and resistance factored design (LRFD) Method as shown in **Figure 3.1**.

In order to perform analysis and design of culverts, the following data was prepared:

- Pipe diameter or span, $D = S = 4$ m
- Seam type: bolted structural plate
- Height of cover, $H = 0.6$ m
- Live load, LL = H-20 Highway Loading
- Weight of Gravelly sand (SM) soil, $w = 19.64$ kN/m³
- Installation type: embankment

The manual calculations were as follows:

ASTM A796/A796M Ref.	CALCULATION	OUTPUT
11.1	<p><u>Check Minimum Allowable Cover</u> Try the 152 by 51 mm corrugation with 2.82 mm wall.</p> $\sqrt{\frac{(AL)d}{EI}} = \sqrt{\frac{142300 \times 50.8}{200 \times 10^3 \times 990.06}} = 0.19$ < 0.23 $H_{min} = \frac{S}{8} = \frac{4}{8} = 0.5 \text{ m} < 0.6 \text{ m}$	∴ ok
18.2.2	<p><u>Backfill Soil Densities Required or Expected</u> SM with 90% standard Proctor density is specifying for construction.</p>	
9.1 6.2.1 6.2.2.1	<p><u>Design Pressure</u> $P_f = 1.95 \text{ EL} + 1.75 \text{ LL}$ $\text{EL} = w \text{ H} = 19.64 \times 0.6 = 11.8 \text{ kN/m}^2$ $\text{LL} = 47.2 \text{ kN/m}^2$ $P_f = 1.95 \times 12 + 1.75 \times 47.2 = 105.6 \text{ kN/m}^2$</p>	$P_f = 105.6 \text{ kN/m}^2$
9.2	<p><u>Factored Thrust</u> $T_f = P_f (S/2)$ $T_f = 105.6 \times (4/2) = 211.2 \text{ N/mm}$</p>	$T_f = 211.2 \text{ N/mm}$
9.3 9.4 Table 1	<p><u>Factored Resistance</u> $R_f = \phi R_n$ $R_n = f_y A$ $R_n = 225 \times 3.294 = 741.2 \text{ N/mm}$ $\phi = 1$ $R_f = 1 \times 741.2 = 741.2 \text{ N/mm} > 211.2 \text{ N/mm}$</p>	∴ ok
8.1.2	<p><u>Buckling Stress</u> $s = 4000 < \frac{r}{k} \sqrt{\frac{24E}{f_u}} = \frac{17.3}{0.22} \sqrt{\frac{24 \times 200 \times 10^3}{310}} =$ 9785.1 mm $f_c = f_u - \frac{f_u^2}{48E} \left(\frac{kS}{r}\right)^2$ $f_c = 310 - \frac{310^2}{48 \times 200 \times 10^3} \left(\frac{0.22 \times 4000}{17.3}\right)^2 = 284.1$ $\text{MPa} > f_y = 225 \text{ MPa}$</p>	∴ ok

ASTM A796/A796M Ref.	CALCULATION	OUTPUT
10.1 10.2	<u>Handling Stiffness</u> $FF = s^2/EI$ $FF = (4000)^2/(200 \times 103 \times 990.06) = 0.081$ $\text{mm/N} < 0.114 \text{ mm/N limit}$	∴ <i>ok</i>
8.1.3.2 Table 1	<u>Seam Strength</u> $(SS) = \phi \times 2 \text{ bolts per Corrugation}$ $\phi = 0.67$ $(SS) = 0.67 \times 613 = 410.7 \text{ N/mm} > 211.2$ mm/N	∴ <i>ok</i>
	<u>For Arch only</u> <u>Check Rise to Span Ratio</u> $\text{Rise/Span} = 1.4/4 = 0.35 \geq 0.3$ <u>Footing Reactions</u> $\text{Footing Reaction} = \text{Thrust}$ $P = EL + LL = 12 + 47.2 = 59.2 \text{ kN/m}^2$ $T = P (S/2) = 59.2 (4/2) = 118.4 \text{ N/mm}$	∴ <i>ok</i> Reactions = 118.4 N/mm

Therefore, the Results 152 by 51 mm corrugation with specified wall minimum thickness of 2.82 mm is an acceptable design.

4.2. CANDE Results

4.2.1. Live Load Calculation

This demonstrates calculating the two-dimensional out-of-plane distribution of live load through soil by AASHTO LRFD for use with CANDE FEM for a Design Truck (H-20) traveling parallel to the span of the culvert.

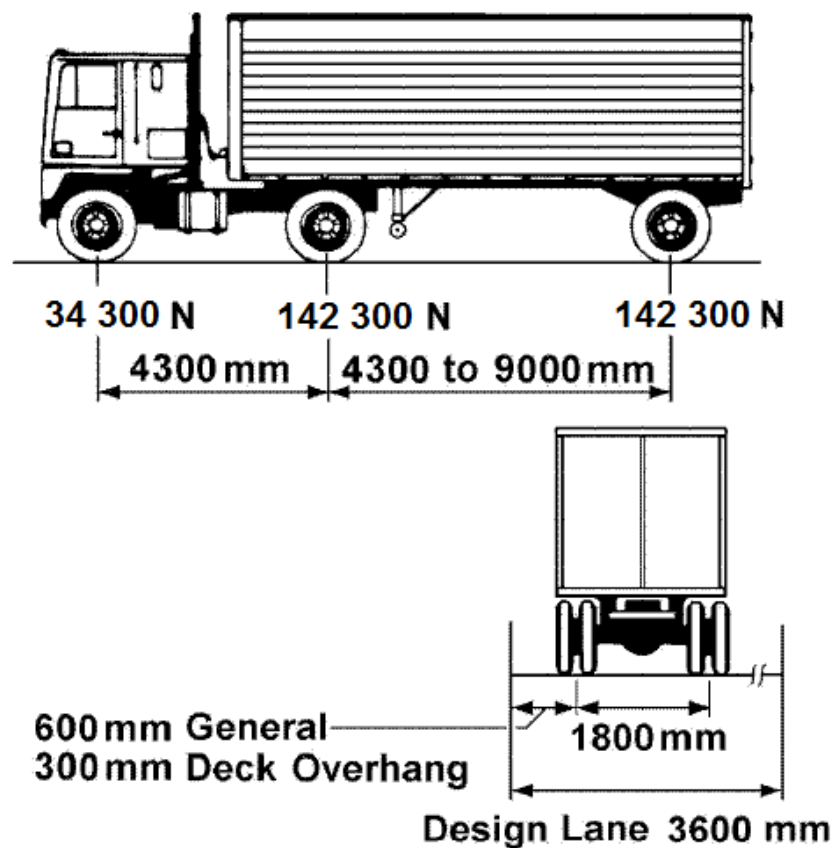


Figure 4.1. AASHTO Design Truck (H-20).^[14]

1. General Properties:

Height of cover, $H_E = 600$ mm

Pipe diameter or span, $D = S = 4000$ mm

Design Truck:

Axle Load, $P_{axle} = 142300$ N

Tire Load, $P_{tire} = P_{axle} / 2 = 71150$ N

Axle Width (distance between tires), $w_{axle} = 1800$ mm

Tire Contact Area (LRFD 3.6.1.2.5):

Contact Width, $w_{\text{tire}} = 510 \text{ mm}$

Contact Length, $L_{\text{tire}} = 250 \text{ mm}$

2. Design Factors:

Live Load Distribution Factor (LRFD 3.6.1.2.6), $LLDF = 1.15$

Multiple Presence of Live Load (LRFD 3.6.1.1.2), $mpf = 1.20$

Live Load Factor (Service I), $LL = 1.0$

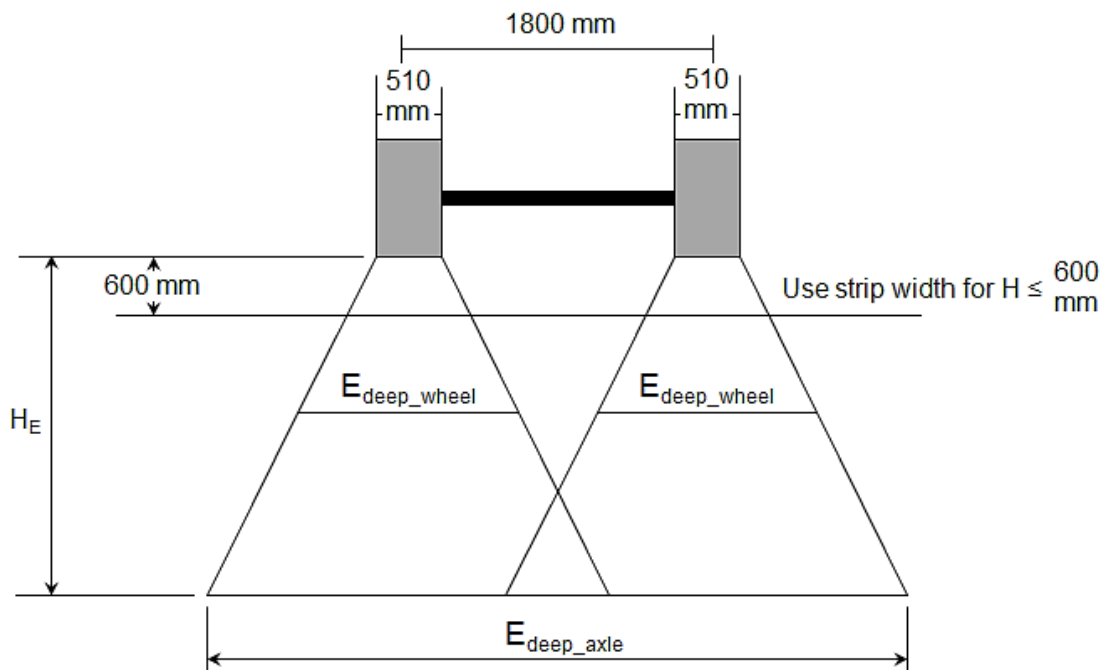
Impact for Buried Components (LRFD 3.6.2.2):

Dynamic Allowance, $IM = 33 (1.0 - 4.1 \times 10^{-4} H_E) \geq 0\%$

$= 33 (1.0 - 4.1 \times 10^{-4} \times 600) = 24.88\%$

Impact Factor, $I_{\text{imp}} = \max \left[1.0, \left(1 + \frac{IM}{100} \right) \right] = 1.25$

3. For Depth of Fill Greater Than 600 mm (LRFD 3.6.1.2.6):



Wheel Load Equivalent Distribution Width, $E_{\text{deep_wheel}} = w_{\text{tire}} + LLDF \times H_E = 510 + 1.15 \times 600 = 1200 \text{ mm}$

Axle Load Equivalent Distribution Width, $E_{\text{deep_axle}} = W_{\text{axle}} + W_{\text{tire}} + \text{LLDF} \times H_E = 1800 + 510 + 1.15 \times 600 = 3000 \text{ mm}$

Wheel Live Load Equivalent Distribution (no overlap), $LL_{\text{deep_wheel}} = \frac{P_{\text{tire}} \times I_{\text{imp}} \times \text{mpf}}{E_{\text{deep_wheel}}} = \frac{71150 \times 1.25 \times 1.20}{1200} = 88.94 \text{ N/mm}$

Axle Live Load Equivalent Distribution (overlap), $LL_{\text{deep_axle}} = \frac{P_{\text{axle}} \times I_{\text{imp}} \times \text{mpf}}{E_{\text{deep_axle}}} = \frac{142300 \times 1.25 \times 1.20}{3000} = 71.15 \text{ N/mm}$

Determine Controlling Distribution (check wheel overlap), $LL_{\text{deep}} = \begin{cases} LL_{\text{deep_wheel}} & \text{if } E_{\text{deep_wheel}} \leq \frac{E_{\text{deep_axle}}}{2} = \frac{3000}{2} = 1500 \\ LL_{\text{deep_axle}} & \text{otherwise} \end{cases}$
 $LL_{\text{deep}} = 88.94 \text{ N/mm}$

4. For Depth of Fill Less Than 600 mm (LRFD 4.6.2.10):

Equivalent Axle Distribution Width, $E_{\text{shallow}} = 24440 + 0.12 \times S = 2440 + 0.12 \times 4000 = 2920 \text{ mm}$

Axle Live Load Distribution, $LL_{\text{shallow}} = \frac{P_{\text{axle}} \times I_{\text{imp}} \times \text{mpf}}{E_{\text{shallow}}} = \frac{142300 \times 1.25 \times 1.20}{2920} = 73.1 \text{ N/mm}$

5. Two-Dimensional Live Load - (Service I):

Two Dimensional Live, $LL_{2D} = \begin{cases} LL_{\text{shallow}} & \text{if } H_E \leq 600 \text{ mm} \\ LL_{\text{deep}} & \text{if } H_E > 600 \text{ mm} \end{cases}$

$LL_{2D} = 73.1 \text{ N/mm}$

If Modelling Full Structure:

Number of Elements over Wheel Length, $n_{\text{elems}} = 2$ (3 nodes) use equal mesh spacing

Load per Interior Node, $I_{\text{int.node}} = \frac{LL_{2D}}{n_{\text{elems}}} = \frac{73.1}{2} = 36.55 \text{ N/mm}$

$$\text{Load per Exterior Node, } l_{\text{ext.node}} = \frac{l_{\text{int.node}}}{2} = \frac{36.55}{2} = 18.28 \text{ N/mm}$$

Apply Wheel Load in Increments (fewer convergence issues),

$$n_{\text{con.wheel}} = 4$$

$$\text{Load per Interior Node per Construction Increment, } l_{\text{int.node_per_con_incr}} = \frac{LL_{2D}}{n_{\text{con.wheel}} \times n_{\text{elems}}} = \frac{73.1}{4 \times 2} = 9.14 \text{ N/mm}$$

(For this problem, the interior node is on the plane of symmetry. Use half of the load above if modelling half the structure)

Use half of the load above if modelling half the structure)

Load per Exterior Node per Construction Increment,

$$l_{\text{ext.node_per_con_incr}} = \frac{l_{\text{int.node}}}{2 \times n_{\text{con.wheel}}} = \frac{36.55}{2 \times 4} = 4.57 \text{ N/mm}$$

4.2.2. Culvers Loads Steps and Elements Simulation

By applying the required data to have full simulation for Round Pipe and Horizontal Ellipse culvert shapes to perform the modelling forms in CANDE program. A half-symmetrical shape was modelled to show soil compaction and construction increments of loads steps that establishing different effects of external forces and internal stresses in the culverts structures.

There are six load steps as shown in **Figure 4.2** for each culvert form. The load step 1 shows site soil and culvert sections referred to number 1 and other load steps 2 to 5 illustrate the effect of incremental backfill soil and its compaction by construction around the pipe.

The nodal live load presented in load step 6 as shown in the **Figure 4.2** as two red dots at the top of the backfill over the crown of the pipe.

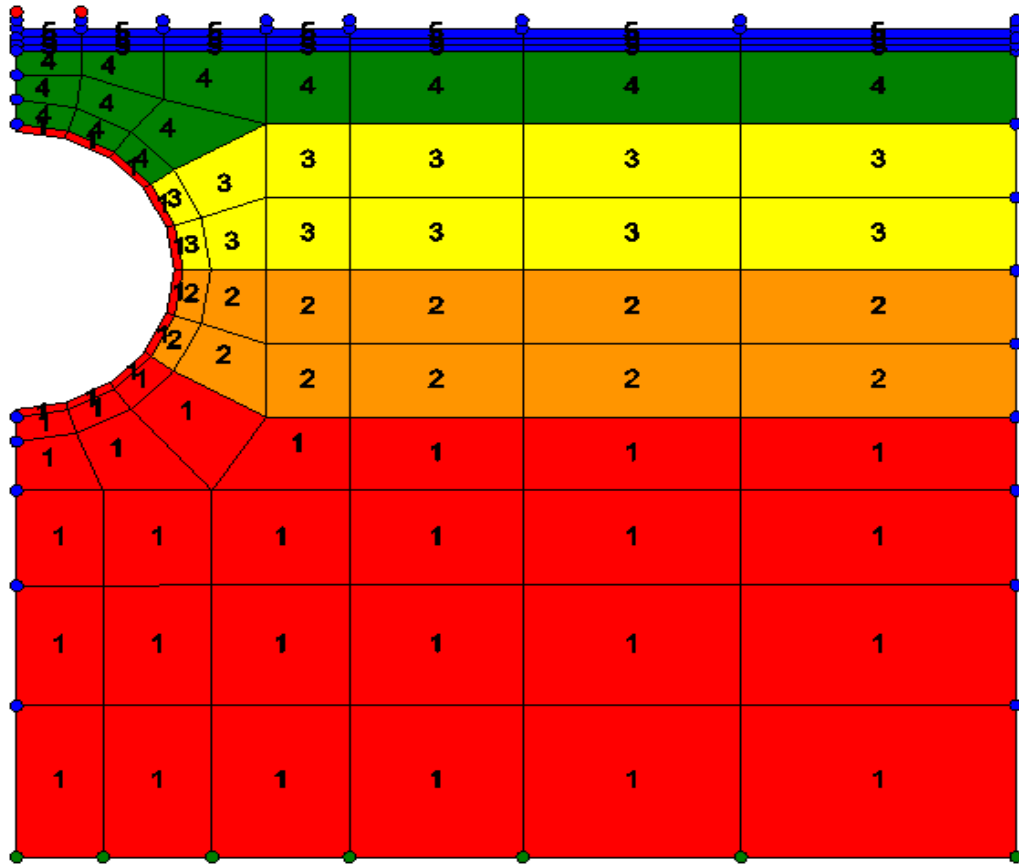


Figure 4.2. Loads steps for Round Pipe and Horizontal Ellipse shapes.

The modelling of Round Pipe and Horizontal Ellipse culvert shapes were divided in to 10 elements and 11 nodes using CANDE program as shown in **Figure 4.3**, in order to obtain the external force and its effect on them.

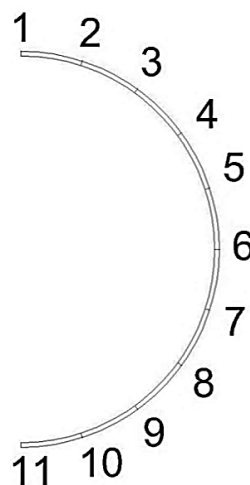


Figure 4.3: View for Round Pipe and Horizontal Ellipse shapes.

For both Arch and Low Profile Arch, culvert shapes were modelling in CANDE program. A half-symmetrical shape was modelled to show soil compaction and construction increments of loads steps that establishing different effects of external forces and internal stresses in the culverts structures.

There are ten load steps as shown in **Figure 4.4** for each culvert form. The load step 1 shows site soil and culvert sections referred to number 1 and other load steps 2 to 9 illustrate the effect of incremental backfill soil and its compaction by construction around the pipe.

The nodal live load presented in load step 10 as shown in the **Figure 4.4** as two red dots at the top of the backfill over the crown of the pipe.

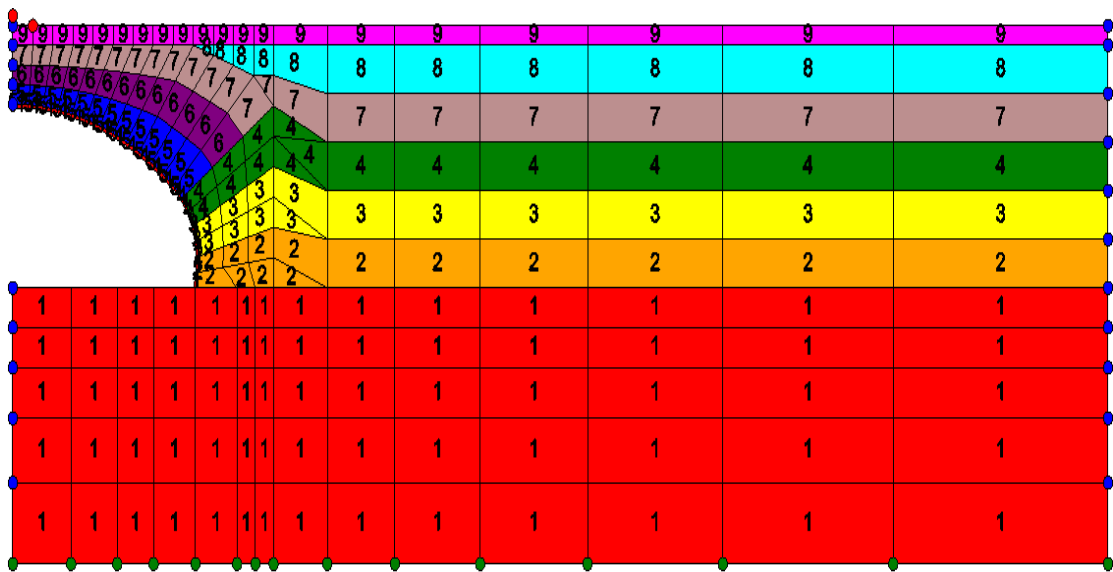


Figure 4.4. Loads steps for Arch and Low Profile Arch shapes.

The modelling of Arch and Low Profile Arch culvert shapes were divided in to 10 elements and 11 nodes using CANDE program as shown in **Figure 4.5**, in order to obtain the external force and its effect on them.

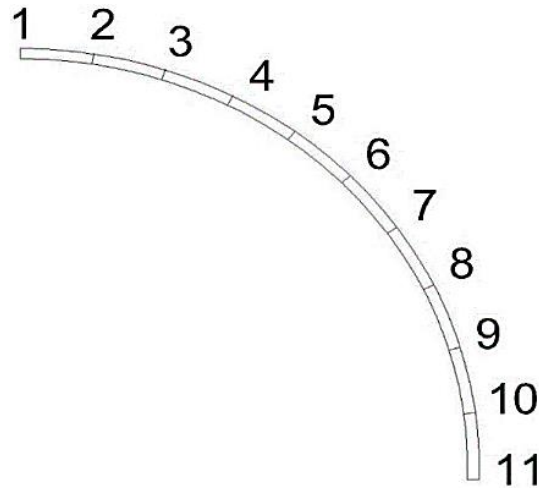


Figure 4.5. View for Arch and Low Profile Arch shapes.

4.2.3. Results of Thrust Forces

The comparison results of maximum thrust force from soil compaction and construction increments of loads steps at each node using manual analysis and CANDE computer program analysis for the four-selected culvert shapes illustrated in graphical presentation as shown in **Figure 4.6**. Horizontal axis presented node number at culverts wall and vertical axis thrust force in (N/mm), and the negative values means ring compression force. The thrust forces for manual calculation and round pipe for CANDE analysis had the same value and they almost twice the value of Horizontal Ellipse, Arch and Low Profile Arch.

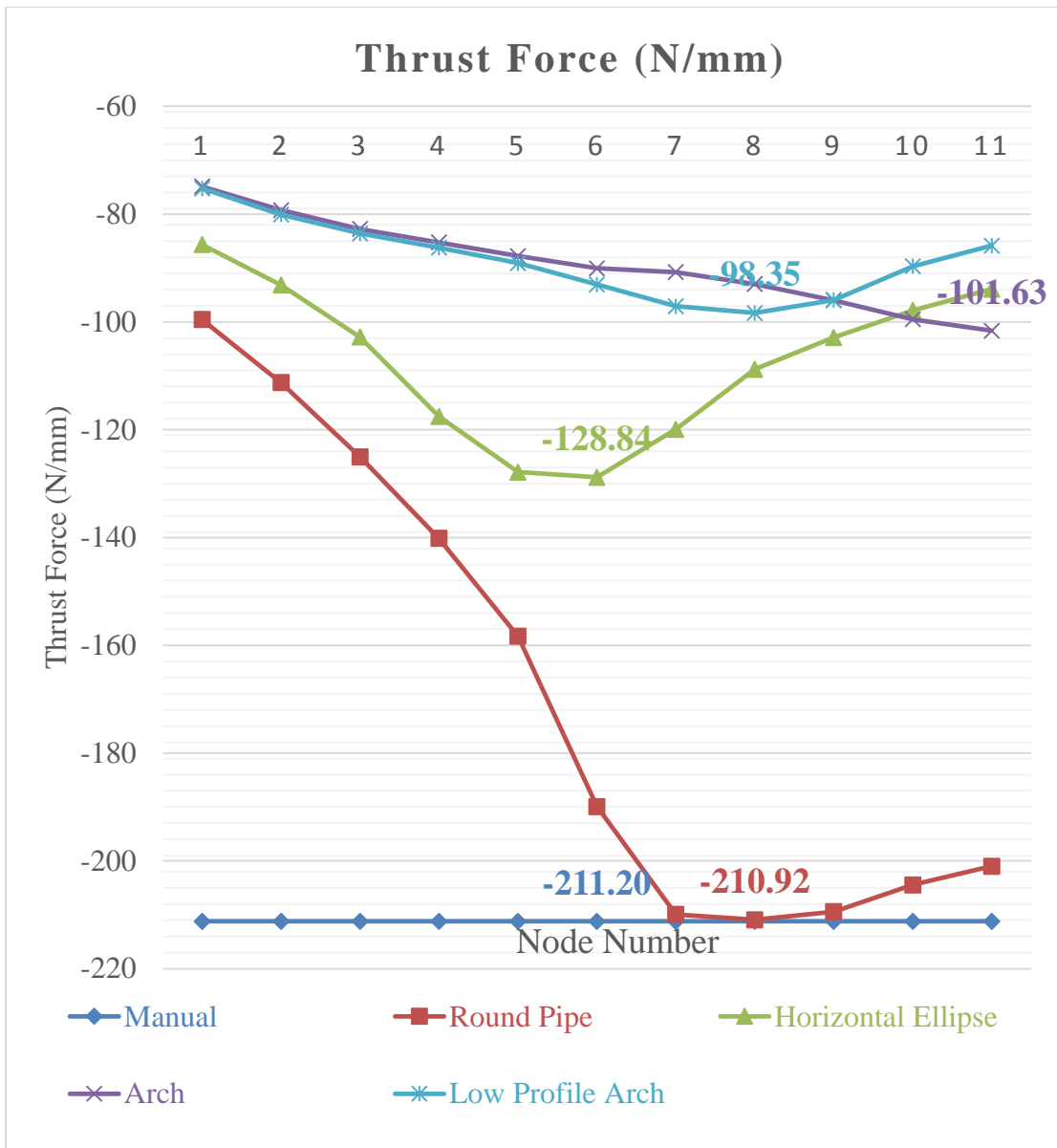


Figure 4.6. The comparison of thrust force between manual and CANDE analysis.

The comparison of thrust forces between manual and CANDE computer program for the selected types of culverts were presented in chart as shown in **Figure 4.7**. Since the manual analysis has taken as a basic reference for comparison of different culverts shapes. Horizontal axis represents the culvert's types and vertical axis is percentage of maximum thrust force in each culvert shape. The thrust forces for manual calculation and round pipe for CANDE analysis had same percentage.

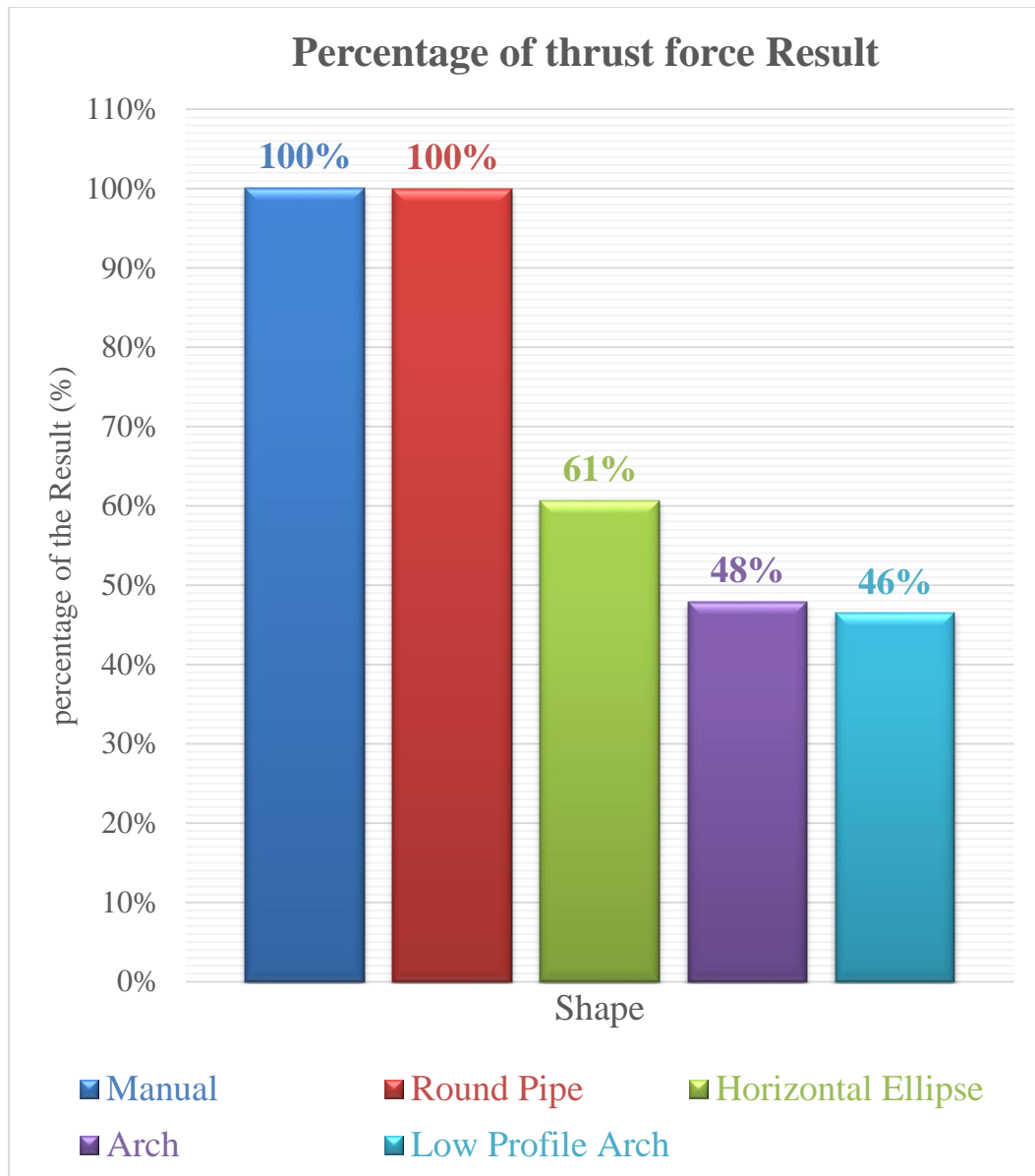


Figure 4.7. The comparison of Percentage thrust force between manual and CANDE program.

4.2.4. Displacements Results

The Results of maximum displacements from their soil compaction and construction incremental load steps for the selected culvert shapes using CANDE analysis computer program were presented graphically as shown in **Figures 4.8** and **4.9** respectively in x-direction and y-direction. The horizontal axis represents nodes number at culvert wall and displacement in each node in vertical axis.

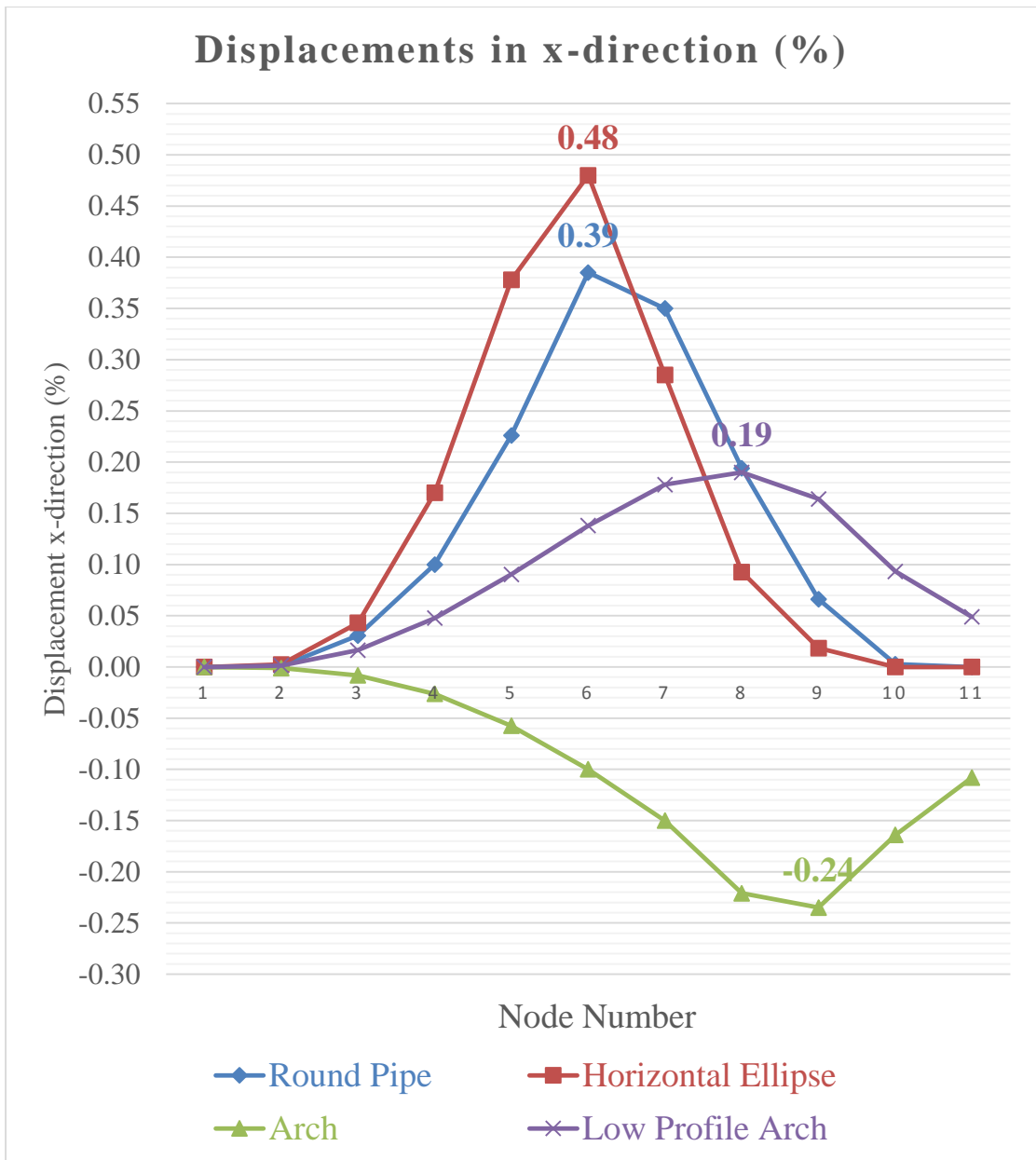


Figure 4.8. The comparison of displacements in x-direction of four types of culverts by CANDE program.

CANDE predicted a deflection less than the actual value in the horizontal and vertical diameters. Previous studies have reported similar findings that CANDE either under predicts the deflection or no correlation can be made between experimental and predicted results. Although other studies have reported good to acceptable predictions, from CANDE, correlating with experimental data.^[16]

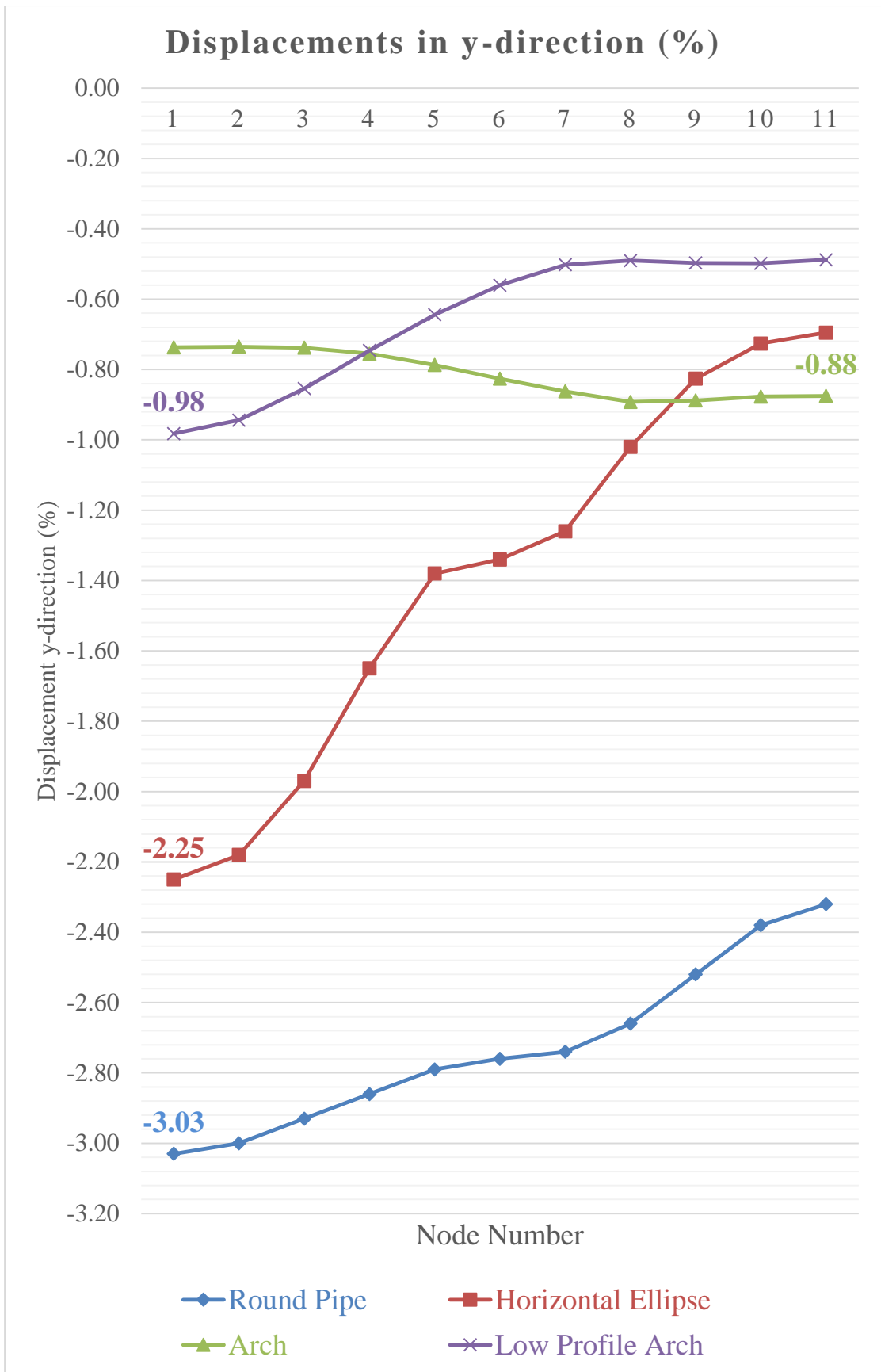


Figure 4.9. The comparison of displacements in y-direction of four types of culverts by CANDE program.

Similar to results of thrust force, the comparison of percentage of displacements in x and y directions for the mentioned four types of culvert was presented graphically in **Figures 4.10** and **4.11**. The basic reference for the comparison purpose is Round Pipe culvert.

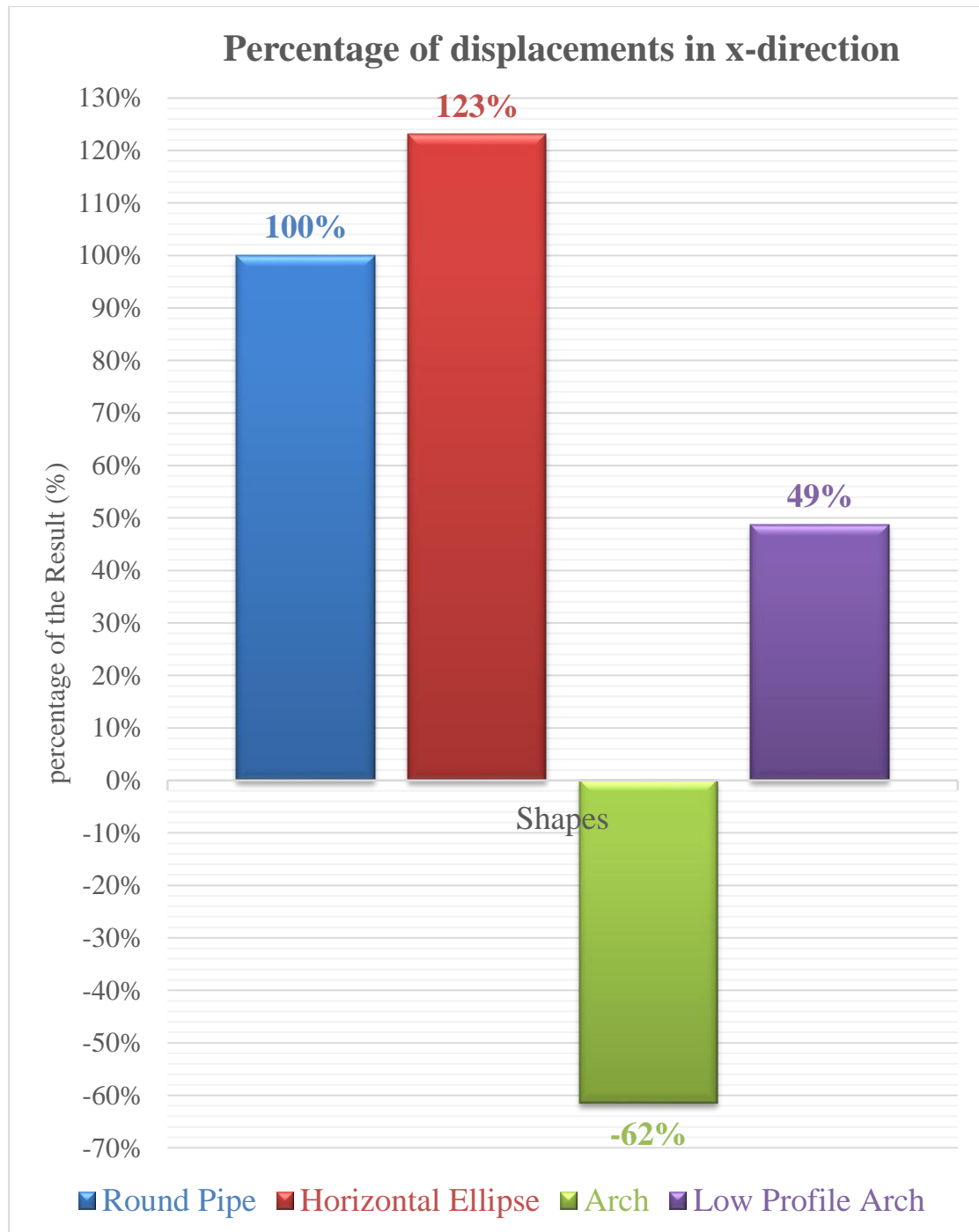


Figure 4.10. The comparison of percentage displacements in x-direction using CANDE program.

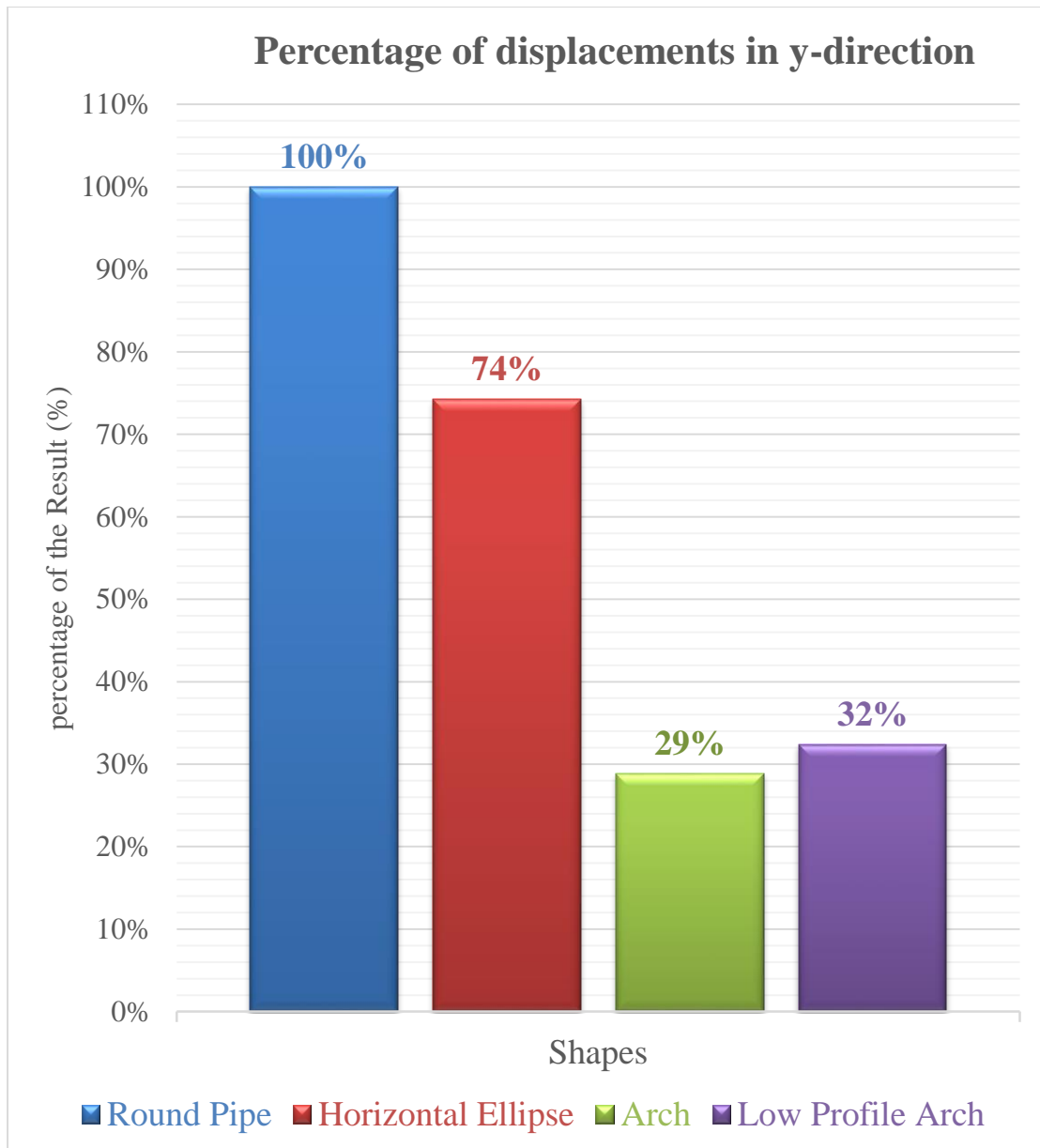


Figure 4.11. The comparison of percentage displacements in y-direction using CANDE program.

4.2.5. Other Results

In **Appendixes**, It was represented the results of bending moments, thrust forces, shear forces, normal pressures, tangential pressures, maximum fibre stresses, thrust stresses, shear stresses, strain ratio, displacements in x-direction and displacements in y-direction that obtained from soil compaction and construction incremental load steps at each node using CANDE program for the round pipe culvert.

4.3. End Area Value

The end area value of culvers is important factor for hydraulic design. Therefore, they were measured in square meter and for comparison purpose, Round Pipe end area value was chosen as basic reference with respect to other three culvert shapes as shown in **Figure 4.12**. The percentage End Area value was presented for all culvert shapes as illustrated in **Figure 4.13**.

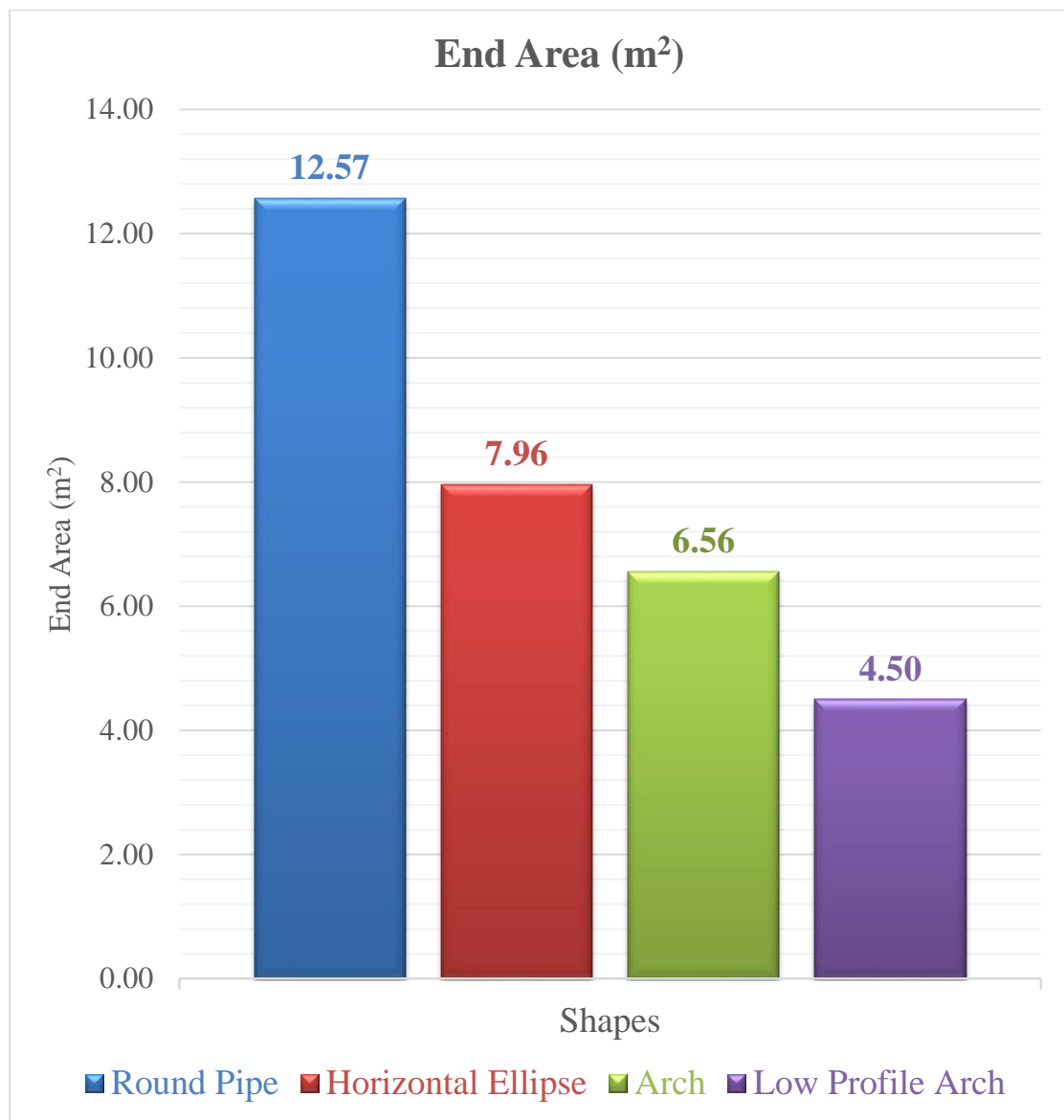


Figure 4.12. Results of End area value of four culvert shapes using CANDE program.

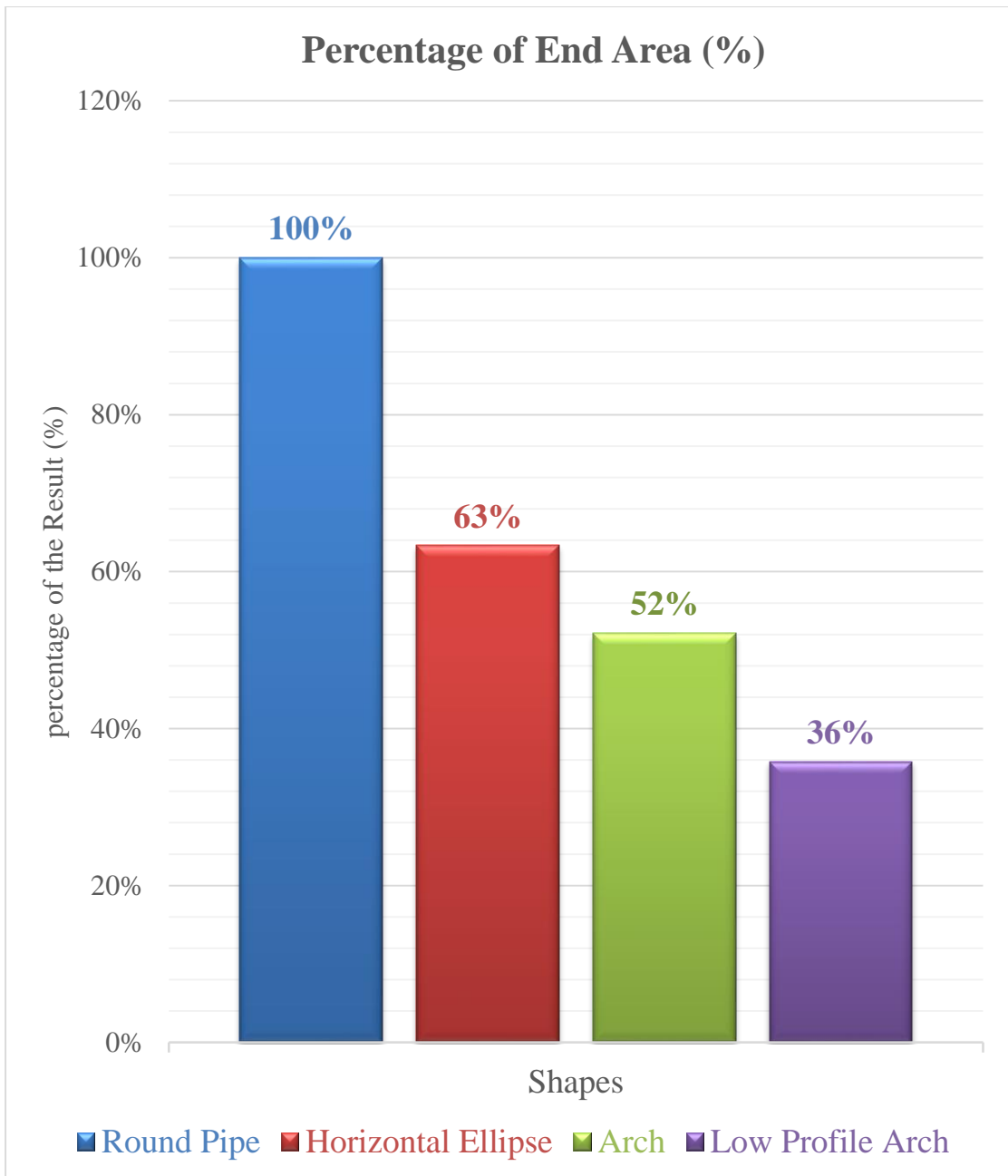


Figure 4.13. The comparison of percentage of end area value.

The end area value of Horizontal Ellipse, Arch and Low Profile Arch were 63%, 52% and 36% respectively in comparison with round pipe culver.

CHAPTER 5

Conclusions and Recommendations

5.1. Summary

This study evaluates the structural performance of four buried corrugated steel plate culvert shapes that were analysed and design under design cover and highway loading.

In this study, all culverts have 4 m span. The embankment fill reached to a height of approximately 0.6 m over the crown of the culvert. The thickness of each steel plate was 2.82 mm. The corrugation profile was 152 by 51 mm, with the pitch being 152 mm and the depth being 51 mm.

5.2. Conclusions

The performance of the culverts was monitored by numerical investigation in account of the thrust force distribution around the culverts as well as the deflection of the culverts during soil compaction and construction increments. The study of the culverts also includes the comparison of manual and numerical predictions given by finite element simulations that were carried out using the CANDE program. Data was collected and analysed for the mentioned four culverts.

The conclusions were made as follows:

- The percentage of thrust forces for the horizontal ellipse, arch and low profile arch culverts were 61%, 48% and 46% respectively in comparison with round pipe. So, thrust force predicted by finite element simulation and manual calculation have equals values for the round shape, but always have smaller values of finite element simulation than manual calculation for non-round shapes.

- All displacements values did not exceeded the 5% limitation as defined in Standard Practice for Structural Design for CANDE analysis results.
- The percentage of the horizontal displacements for horizontal ellipse, arch and low profile arch culverts were 123%, 62% and 49% respectively in comparison with round pipe. Moreover, the horizontal displacements were very small and can be ignored.
- The percentage of vertical displacements for the horizontal ellipse, arch and low profile arch culverts were 74%, 29% and 32% respectively in comparison with round pipe.
- The manual calculation was not able to predict the value and change at each node of thrust force accurately for the corrugated steel plate culverts in comparison with CANDE-2013 program. CANDE had a tendency to predict the culverts deflections.
- The Critical shape of this type of culverts was considered to be the round pipe, because it was slightly close to reach its vertical deflection limit.
- From all of these investigations, the most important value is the End Area of all culvert shapes. Where the round pipe is the perfect shape to be used for hydraulic usage than the other shapes and they all have the same structural plate thickness and corrugation profile. However, the round pipe has the biggest percentage value of end area. The end area for the horizontal ellipse, arch and low profile arch culverts were 63%, 52%, and 36% respectively in comparison with round pipe.
- Finally, although it may be on the conservative side, it is safer to use CANDE as a design tool for these types of structures. Analysis

of this type of structures using CANDE should be subjected to further research.

5.3. Recommendations

- For officials and researchers to do further study of culvert's construction, installation, cost and its maintenance.
- In addition, other corrugated sheets and corrugated conduits applications such as storage and bridges.
- Finite element simulation of live load is a better method for converting the concentrated load to line load. A simpler technique must be used to model this type of loads for plane strain analysis.

References

1. Moser, A. and Folkman, S. (2008) *Buried Pipe Design*. Third Edition. United States of America: McGraw-Hill Companies, Inc.
2. Abdel-Sayed, G. and Bakht, B. (1994) *Soil-steel Bridges: Design and Construction*, Jaeger, L. G. (ed.). United States of America: McGraw-Hill Companies, Inc.
3. Moreland, A. (2004) *Experimental and Numerical Investigation of A Deeply Buried Corrugated Steel Multi Plate Pipe*. Master of Science. Ohio University.
4. National Corrugated Steel Pipe Association (NCSPA) (2008) *Corrugated Steel Pipe Design Manual*. First Edition, (ed.). Dallas: (NCSPA).
5. Yu, W.-W. and A. LaBoube, R. (2010) *Cold-Formed Steel Design*. Fourth Edition. United States of America: John Wiley & Sons, Inc., Hoboken, New Jersey.
6. Corrugated Steel Pipe Institute (CSPI) (2007) *Handbook of Steel Drainage & Highway Construction Products*. Second Edition. Cambridge, Ontario, Canada: (CSPI).
7. *Steel and Aluminium structural plate, versatile and economical* (no date) *Hebei Anrun Anti-corrosion Steel Pipe Industry Co., Ltd.* Available at: <http://www.metal-culvert.com/culvert/steel-and-aluminum-structural-plate.html>.
8. David V. Hutton (2004) *Fundamentals of Finite Element Analysis*. First Edition. United States of America: McGraw-Hill Companies, Inc.
9. G. Katona, M. (2013) *CANDE-2013 Culvert Analysis and Design User Manual and Guideline, National Cooperative Highway Research Project*. NCHRP 15-28. Available at: CandeForCulverts.com.

10. ROSEKE, B. and A COMMENT, L. (2012) ‘Structural Design of Corrugated Steel Pipe (AASHTO Method)’, Roseke, B. *Culvert Design*, 22 June. Available at: <http://culvertdesign.com/structural-design-of-corrugated-steel-pipe-aashto-method/>.
11. *Highlights of 2013 CHBDC Supplement #3 (2013) Corrugated Steel Pipe Institute*. Association of Canadian corrugated steel pipe: Corrugated Steel Pipe Institute. Available at: <http://www.cspi.ca/node/400>.
12. American Society for Testing and Materials (ASTM) (2011) ‘Standard Practice for Structural Design of Corrugated Steel Pipe, Pipe-Arches, and Arches for Storm and Sanitary Sewers and Other Buried Applications’. ASTM (A796/A796M – 10). Available at: www.astm.org.
13. G. Katona, M. (2013) *CANDE-2013 Culvert Analysis and Design Solution Methods and Formulations, National Cooperative Highway Research Project*. NCHRP 15-28. Available at: CandeForCulverts.com.
14. G. Katona, M. (2007) *CANDE-2007 Culvert Analysis and Design Tutorial of Applications, National Cooperative Highway Research Project*. NCHRP 15-28. Available at: CandeForCulverts.com.
15. American Association of State Highway and Transportation Officials (AASHTO) (2012) ‘AASHTO LRFD Bridge Design Specifications’. AASHTO. Available at: www.transportation.org.
16. Sharma, S., & Hardcastle, J.H (1993). "Evaluation of Culvert Deformations Using the Finite Element Method, Field performance of Structures and Non-destructive evaluation of Subsurface." *Transportation Research Record* 141 5, TRB, Washington, D.C. pp.32-38.

Appendixes

```

*****
*           Program Title           CANDE-2013           *
*           Version                 3/1/2013            *
*           License No.             xxxxxx              *
*****

```

```

TITLE: Round Pipe
LEVEL: 2
USER: MOSAB

```

GENERAL BEAM INFORMATION

Beam Info. (General)-Beam Group 1-Load Step 1(1 of 2)

Node Number	X Coord. (mm)	Y Coord. (mm)	X Displ. (mm)	Y Displ. (mm)	Bending Moment (N-mm/mm)	Thrust Force (N/mm)
1	0.00	2000.25	0.00	-29.17	12.46	0.01
2	618.18	1902.33	0.00	-29.16	11.78	0.01
3	1175.76	1618.20	0.02	-29.13	9.81	0.01
4	1618.26	1175.69	0.05	-29.10	6.74	0.00
5	1902.36	618.09	0.11	-29.07	2.88	0.00
6	2000.25	0.00	0.17	-29.06	-1.41	0.00
7	1902.24	-618.45	0.23	-29.07	-5.69	0.00
8	1618.04	-1175.99	0.28	-29.09	-9.56	-0.39
9	1175.46	-1618.42	0.24	-29.05	-329.66	-1.48
10	617.83	-1902.44	0.05	-28.67	81.33	-1.75
11	0.00	-2000.25	0.00	-28.37	455.36	-0.89

Beam Info. (General)-Beam Group 1-Load Step 1(2 of 2)

Node Number	Shear Force (N/mm)	Normal Pressure (kPa)	Tang. Pressure (kPa)	Strain-Interior Wall (mm/mm)	Strain-Exterior Wall (mm/mm)
1	0.00	0.00	0.00	0.0000	0.0000
2	0.00	0.00	0.00	0.0000	0.0000
3	0.00	0.00	0.00	0.0000	0.0000
4	0.01	0.00	0.00	0.0000	0.0000
5	0.01	0.00	0.00	0.0000	0.0000
6	0.01	0.00	0.00	0.0000	0.0000
7	0.01	0.00	0.00	0.0000	0.0000
8	0.26	-0.99	-1.09	0.0000	0.0000
9	-0.07	1.11	-2.24	0.0000	0.0000
10	-0.63	-0.97	1.03	0.0000	0.0000
11	-0.57	-3.04	4.30	0.0001	-0.0000

Beam Info. (General)-Beam Group 1-Load Step 2(1 of 2)

Node Number	X Coord. (mm)	Y Coord. (mm)	X Displ. (mm)	Y Displ. (mm)	Bending Moment (N-mm/mm)	Thrust Force (N/mm)
1	0.00	2000.25	0.00	-43.88	1020.96	1.51
2	618.18	1902.33	0.14	-43.01	878.35	1.37
3	1175.76	1618.20	1.22	-40.90	464.55	1.16
4	1618.26	1175.69	3.44	-38.67	-179.93	0.85
5	1902.36	618.09	5.91	-37.42	-992.02	0.44
6	2000.25	0.00	6.86	-37.27	-1892.21	-3.17
7	1902.24	-618.45	5.16	-36.99	-3.48.75	-11.26
8	1618.04	-1175.99	2.79	-35.77	127.86	-21.22
9	1175.46	-1618.42	1.00	-33.95	216.36	-29.51
10	617.83	-1902.44	0.10	-32.11	703.51	-33.26
11	0.00	-2000.25	0.00	-31.29	1025.39	-34.69

Beam Info. (General)-Beam Group 1-Load Step 2(2 of 2)

Node Number	Shear Force (N/mm)	Normal Pressure (kPa)	Tang. Pressure (kPa)	Strain-Interior Wall (mm/mm)	Strain-Exterior Wall (mm/mm)
1	0.01	0.00	0.00	0.0001	-0.0001
2	0.44	0.00	0.00	0.0001	-0.0001
3	0.85	0.00	0.00	0.0001	-0.0001
4	1.16	0.00	0.00	0.0000	0.0000
5	1.37	0.00	0.00	-0.0001	0.0001
6	-0.51	4.58	-10.97	-0.0002	0.0002
7	-1.61	-8.32	-15.65	-0.0001	0.0000
8	-0.45	-11.59	-16.81	0.0000	0.0000
9	-0.46	-13.75	-9.81	0.0000	-0.0001
10	-0.65	-17.04	-2.59	0.0000	-0.0001
11	-0.38	-20.34	4.63	0.0001	-0.0002

Beam Info. (General)-Beam Group 1-Load Step 3(1 of 2)

Node Number	X Coord. (mm)	Y Coord. (mm)	X Displ. (mm)	Y Displ. (mm)	Bending Moment (N-mm/mm)	Thrust Force (N/mm)
1	0.00	2000.25	0.00	-43.56	-967.42	-3.10
2	618.18	1902.33	-0.13	-44.33	-674.22	-2.81
3	1175.76	1618.20	-0.96	-45.96	176.52	-2.39
4	1618.26	1175.69	-1.93	-46.93	1501.51	-4.20
5	1902.36	618.09	-1.07	-46.48	1602.57	-18.13
6	2000.25	0.00	1.82	-46.00	-1371.15	-44.53
7	1902.24	-618.45	3.14	-46.16	-1470.44	-70.41
8	1618.04	-1175.99	2.27	-45.64	-504.54	-91.91
9	1175.46	-1618.42	0.87	-44.11	-39.57	-109.8
10	617.83	-1902.44	0.03	-42.24	702.78	-121.1
11	0.00	-2000.25	0.00	-41.35	1123.20	-128.1

Beam Info. (General)-Beam Group 1-Load Step 3(2 of 2)

Node Number	Shear Force (N/mm)	Normal Pressure (kPa)	Tang. Pressure (kPa)	Strain-Interior Wall (mm/mm)	Strain-Exterior Wall (mm/mm)
1	-0.02	0.00	0.00	-0.0001	0.0001
2	-0.91	0.00	0.00	-0.0001	0.0001
3	-1.74	0.00	0.00	0.0000	0.0000
4	-1.14	-5.18	-7.13	0.0002	-0.0002
5	2.30	-16.82	-36.28	0.0002	-0.0002
6	2.46	-15.01	-44.67	-0.0002	0.0001
7	-0.69	-32.52	-36.13	-0.0003	0.0001
8	-1.14	-47.21	-32.64	-0.0002	-0.0001
9	-0.96	-54.21	-24.97	-0.0002	-0.0001
10	-0.93	-61.34	-11.49	-0.0001	-0.0003
11	-0.42	-68.48	1.98	0.0000	-0.0003

Beam Info. (General)-Beam Group 1-Load Step 4(1 of 2)

Node Number	X Coord. (mm)	Y Coord. (mm)	X Displ. (mm)	Y Displ. (mm)	Bending Moment (N-mm/mm)	Thrust Force (N/mm)
1	0.00	2000.25	0.00	-67.69	-332.74	-79.21
2	618.18	1902.33	-0.09	-67.82	188.20	-83.90
3	1175.76	1618.20	-0.06	-67.60	766.69	-91.27
4	1618.26	1175.69	0.92	-66.50	925.10	-102.5
5	1902.36	618.09	3.73	-64.97	1313.35	-120.9
6	2000.25	0.00	7.70	-64.22	-3395.89	-152.5
7	1902.24	-618.45	7.46	-64.03	-2055.20	-174.7
8	1618.04	-1175.99	4.22	-62.21	134.65	-182.4
9	1175.46	-1618.42	1.45	-59.20	248.77	-187.5
10	617.83	-1902.44	0.05	-56.11	1217.72	-186.9
11	0.00	-2000.25	0.00	-54.75	1650.46	-185.2

Beam Info. (General)-Beam Group 1-Load Step 4(2 of 2)

Node Number	Shear Force (N/mm)	Normal Pressure (kPa)	Tang. Pressure (kPa)	Strain-Interior Wall (mm/mm)	Strain-Exterior Wall (mm/mm)
1	-0.79	-36.91	0.46	-0.0002	-0.0001
2	-0.88	-41.80	-7.84	-0.0001	-0.0001
3	-0.59	-46.69	-16.15	0.0000	-0.0002
4	-0.44	-50.64	-19.66	0.0000	-0.0003
5	3.45	-73.31	-37.11	0.0000	-0.0003
6	2.69	-60.98	-59.46	-0.0006	0.0002
7	-2.82	-85.18	-10.58	-0.0005	0.0000
8	-1.84	-96.43	-16.19	-0.0002	-0.0003
9	-0.87	-91.57	-1.15	-0.0002	-0.0003
10	-1.12	-94.77	2.09	-0.0001	-0.0004
11	-0.26	-97.97	5.34	-0.0001	-0.0005

Beam Info. (General)-Beam Group 1-Load Step 5(1 of 2)

Node Number	X Coord. (mm)	Y Coord. (mm)	X Displ. (mm)	Y Displ. (mm)	Bending Moment (N-mm/mm)	Thrust Force (N/mm)
1	0.00	2000.25	0.00	-73.05	-130.92	-96.55
2	618.18	1902.33	-0.08	-73.02	337.29	-103.0
3	1175.76	1618.20	0.12	-72.42	780.93	-112.4
4	1618.26	1175.69	1.40	-71.00	831.98	-126.0
5	1902.36	618.09	4.50	-69.29	1320.81	-145.6
6	2000.25	0.00	8.68	-68.49	-3734.65	-178.7
7	1902.24	-618.45	8.22	-68.24	-2183.72	-200.6
8	1618.04	-1175.99	4.59	-66.19	223.67	-205.4
9	1175.46	-1618.42	1.56	-62.91	278.03	-207.7
10	617.83	-1902.44	0.06	-59.56	1328.22	-204.4
11	0.00	-2000.25	0.00	-58.09	1770.58	-201.0

Beam Info. (General)-Beam Group 1-Load Step 5(2 of 2)

Node Number	Shear Force (N/mm)	Normal Pressure (kPa)	Tang. Pressure (kPa)	Strain-Interior Wall (mm/mm)	Strain-Exterior Wall (mm/mm)
1	-0.77	-45.92	-1.33	-0.0001	-0.0001
2	-0.73	-51.56	-10.55	-0.0001	-0.0002
3	-0.40	-57.20	-19.76	-0.0001	-0.0003
4	-0.43	-61.88	-23.42	-0.0001	-0.0003
5	3.65	-86.76	-36.83	0.0000	-0.0004
6	2.80	-72.69	-64.52	-0.0007	0.0002
7	-3.16	-98.13	-4.74	-0.0005	0.0000
8	-1.97	-108.61	-12.90	-0.0003	-0.0003
9	-0.88	-101.30	4.29	-0.0003	-0.0003
10	-1.19	-103.74	4.84	-0.0001	-0.0004
11	-0.22	-106.17	5.38	-0.0001	-0.0005

Beam Info. (General)-Beam Group 1-Load Step 6(1 of 2)

Node Number	X Coord. (mm)	Y Coord. (mm)	X Displ. (mm)	Y Displ. (mm)	Bending Moment (N-mm/mm)	Thrust Force (N/mm)
1	0.00	2000.25	0.00	-76.91	792.00	-99.57
2	618.18	1902.33	0.02	-76.22	712.98	-111.3
3	1175.76	1618.20	0.78	-74.50	313.60	-125.1
4	1618.26	1175.69	2.54	-72.57	468.02	-140.2
5	1902.36	618.09	5.74	-70.80	1286.06	-158.4
6	2000.25	0.00	9.79	-70.01	-4033.88	-190.0
7	1902.24	-618.45	8.88	-69.68	-2026.76	-210.0
8	1618.04	-1175.99	4.93	-67.47	209.31	-211.0
9	1175.46	-1618.42	1.68	-63.96	325.60	-209.4
10	617.83	-1902.44	0.07	-60.40	1421.18	-203.7
11	0.00	-2000.25	0.00	-58.85	1860.52	-198.6

Beam Info. (General)-Beam Group 1-Load Step 6(2 of 2)

Node Number	Shear Force (N/mm)	Normal Pressure (kPa)	Tang. Pressure (kPa)	Strain- Interior Wall (mm/mm)	Strain- Exterior Wall (mm/mm)
1	-0.13	-51.76	-11.74	0.0000	-0.0002
2	0.38	-56.45	-18.32	-0.0001	-0.0002
3	0.20	-61.13	-24.89	-0.0001	-0.0002
4	-0.78	-68.42	-23.14	-0.0001	-0.0003
5	3.60	-94.65	-32.76	-0.0001	-0.0004
6	2.65	-76.50	-63.89	-0.0008	0.0002
7	-3.39	-104.38	0.47	-0.0005	0.0000
8	-1.88	-110.80	-6.23	-0.0003	-0.0003
9	-0.97	-102.23	9.60	-0.0002	-0.0003
10	-1.23	-103.49	7.39	-0.0001	-0.0005
11	-0.18	-104.75	5.18	0.0000	-0.0005

STEEL BEAM INFORMATION

Beam Info. (Steel)-Beam Group 1-Load Step 1

Node Number	Max. Fiber Stress (kPa)	Thrust Stress (kPa)	Shear Stress (kPa)	Strain Ratio max/yield
1	337.29	2.18	0.02	0.001
2	318.83	1.98	0.64	0.001
3	265.56	1.68	1.22	0.001
4	182.59	1.22	1.68	0.001
5	78.04	0.64	1.98	0.000
6	-37.85	0.00	2.08	0.000
7	-153.81	-0.64	1.98	0.001
8	-375.73	-118.61	78.57	0.002
9	-9316.26	-447.81	-22.04	0.041
10	-2717.80	-529.97	-190.43	0.012
11	-12520.95	-271.19	-172.58	0.055

Beam Info. (Steel)-Beam Group 1-Load Step 2

Node Number	Max. Fiber Stress (kPa)	Thrust Stress (kPa)	Shear Stress (kPa)	Strain Ratio max/yield
1	27923.35	458.02	3.39	0.123
2	24044.09	415.27	134.94	0.106
3	12850.24	353.25	256.66	0.056
4	5097.13	256.65	353.26	0.022
5	26821.57	134.93	415.28	0.118
6	-51864.36	-961.21	-155.79	0.228
7	-12800.87	-3419.09	-489.71	0.056
8	-9880.81	-6441.16	-137.05	0.043
9	-14776.98	-8956.57	-139.61	0.065
10	-29020.79	-10095.37	-196.25	0.128
11	-38115.66	-10531.33	-116.14	0.168

Beam Info. (Steel)-Beam Group 1-Load Step 3

Node Number	Max. Fiber Stress (kPa)	Thrust Stress (kPa)	Shear Stress (kPa)	Strain Ratio max/yield
1	-26966.57	-941.64	-6.97	0.119
2	-18991.19	-853.76	-277.43	0.083
3	-5474.74	-726.24	-527.68	0.024
4	-41666.12	-1273.42	-345.86	0.183
5	-48614.38	-5502.94	696.70	0.214
6	-50401.98	-13516.27	745.27	0.222
7	-60930.14	-21373.26	-210.19	0.268
8	-41472.24	-27899.29	-347.03	0.182
9	-34402.01	-33337.67	-292.81	0.151
10	-55658.68	-36752.98	-282.05	0.245
11	-69089.60	-38874.09	-125.99	0.304

Beam Info. (Steel)-Beam Group 1-Load Step 4

Node Number	Max. Fiber Stress (kPa)	Thrust Stress (kPa)	Shear Stress (kPa)	Strain Ratio max/yield
1	-32995.41	-24044.29	-238.68	0.145
2	-30531.16	-25468.20	-266.62	0.134
3	-48329.49	-27704.58	-178.72	0.212
4	-55985.22	-31098.80	-132.58	0.246
5	-72034.35	-36703.27	1047.96	0.317
6	-137640.72	-46286.37	817.16	0.605
7	-108305.60	-53017.65	-856.07	0.476
8	-58991.27	-55369.04	-558.78	0.259
9	-63598.96	-56906.70	-262.67	0.280
10	-89479.47	-56721.44	-340.00	0.393
11	-100611.74	-56212.26	-80.00	0.442

Beam Info. (Steel)-Beam Group 1-Load Step 5

Node Number	Max. Fiber Stress (kPa)	Thrust Stress (kPa)	Shear Stress (kPa)	Strain Ratio max/yield
1	-32830.63	-29308.65	-233.02	0.144
2	-40340.60	-31266.96	-221.13	0.177
3	-55135.92	-34127.74	-119.98	0.242
4	-60622.63	-38241.15	-130.93	0.266
5	-79722.01	-44190.36	1107.53	0.350
6	-154715.59	-54248.09	850.16	0.680
7	-119637.82	-60892.56	-959.78	0.526
8	-68359.31	-62342.32	-597.04	0.300
9	-70512.68	-63032.97	-267.89	0.310
10	-97786.96	-62055.85	-362.03	0.430
11	-108642.75	-61011.70	-67.30	0.477

Beam Info. (Steel)-Beam Group 1-Load Step 6

Node Number	Max. Fiber Stress (kPa)	Thrust Stress (kPa)	Shear Stress (kPa)	Strain Ratio max/yield
1	-51529.14	-30223.31	-39.38	0.226
2	-52963.39	-33783.07	116.02	0.233
3	-46402.27	-37966.05	59.41	0.204
4	-55147.99	-42557.54	-235.85	0.242
5	-82665.38	-48068.73	1091.84	0.363
6	-166181.57	-57664.58	803.74	0.730
7	-118252.67	-63729.96	-1028.81	0.520
8	-69661.87	-64031.26	-570.51	0.306
9	-72329.45	-63570.56	-293.91	0.318
10	-100063.61	-61831.90	-372.31	0.440
11	-110344.38	-60294.10	-54.09	0.485

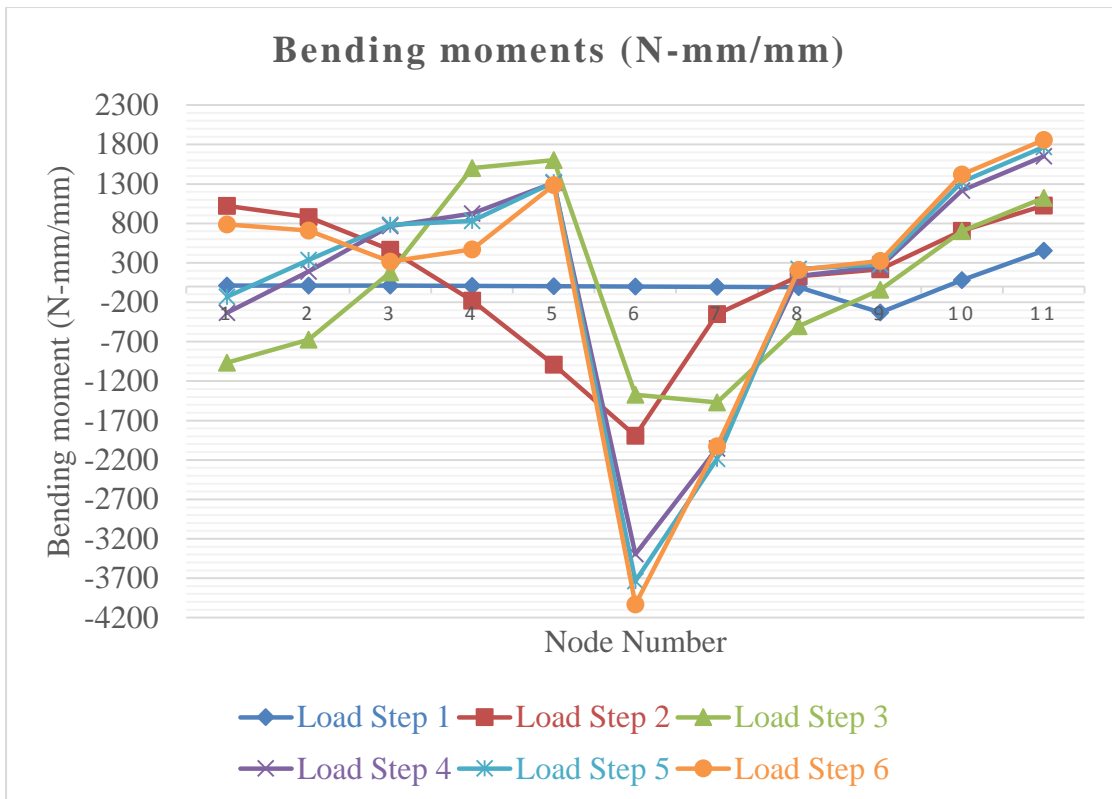


Figure B.1. Result of bending moments for Round Pipe culvert using CANDE program.

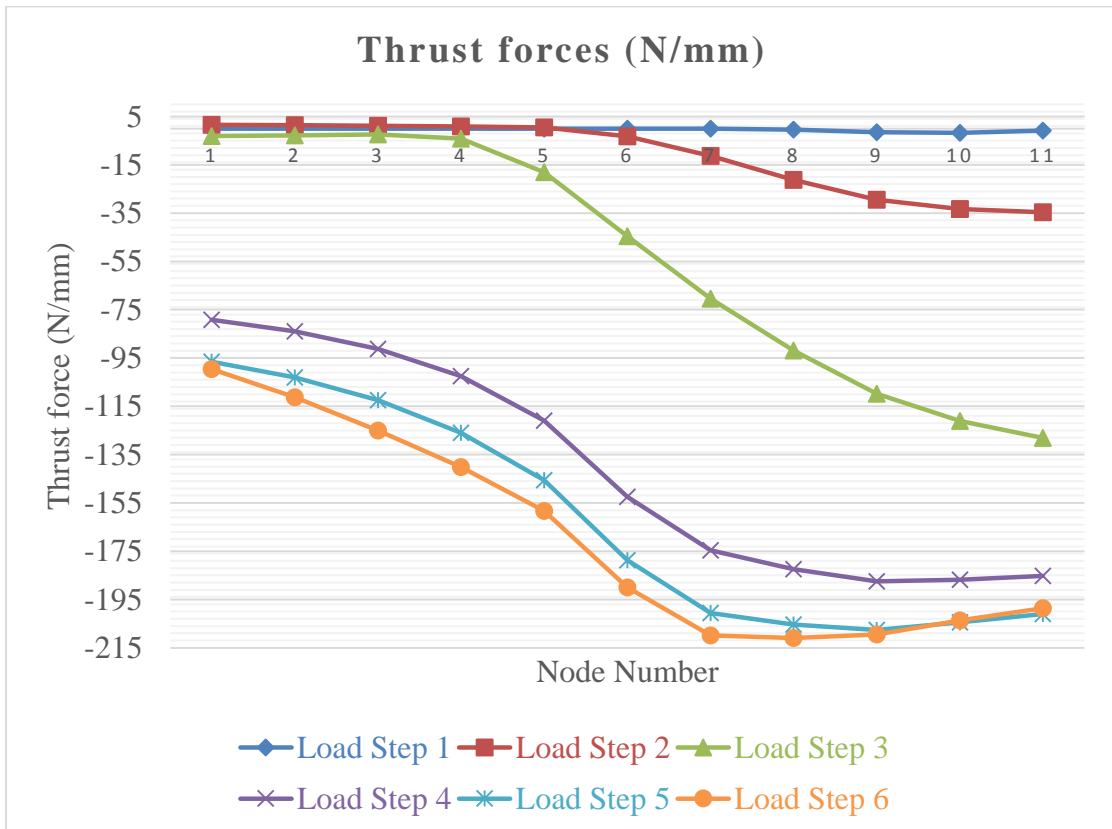


Figure B.2. Result of thrust force for Round Pipe culvert using CANDE program.

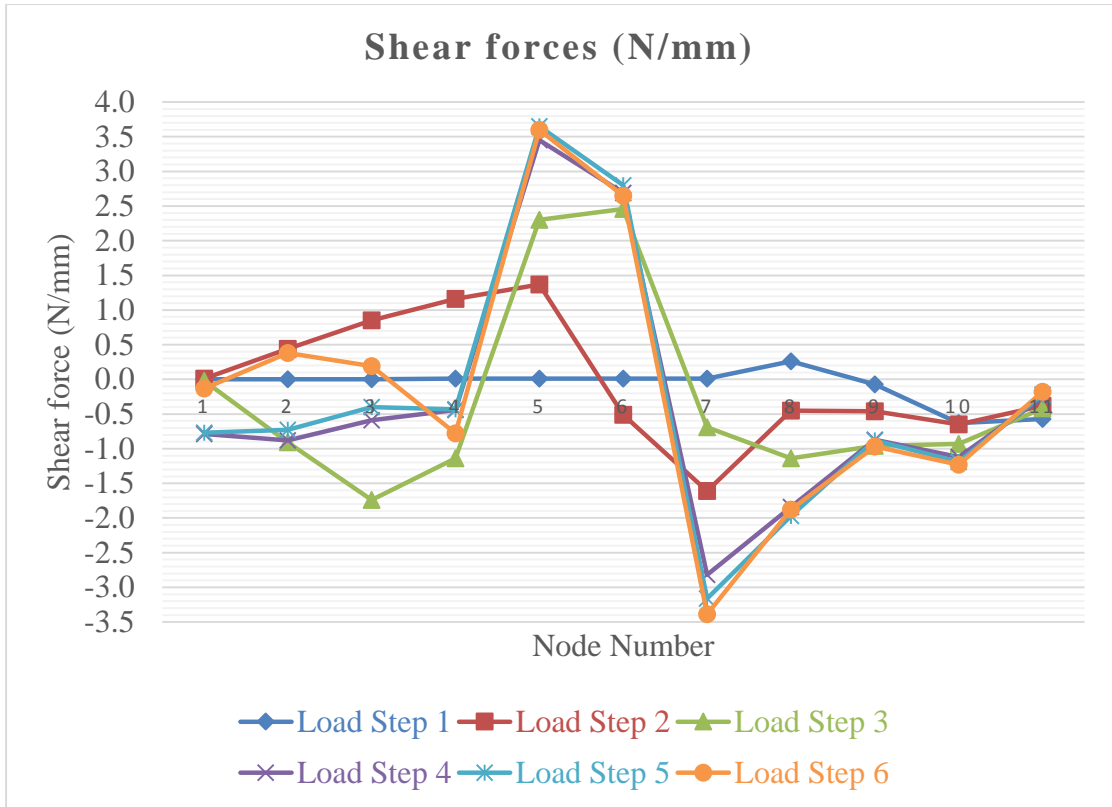


Figure B.3. Result of shear force for Round Pipe culvert using CANDE program.

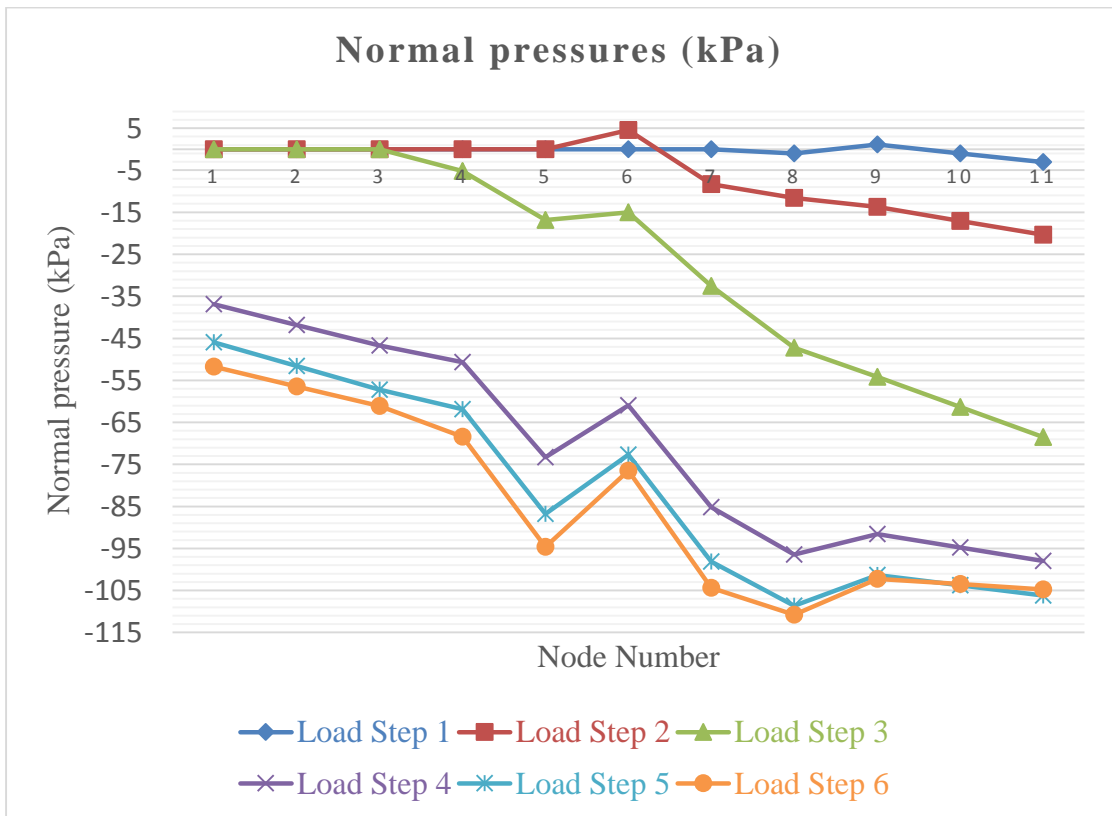


Figure B.4. Result of normal pressure for Round Pipe culvert using CANDE program.

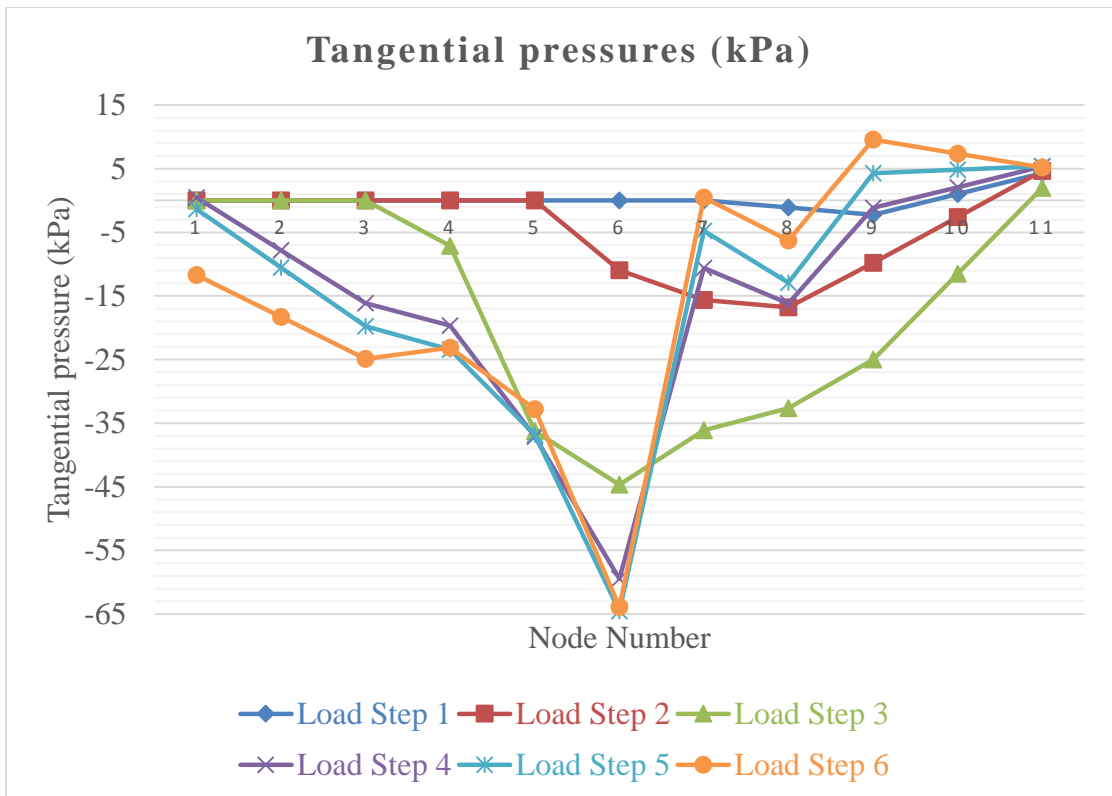


Figure B.5. Result of tangential pressure for Round Pipe culvert using CANDE program.

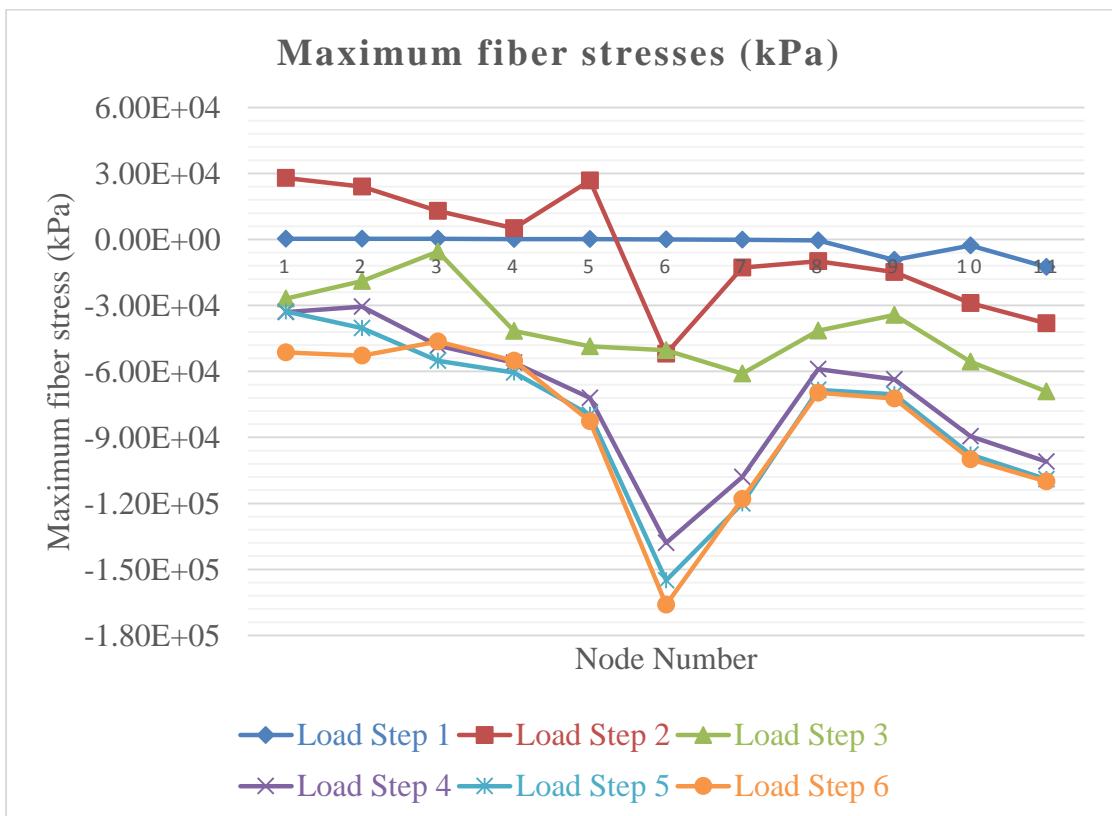


Figure B.6. Result of maximum fiber stresses for Round Pipe culvert using CANDE program.

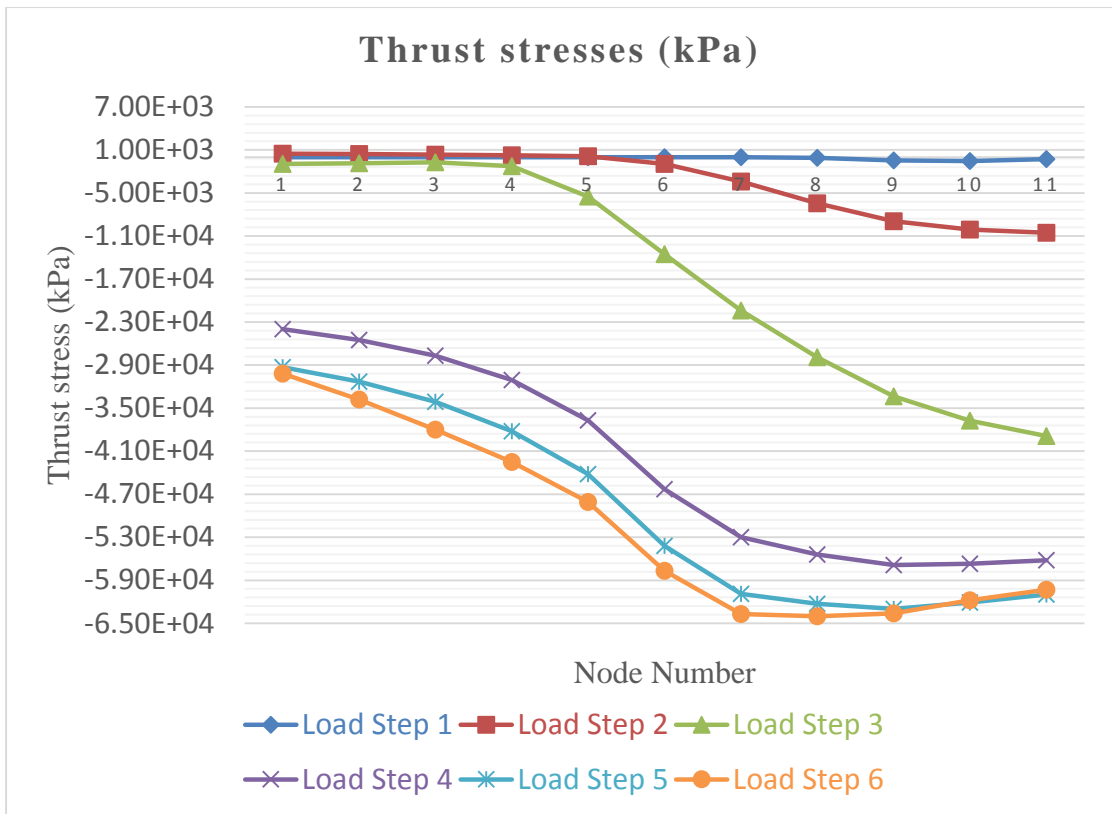


Figure B.7. Result of thrust stresses for Round Pipe culvert using CANDE program.

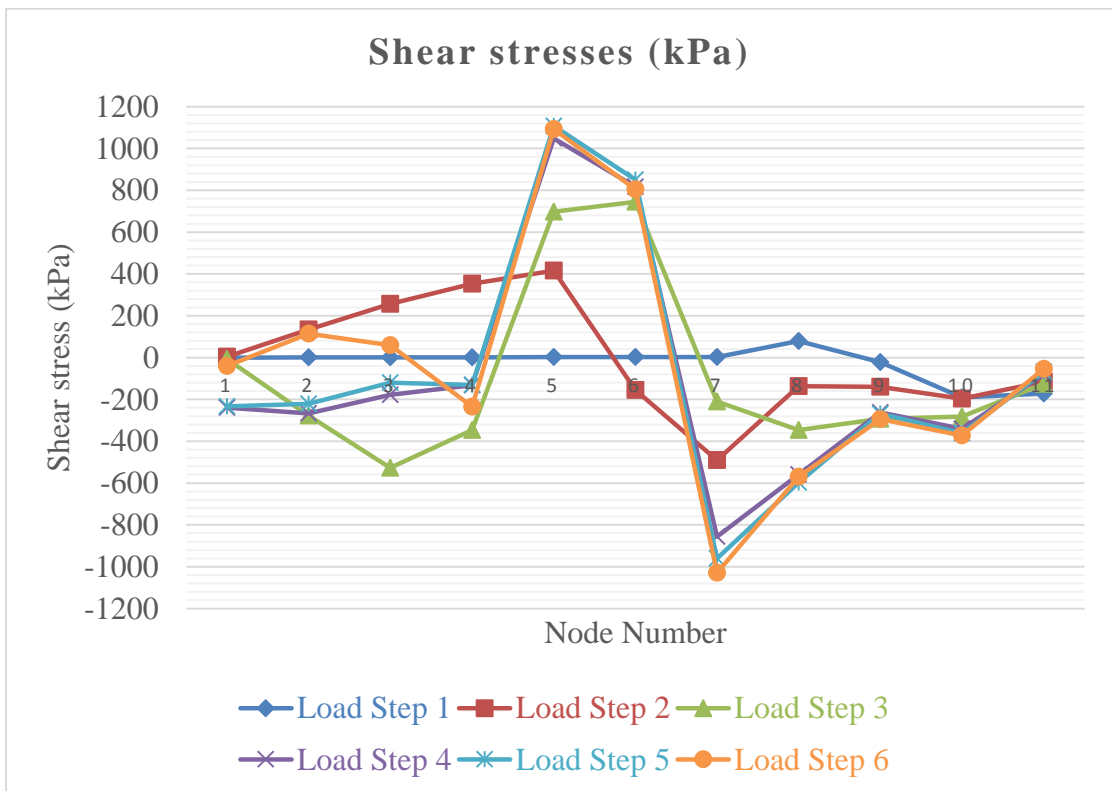


Figure B.8. Result of shear stresses for Round Pipe culvert using CANDE program.

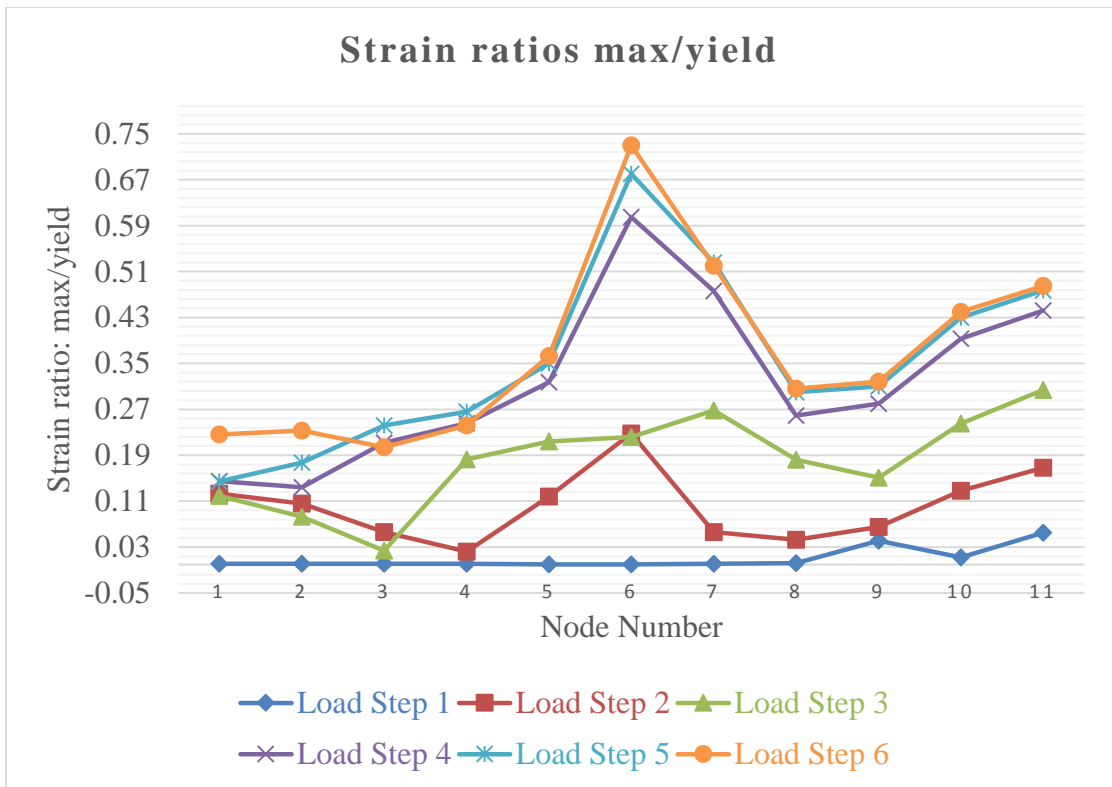


Figure B.9. Result of strain ratios for Round Pipe culvert using CANDE program.

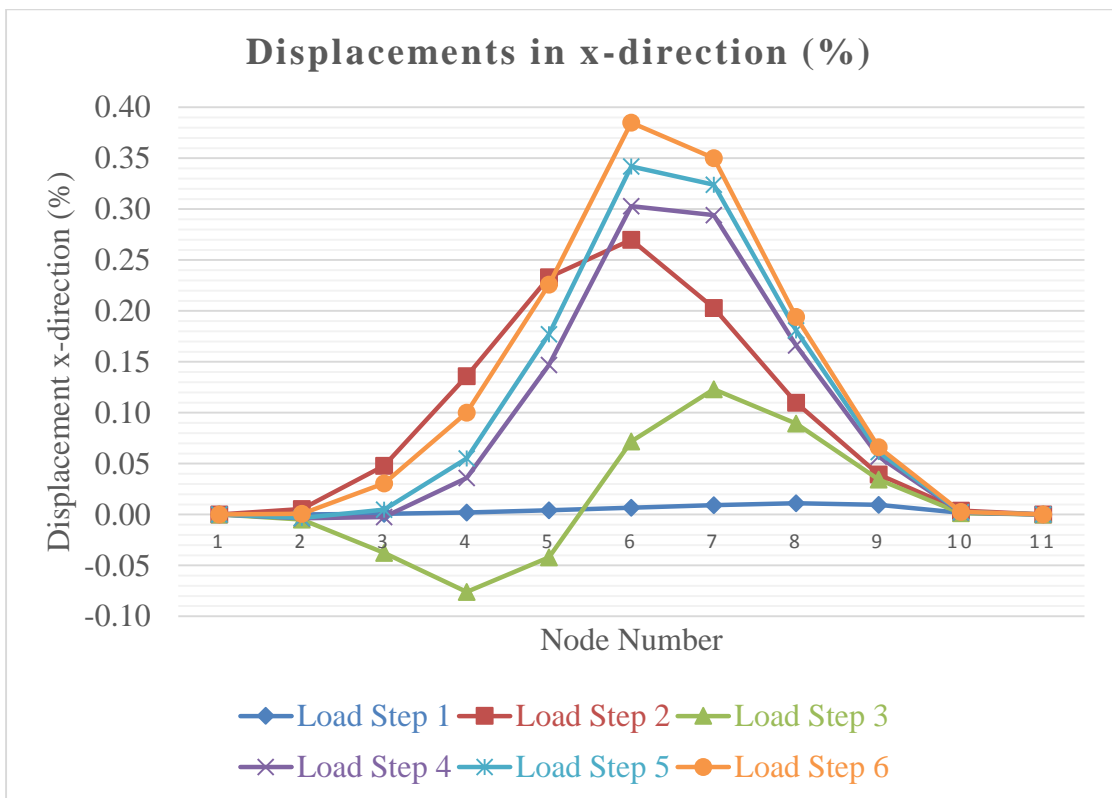


Figure B.10. Result of displacements x-direction for Round Pipe culvert using CANDE program.

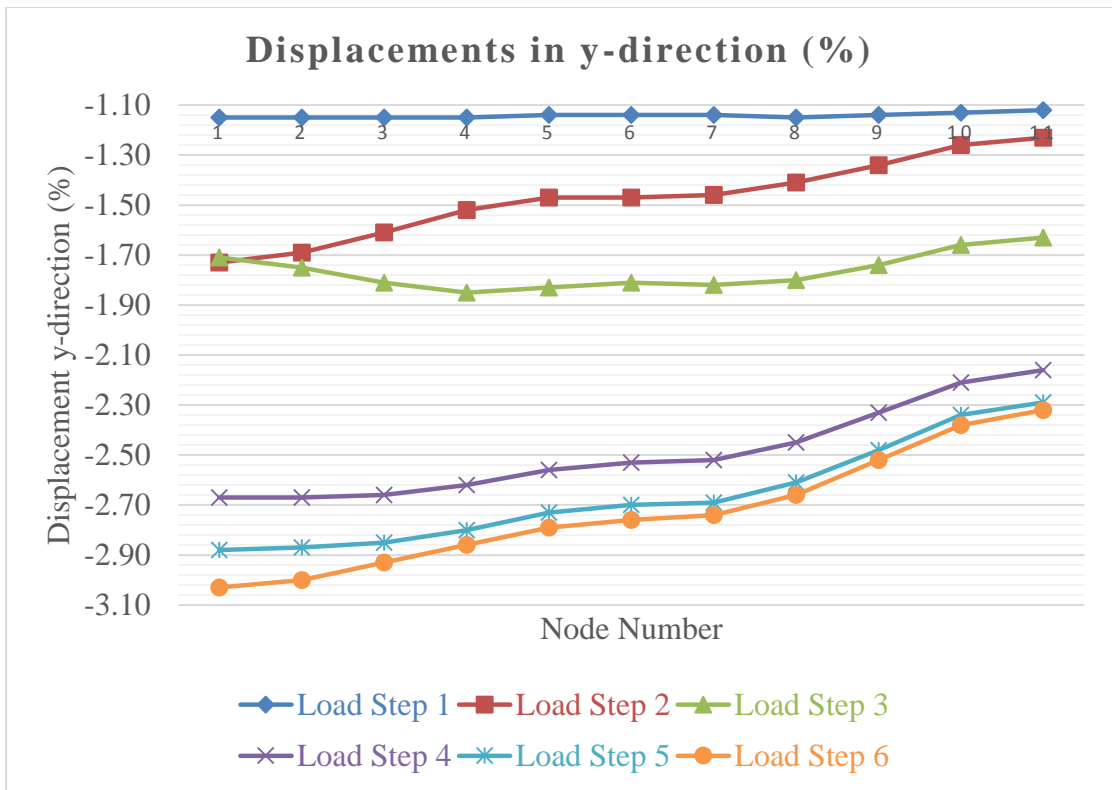


Figure B.11. Result of displacements y-direction for Round Pipe culvert using CANDE program.